Aymeric FREREJEAN

Micro and Nanotechnologies for Integrated Systems
2024

Chalmers University of Technology
Department of Microtechnology and Nanoscience - MC2
Gothenburg, Sweden
www.chalmers.se

Optomechanical ground-state cooling with Fano-membrane in the middle

from 03/11/2024 to 08/30/2024

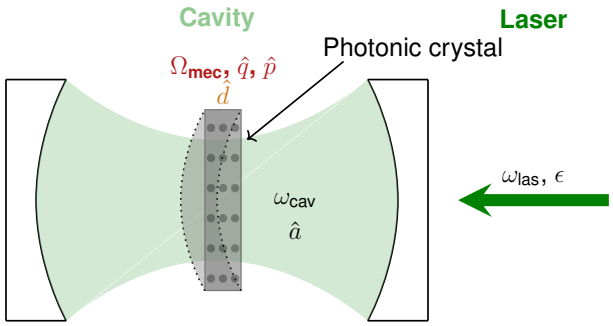

Under the supervision of:

- **Supervisor: Janine SPLETTSTÖSSER, janines@chalmers.se**
- **PoliTO Thesis Supervisor: Carlo RICCIARDI, carlo.ricciardi@polito.it**

Confidentiality: No

Politecnico di Torino

Corso Duca degli Abruzzi, 24
10129 Torino, ITALIA

politecnicoditorino@pec.polito.it
https://www.polito.it/

Master project 2024
Micro and Nanotechnologies for Integrated Systems

Master Thesis Report
Relazione di Tirocinio di Fine Studi

Last Semester of MNIS Program, Spring 2024

AYMERIC FREREJEAN

Politecnico di Torino
Torino, Italia

Department of Microtechnology and Nanoscience - MC2
Chalmers University of Technology
Gothenburg, Sweden

© AYMERIC FREREJEAN, 2024.

Supervisor: Janine Splettstößer, Department of Microtechnology and Nanoscience
PoliTO Thesis Supervisor: Carlo Ricciardi, Politecnico di Torino

Master project report 2024
Department of Microtechnology and Nanoscience - MC2
Chalmers University of Technology
SE-412 96 Gothenburg
Sweden
Telephone +46 31 772 1000

Typeset in LaTeX
Gothenburg, Sweden 2024

List of Acronyms

Below is the list of acronyms that have been used throughout this thesis listed in alphabetical order:

BCH	Baker-Campbell-Hausdorff
CM	Covariance Matrix
MQLE	Markovian Quantum Langevin Equation
RWA	Rotating Wave Approximation

Contents

List of Figures

List of Tables

1
Introduction

Optomechanics is the study of the interaction between light and mechanical motion. In a typical optomechanical system, light is confined within an optical cavity and interacts with a mechanical element, such as a mirror or membrane. The mechanical element can move in response to the light field, while the light exerts radiation pressure on the mechanical element, causing it to move.

This interaction between light and mechanical motion leads to various intriguing phenomena, such as optomechanical interactions, which generally stem from the exchange of momentum between the electromagnetic field and a mechanical resonator. This exchange enables quantum control over both photonic and phononic modes. Optomechanical systems, being highly sensitive, are then well suited for applications such as gravitational wave sensing, signal processing, and quantum information processing.

One particularly notable phenomenon in these systems is optical cooling, where the light field is tuned to reduce the vibrational energy of the mechanical element, bringing it close to its quantum ground state. Cavity optomechanical systems achieve sideband cooling through the strong interaction between light and mechanical motion. Reaching the quantum ground state is a crucial prerequisite for observing genuine quantum phenomena. Thus, optomechanical cavities provide an excellent platform for studying and utilizing quantum effects on a mesoscopic scale, as well as for observing quantum states in macroscopic objects.

For many applications, the spectral selectivity of the cavity is a critical figure of merit. However, in a linear Fabry-Perot cavity, reducing the cavity length while maintaining a fixed loss level typically results in an increase in linewidth and a decrease in spectral selectivity. A solution to this is the use of a structured ultrathin Fano-membrane, which enables the realization of narrow-linewidth cavities.

In this work, we aim to investigate the properties of a Fano-cavity and its potential applications in optomechanical systems. Reaching the quantum ground state has been a long-standing goal in the field of optomechanics, already investigated in various systems. We will explore the possibility of achieving this goal developing a theoretical model of the so-called Fano-membrane-in-the-middle system. Our work is to assume, derive, simulate, analyze and optimize the system in light of the already investigated Fano-membrane-based-optomechanical systems.

2

Theory

The aim of this chapter is to provide a theoretical background on the concepts and methods used in the thesis. The chapter is divided into three sections. The first section gives a brief overview of quantum mechanics, focusing on the concepts and results that are relevant to the thesis. The second section discusses the concept of rotating frames and the rotating wave approximation, which are essential for understanding the dynamics of quantum systems. The third section introduces the equivalence between the Schrödinger and Heisenberg pictures and the concept of the covariance matrix, which is used to describe the statistical properties of quantum states.

Crash course on Quantum Mechanics, here we are!

Nota bene: unless otherwise mentioned, $\hbar$ is set to 1.

2.1 Usefull quantum physics Results

Quantum Mechanics:

Operators:
Operators are mathematical objects that act on a quantum state to produce another quantum state.

The commutator of two operators $\hat{A}$ and $\hat{B}$ is defined as

$$[\hat{A}, \hat{B}] = \hat{A}\hat{B} - \hat{B}\hat{A}. \tag{2.1}$$

The commutator of two operators is a measure of how much they fail to commute. If the commutator is zero, the operators commute.

The anticommutator of two operators $\hat{A}$ and $\hat{B}$ is defined as

$$\{\hat{A}, \hat{B}\}_+ = \hat{A}\hat{B} + \hat{B}\hat{A}. \tag{2.2}$$

Useful quantum mechanics relations:

$$\hat{p}^2 + \hat{q}^2 = 2\hat{b}^\dagger\hat{b} + 1, \tag{2.3}$$
$$[\hat{q}, \hat{p}] = i, \tag{2.4}$$
$$\left[\hat{p}, \hat{q}^2\right] = -2i\hat{q}, \tag{2.5}$$
$$\left[\hat{q}, \hat{p}^2\right] = 2i\hat{p}. \tag{2.6}$$

A detailled derivation of those results can be found in Appendix A.

Complex Conjugate:
The complex conjugate of a complex number $z = a + ib$ is denoted z^* and is defined as $z^* = a - ib$.

Transpose:
The transpose of a matrix M is denoted M^T and is defined as the matrix obtained by exchanging the rows and columns of M.

Adjoint:
The adjoint of an operator $\hat{A}$ is denoted $\hat{A}^\dagger$ and is defined as the complex conjugate of the operator's transpose.

Expectation Value:
The expectation value of an operator $\hat{A}$ in a state $|\psi\rangle$ is denoted $\left\langle \hat{A} \right\rangle$ and is defined as

$$\left\langle \hat{A} \right\rangle = \langle\psi| \hat{A} |\psi\rangle . \tag{2.7}$$

The expectation value of an operator is the average value of the observable $\hat{A}$ in the state $|\psi\rangle$.

Hermitian Operators:
An operator $\hat{A}$ is hermitian if it satisfies

$$\hat{A} = \hat{A}^\dagger. \tag{2.8}$$

The expectation value of a hermitian operator is real:

$$\left\langle \hat{A} \right\rangle = \left\langle \hat{A}^\dagger \right\rangle . \tag{2.9}$$

Unitary Operators:
An operator $\hat{U}$ is unitary if it satisfies

$$\hat{U}\hat{U}^\dagger = \hat{U}^\dagger\hat{U} = \mathbb{1}. \tag{2.10}$$

The inverse of a unitary operator is its adjoint.

Boson Operators:
Boson operators are operators that satisfy the boson commutation relations:

$$[\hat{a}, \hat{a}^\dagger] = 1. \tag{2.11}$$

The boson operators $\hat{a}$ and $\hat{a}^\dagger$ are the annihilation and creation operators, respectively. They act on the Fock states $|n\rangle$ as

$$\hat{a}\,|n\rangle = \sqrt{n}\,|n-1\rangle\,, \tag{2.12}$$
$$\hat{a}^\dagger\,|n\rangle = \sqrt{n+1}\,|n+1\rangle\,. \tag{2.13}$$

The number operator $\hat{n} = \hat{a}^\dagger\hat{a}$ counts the number of bosons in a given state.

Harmonic Oscillator:
The hamiltonian of a harmonic oscillator is given by

$$\hat{H} = \hbar\omega\left(\hat{a}^\dagger\hat{a} + \frac{1}{2}\right), \tag{2.14}$$

where ω is the frequency of the oscillator.

Baker-Campbell-Hausdorff formula:

$$e^{t\hat{A}}\hat{B}e^{-t\hat{A}} = \hat{B} + t[\hat{A},\hat{B}] + \frac{t^2}{2!}[\hat{A},[\hat{A},\hat{B}]] + \frac{t^3}{3!}[\hat{A},[\hat{A},[\hat{A},\hat{B}]]] + \ldots, \tag{2.15}$$

This formula expresses the transformation of an operator $\hat{B}$ under the adjoint action of an exponential operator $e^{\hat{A}}$.

BCH expansion of the exponential of a commutator:

$$\frac{d\,e^{i\hat{K}}}{dt}e^{-i\hat{K}} = i\frac{d\hat{K}}{dt} + \frac{i^2}{2}\left[\hat{K}, \frac{d\hat{K}}{dt}\right] + \frac{i^3}{3!}\left[\hat{K}, \left[\hat{K}, \frac{d\hat{K}}{dt}\right]\right] + \ldots. \tag{2.16}$$

In the case where $\hat{K}$ commutes with $\frac{d\hat{K}}{dt}$, only the first term survives.

2.2 Rotating Frames

Let us consider a system with density matrix ρ and a possibly time-dependent hamiltonian $\hat{H}(t)$. This system evolves according to the von Neumann's equation

$$\frac{d}{dt}\rho = -\frac{i}{\hbar}[\hat{H}(t), \rho]. \tag{2.17}$$

We can always move to a *rotating frame* by defining a new density matrix

$$\tilde{\rho} = U(t)\rho U^\dagger(t) \tag{2.18}$$

with $U(t)$ an unitary operator. ρ' evolves also according to the von Neumann's equation

$$\frac{d}{dt}\tilde{\rho} = -\frac{i}{\hbar}[\tilde{H}(t), \rho]. \tag{2.19}$$

but with an effective hamiltonian

$$\tilde{H}(t) = i\frac{dU}{dt}U^\dagger + UHU^\dagger. \tag{2.20}$$

Eliminating time-dependences

A useful application of rotating frames is to remove the time-dependency of the hamiltonian.

Let us consider a classical hamiltonian of a pumped cavity:

$$\hat{H} = \omega\hat{a}^\dagger\hat{a} + \epsilon\hat{a}^\dagger e^{(-i\omega_p t)} + \epsilon^*\hat{a}e^{(i\omega_p t)} \tag{2.21}$$

and a appropriate unitary operator

$$U = e^{i\omega_p t\hat{a}^\dagger\hat{a}}. \tag{2.22}$$

Choosing this operator, we move to a frame rotating at the laser pump frequency ω_p. Defining $\alpha = \omega_p t$, we compute the effective hamiltonian in the rotating frame.

On the first hand, we have

$$i\frac{dU}{dt}U^\dagger = i\frac{d}{dt}e^{i\alpha\hat{a}^\dagger\hat{a}}e^{-i\alpha\hat{a}^\dagger\hat{a}} \tag{2.23}$$

and using the BCH expansion (2.16), we obtain

$$\begin{aligned} i\frac{dU}{dt}U^\dagger &= i\left(i\frac{d}{dt}\alpha\hat{a}^\dagger\hat{a} + \frac{i^2}{2}\left[\alpha\hat{a}^\dagger\hat{a}, \frac{d}{dt}\alpha\hat{a}^\dagger\hat{a}\right] + \dots\right) \\ &= i\cdot i\omega_p\hat{a}^\dagger\hat{a} + i\cdot\frac{i^2}{2}\left[\omega_p t\hat{a}^\dagger\hat{a}, \omega_p\hat{a}^\dagger\hat{a}\right] + \dots \\ &= -\omega_p\hat{a}^\dagger\hat{a}. \end{aligned} \tag{2.24}$$

On the other hand,

$$UHU^\dagger = U\omega\hat{a}^\dagger\hat{a}U^\dagger + U\epsilon\hat{a}^\dagger e^{(-i\omega_p t)}U^\dagger + U\epsilon^*\hat{a}e^{(i\omega_p t)}U^\dagger. \tag{2.25}$$

U having no effect on $\hat{a}^\dagger\hat{a}$, we have

$$\begin{aligned} U\omega_a\hat{a}^\dagger\hat{a}\,U^\dagger &= e^{i\alpha\hat{a}^\dagger\hat{a}}\omega_a\hat{a}^\dagger\hat{a}\,e^{-i\alpha\hat{a}^\dagger\hat{a}} \\ &= \omega_a e^{i\alpha\hat{a}^\dagger\hat{a}}\,\hat{a}^\dagger\hat{a}\,e^{-i\alpha\hat{a}^\dagger\hat{a}} \\ &= \omega_a\hat{a}^\dagger\hat{a}. \end{aligned} \tag{2.26}$$

Using (2.15), we derive

$$\begin{aligned}
e^{i\alpha\hat{a}^\dagger\hat{a}}\,\hat{a}\,e^{-i\alpha\hat{a}^\dagger\hat{a}} &= \hat{a} + i\alpha\left[\hat{a}^\dagger\hat{a},\hat{a}\right] \\
&\quad + \frac{(i\alpha)^2}{2!}\left[\hat{a}^\dagger\hat{a},\left[\hat{a}^\dagger\hat{a},\hat{a}\right]\right] \\
&\quad + \frac{(i\alpha)^3}{3!}\left[\hat{a}^\dagger\hat{a},\left[\hat{a}^\dagger\hat{a},\left[\hat{a}^\dagger\hat{a},\hat{a}\right]\right]\right] + \cdots \\
&= \hat{a} + i\alpha(-1)\hat{a} + \frac{(i\alpha)^2}{2!}\left[\hat{a}^\dagger\hat{a},(-1)\hat{a}\right] + \cdots \\
&= \hat{a} - i\alpha\hat{a} + \frac{(i\alpha)^2}{2!}\left(\hat{a}^\dagger\hat{a}(-1)\hat{a} - (-1)\hat{a}\hat{a}^\dagger\hat{a}\right) + \cdots \\
&= \hat{a} + i\alpha(-1)\hat{a} + \frac{(i\alpha)^2}{2!}(-1)\left(\hat{a}^\dagger\hat{a} - \hat{a}\hat{a}^\dagger\right) + \cdots \\
&= \hat{a} + i\alpha(-1)\hat{a} + \frac{(i\alpha)^2}{2!}(-1)(-1)\hat{a} + \cdots \\
&= \hat{a} - i\alpha\hat{a} + \frac{(-x^2)}{2!}\hat{a} + \cdots \\
&= \hat{a} + i\alpha(-1)\hat{a} + \frac{(i\alpha)^2}{2!}(-1)^2\hat{a} + \frac{(i\alpha)^3}{3!}(-1)^3\hat{a} + \cdots \\
&= \left(1 + \sum_{j=1}^{\infty}\frac{(i\alpha)^j}{j!}(-1)^j\right)\hat{a} \\
&= \sum_{j=0}^{\infty}\frac{(i\alpha)^j}{j!}(-1)^j\hat{a} \\
&= \sum_{j=0}^{\infty}\frac{(-i\alpha)^j}{j!}\hat{a} \\
&= e^{-i\alpha}\hat{a}.
\end{aligned}$$

We obtain

$$e^{i\alpha\hat{a}^\dagger\hat{a}}\,\hat{a}\,e^{-i\alpha\hat{a}^\dagger\hat{a}} = e^{-i\alpha}\hat{a}, \tag{2.27}$$

$$e^{i\alpha\hat{a}^\dagger\hat{a}}\,\hat{a}^\dagger\,e^{-i\alpha\hat{a}^\dagger\hat{a}} = e^{i\alpha}\hat{a}^\dagger, \tag{2.28}$$

leading to

$$U\,\epsilon\hat{a}^\dagger e^{-i\omega_p t}\,U^\dagger = \epsilon\hat{a}^\dagger, \tag{2.29}$$

$$U\,\epsilon^*\hat{a}e^{i\omega_p t}\,U^\dagger = \epsilon^*\hat{a}. \tag{2.30}$$

Thus, the effective hamiltonian in the rotating frame reads

$$\hat{H} = (\omega_a - \omega_p)\,\hat{a}^\dagger\hat{a} + \epsilon\hat{a}^\dagger + \epsilon^*\hat{a}. \tag{2.31}$$

We conclude that in this rotating frame, the hamiltonian remains time-independent, but it evolves based on the detuned frequency $\Delta = \omega_a - \omega_p$. This concept of detuning a frequency is crucial in quantum optics applications because it provides a straightforward method to adjust the parameters of the system.

2.3 Rotating Wave Approximation

Let us consider a two-level atomic system interacting with a coherent input field. The hamiltonian describing such a system typically includes a part for the free evolution of the atom and another part for the interaction with the field.

In the interaction picture, the interaction hamiltoniancan be expressed as

$$\hat{H}_{\text{int}}(t) = \hbar\Omega \left(e^{i(\omega-\omega_0)t}\hat{\sigma}_+ + e^{-i(\omega-\omega_0)t}\hat{\sigma}_- + e^{i(\omega+\omega_0)t}\hat{\sigma}_+ + e^{-i(\omega+\omega_0)t}\hat{\sigma}_- \right),$$

where:

- Ω is the Rabi frequency, representing the strength of the coupling,
- $\hat{\sigma}_+ = |0\rangle\langle 1|$ and $\hat{\sigma}_- = |1\rangle\langle 0|$ are the raising and lowering operators.

In many practical situations, ω is chosen to be close to ω_0, making $\Delta = \omega - \omega_0$ small. However, the terms oscillating at $\omega + \omega_0$ are far off-resonant. The RWA involves neglecting the rapidly oscillating terms, which are assumed to average out over time and hence will have a small contribution to the dynamics.

The interaction hamiltonian under the RWA is given by:

$$\hat{H}_{\text{int}}^{\text{RWA}}(t) = \hbar\Omega \left(e^{i\Delta t}\hat{\sigma}_+ + e^{-i\Delta t}\hat{\sigma}_- \right),$$

This simplified hamiltonian is much easier to handle and captures the essential physics of the system under the near-resonance condition.

2.4 Equivalence Schrödinger / Heisenberg Picture

The Schrödinger equation of a system described by an hermitian hamiltonian $\hat{H}$ is given by

$$\frac{d}{dt}|\psi\rangle = -\frac{i}{\hbar}\hat{H}|\psi\rangle . \tag{2.32}$$

Let $\hat{A}$ be an hermitian operator.

We compute the time derivative of $\left\langle \hat{A} \right\rangle$:

$$\begin{aligned}
\frac{d}{dt}\left\langle \hat{A} \right\rangle &= \frac{d}{dt}\langle\psi|\,\hat{A}\,|\psi\rangle \\
&= \left(\frac{d}{dt}\langle\psi|\right)\hat{A}\,|\psi\rangle + \langle\psi|\,\hat{A}\left(\frac{d}{dt}\,|\psi\rangle\right) \\
&= \left(-\frac{i}{\hbar}\hat{H}\,|\psi\rangle\right)^{*}\hat{A}\,|\psi\rangle + \langle\psi|\,\hat{A}\left(-\frac{i}{\hbar}\hat{H}\,|\psi\rangle\right) \\
&= \left(\frac{i}{\hbar}\langle\psi|\,\hat{H}\right)\hat{A}\,|\psi\rangle - \frac{i}{\hbar}\langle\psi|\,\hat{A}\left(\hat{H}\,|\psi\rangle\right) \\
&= \frac{i}{\hbar}\left(\langle\psi|\,\hat{H}\hat{A} - \hat{A}\hat{H}\,|\psi\rangle\right) \\
&= \frac{i}{\hbar}\langle\psi|\,[\hat{H},\hat{A}]\,|\psi\rangle \\
&= \frac{i}{\hbar}[\hat{H},\hat{A}].
\end{aligned}$$

In the Heisenberg picture, the evolution of the expectation value of an observable $\hat{A}$ follows

$$\frac{d}{dt}\left\langle \hat{A} \right\rangle = \frac{i}{\hbar}[\hat{H},\hat{A}]. \tag{2.33}$$

In the Schrödinger picture approach, the state $\rho(t)$ of a system with density matrix ρ evolves in time and $\hat{A}$ is time-independent.

In the Heisenberg picture, the state ρ is fixed at $\rho(0)$ and we transfer the time evolution to the operator. The time-dependent operator $\hat{A}(t)$ satisfies the Heisenberg equation

$$\frac{d}{dt}\hat{A}(t) = \frac{i}{\hbar}[\hat{H},\hat{A}]. \tag{2.34}$$

2.5 Covariance Matrix

The covariance matrix is a mathematical tool used to describe the statistical properties of quantum states, particularly for systems involving multiple operators. It quantifies the correlations between the latter.

Given the vector of operators

$$\hat{Y} = \begin{bmatrix} \hat{q}_1 & \hat{p}_1 & \dots & \hat{q}_N & \hat{p}_N \end{bmatrix}^T, \tag{2.35}$$

we define their first moments as $y_i = \left\langle \hat{Y}_i \right\rangle$. Moreover, we define the covariance matrix (CM) σ as

$$\sigma_{ij} = \frac{1}{2}\left\langle \hat{Y}_i\hat{Y}_j + \hat{Y}_j\hat{Y}_i \right\rangle - \left\langle \hat{Y}_i \right\rangle\left\langle \hat{Y}_j \right\rangle = \frac{1}{2}\left\langle \delta\hat{Y}_i, \delta\hat{Y}_j \right\rangle, \tag{2.36}$$

where

$$\delta\hat{Y}_i = \hat{Y}_i - \left\langle \hat{Y}_i \right\rangle \tag{2.37}$$

is the deviation of the operator $\hat{Y}_i$ from its mean value.

The covariance matrix is constructed in that what in order to have nice properties. The matrix σ is a real, symmetric, and positive matrix. For example, if $N = 1$, the covariance matrix is

$$\sigma = \begin{bmatrix} \langle \delta\hat{q}^2 \rangle & \langle \delta\hat{q}\delta\hat{p} \rangle \\ \langle \delta\hat{p}\delta\hat{q} \rangle & \langle \delta\hat{p}^2 \rangle \end{bmatrix}$$

and for $N = 2$, the covariance matrix is

$$\sigma = \begin{bmatrix} \langle \delta\hat{q}_1^2 \rangle & \langle \delta\hat{q}_1\delta\hat{p}_1 \rangle & \langle \delta\hat{q}_1\delta\hat{q}_2 \rangle & \langle \delta\hat{q}_1\delta\hat{p}_2 \rangle \\ \langle \delta\hat{p}_1\delta\hat{q}_1 \rangle & \langle \delta\hat{p}_1^2 \rangle & \langle \delta\hat{p}_1\delta\hat{q}_2 \rangle & \langle \delta\hat{p}_1\delta\hat{p}_2 \rangle \\ \langle \delta\hat{q}_2\delta\hat{q}_1 \rangle & \langle \delta\hat{q}_2\delta\hat{p}_1 \rangle & \langle \delta\hat{q}_2^2 \rangle & \langle \delta\hat{q}_2\delta\hat{p}_2 \rangle \\ \langle \delta\hat{p}_2\delta\hat{q}_1 \rangle & \langle \delta\hat{p}_2\delta\hat{p}_1 \rangle & \langle \delta\hat{p}_2\delta\hat{q}_2 \rangle & \langle \delta\hat{p}_2^2 \rangle \end{bmatrix}.$$

The diagonal elements of the covariance matrix are the variances of the operators, while the off-diagonal elements represent their correlations.

3
Methods

The purpose of this chapter is to introduce the theoretical frameworks that underpin this thesis. These frameworks lay the groundwork for the in-depth exploration of the thesis's central project, which is the study of the Fano-membrane-in-the-middle optomechanical system.

3.1 Quantum Langevin Equations

The quantum Langevin equations are a set of stochastic differential equations used to describe the dynamics of a system interacting with a dissipative environment or a reservoir. They incorporate both the coherent dynamics of the system and the effects of noise and dissipation due to the environment.

In the quantum Langevin framework, the equations account for:

- Dissipation: Energy loss from the system to the environment ;
- Fluctuations: Random noise with quantum origin.

We use this approach to describe the behavior of open quantum systems such as optical cavities, mechanical resonators and atomic ensembles subject to quantum noise and damping. A formulation of quantum damping theory, in which the explicit nature of inputs from a heat bath and of outputs into it is taken into account, has been developped in [2]. Based on this work, we derive the quantum Langevin equations in the following sections.

3.1.1 Background

We derive the quantum Langevin equations formulating the system in terms of a somewhat idealized class of hamiltonians, in which a finite system is coupled to a heat bath of harmonic oscillators.

The following four assumptions are made:

1. The system is linear ;
2. The rotating wave approximation is made ;
3. The bath spectrum is flat, implying that all frequencies contribute equally to the dynamics ;

4. The coupling constant is independent of frequency.

We consider a system interacting with a heat bath, described by the Hamiltonian:

$$\hat{H} = \hat{H}_{\text{sys}} + \hat{H}_B + \hat{H}_{\text{int}}, \tag{3.1}$$

where

$$\hat{H}_B = \hbar \int_{-\infty}^{\infty} d\omega\, \omega\, \hat{b}^\dagger(\omega)\hat{b}(\omega),$$
$$\hat{H}_{\text{int}} = i\hbar \int_{-\infty}^{\infty} d\omega\, \kappa(\omega) \left[\hat{b}^\dagger(\omega)\hat{c} - \hat{c}^\dagger\hat{b}(\omega)\right],$$

$\hat{b}(\omega)$ being the boson anhillation operator for the bath with

$$[\hat{b}(\omega), \hat{b}^\dagger(\omega')] = \delta(\omega - \omega') \tag{3.2}$$

and $\hat{c}$ is one of several possible system operators.

In practice the range of Ω is $(0, +\infty)$, but a range of $(-\Omega, +\infty)$ can arise when we go into a frame rotating with a very large angular frequency Ω, as is common in quantum optics.

3.1.2 Derivation of the Quantum Langevin Equations

From (3.1) we derive the Heisenberg equations of motion for the system operators.

For the bosonic operators, we have:

$$\begin{aligned}
\dot{\hat{b}}(\omega) &= -\frac{i}{\hbar}\left[\hat{b}(\omega), \hat{H}\right] \\
&= -\frac{i}{\hbar}\left(\left[\hat{b}(\omega), \hat{H}_{\text{sys}}\right] + \left[\hat{b}(\omega), \hat{H}_B\right] + \left[\hat{b}(\omega), \hat{H}_{\text{int}}\right]\right) \\
&= \frac{i}{\hbar}\Bigg(\hat{b}(\omega)\hbar\int_{-\infty}^{\infty} d\omega'\, \omega'\, \hat{b}^\dagger(\omega')\hat{b}(\omega') - \hbar\int_{-\infty}^{\infty} d\omega'\, \omega'\, \hat{b}^\dagger(\omega')\hat{b}(\omega')\hat{b}(\omega) \\
&\quad + \hat{b}(\omega) i\hbar \int_{-\infty}^{\infty} d\omega'\, \kappa(\omega')\left[\hat{b}^\dagger(\omega')\hat{c} - \hat{c}^\dagger\hat{b}(\omega')\right] - i\hbar\int_{-\infty}^{\infty} d\omega'\, \kappa(\omega')\left[\hat{b}^\dagger(\omega')\hat{c} - \hat{c}^\dagger\hat{b}(\omega')\right]\hat{b}(\omega)\Bigg) \\
&= \frac{i}{\hbar}\Bigg(\hbar\int_{-\infty}^{\infty} d\omega'\, \omega'\, \hat{b}(\omega)\hat{b}^\dagger(\omega')\hat{b}(\omega') - \hbar\int_{-\infty}^{\infty} d\omega'\, \omega'\, \hat{b}^\dagger(\omega')\hat{b}(\omega)\hat{b}(\omega') \\
&\quad + i\hbar\int_{-\infty}^{\infty} d\omega'\, \kappa(\omega')\hat{b}(\omega)\left[\hat{b}^\dagger(\omega')\hat{c} - \hat{c}^\dagger\hat{b}(\omega')\right] - i\hbar\int_{-\infty}^{\infty} d\omega'\, \kappa(\omega')\left[\hat{b}^\dagger(\omega')\hat{c} - \hat{c}^\dagger\hat{b}(\omega')\right]\hat{b}(\omega)\Bigg) \\
&= -i\int_{-\infty}^{\infty} d\omega'\, \omega'\left[\hat{b}(\omega)\hat{b}^\dagger(\omega')\right]\hat{b}(\omega') + \int_{-\infty}^{\infty} d\omega'\, \kappa(\omega')\left[\hat{b}(\omega), \hat{b}^\dagger(\omega')\hat{c}\right]
\end{aligned}$$

Substituting $[\hat{b}(\omega), \hat{b}^\dagger(\omega')] = \delta(\omega - \omega')$, we obtain the time evolution of the operator $\hat{b}(\omega)$:

$$\dot{\hat{b}}(\omega) = -i\omega\hat{b}(\omega) + \kappa(\omega)\hat{c}. \tag{3.3}$$

For an arbitrary system operator $\hat{a}$, we have:

$$\begin{aligned}
\dot{\hat{a}} &= -\frac{i}{\hbar}\left[\hat{a}, \hat{H}\right] \\
&= -\frac{i}{\hbar}\left[\hat{a}, \hat{H}_{\text{sys}}\right] - \frac{1}{i\hbar}\left[\hat{a}, \hbar\int_{-\infty}^{\infty} d\omega\, \omega\, \hat{b}^\dagger(\omega)\hat{b}(\omega)\right] \\
&\quad - \frac{i}{\hbar}\left[\hat{a}, i\hbar\int_{-\infty}^{\infty} d\omega\, \kappa(\omega)\left[\hat{b}^\dagger(\omega)\hat{c} - \hat{c}^\dagger\hat{b}(\omega)\right]\right] \\
&= -\frac{i}{\hbar}\left[\hat{a}, \hat{H}_{\text{sys}}\right] + \int_{-\infty}^{\infty} d\omega\, \kappa(\omega)\left\{\hat{b}^\dagger(\omega)\left[\hat{a}, \hat{c}\right] - \left[\hat{a}, \hat{c}^\dagger\right]\hat{b}(\omega)\right\}. \qquad (3.4)
\end{aligned}$$

Then, we verify that

$$\hat{b}(\omega) = e^{-i\omega(t-t_0)}\hat{b}_0(\omega) + \kappa(\omega)\int_{t_0}^{t} e^{-i\omega(t-t')}\hat{c}(t')\, dt' \qquad (3.5)$$

where $\hat{b}_0(\omega)$ is the value of $\hat{b}_(\omega)$ at $t = t_0$, is solution to the differential equation (3.3):

$$\begin{aligned}
\frac{d}{dt}\hat{b}(\omega) &= -i\omega e^{-i\omega(t-t_0)}\hat{b}_0(\omega) + \kappa(\omega)\frac{d}{dt}\left(\int_{t_0}^{t} e^{-i\omega(t-t')}\hat{c}(t')\, dt'\right) \\
&= -i\omega e^{-i\omega(t-t_0)}\hat{b}_0(\omega) + \kappa(\omega)\left(e^{-i\omega(t-t)}\hat{c}(t) + \int_{t_0}^{t}\frac{\partial}{\partial t}\left(e^{-i\omega(t-t')}\right)\hat{c}(t')\, dt'\right) \\
&= -i\omega e^{-i\omega(t-t_0)}\hat{b}_0(\omega) + \kappa(\omega)\left(\hat{c}(t) + (-i\omega)\int_{t_0}^{t} e^{-i\omega(t-t')}\hat{c}(t')\, dt'\right) \\
&= -i\omega e^{-i\omega(t-t_0)}\hat{b}_0(\omega) - i\omega\kappa(\omega)\int_{t_0}^{t} e^{-i\omega(t-t')}\hat{c}(t')\, dt' + \kappa(\omega)\hat{c}(t) \\
&= -i\omega\hat{b}(\omega) + \kappa(\omega)\hat{c}(t).
\end{aligned}$$

Thus, we have shown that (3.5) is a solution to (3.3).

We derive $\hat{b}(\omega)^\dagger$:

$$\hat{b}(\omega)^\dagger = e^{i\omega(t-t_0)}\hat{b}_0(\omega)^\dagger + \kappa^*(\omega)\int_{t_0}^{t} e^{i\omega(t-t')}\hat{c}(t')^\dagger\, dt'. \qquad (3.6)$$

Starting from (3.4) and substituting (3.5) and (3.6), we have:

$$
\begin{aligned}
\dot{\hat{a}} &= -\frac{i}{\hbar}\left[\hat{a}, \hat{H}_{\text{sys}}\right] + \int d\omega\, \kappa(\omega) \left\{\hat{b}^\dagger(\omega)\left[\hat{a}, \hat{c}\right] - \left[\hat{a}, \hat{c}^\dagger\right]\hat{b}(\omega)\right\} \\
&= -\frac{i}{\hbar}\left[\hat{a}, \hat{H}_{\text{sys}}\right] \\
&\quad + \int d\omega\, \kappa(\omega) \left(e^{i\omega(t-t_0)}\hat{b}_0^\dagger(\omega) + \kappa^*(\omega)\int_{t_0}^{t} e^{i\omega(t-t')}\hat{c}(t')^\dagger\, dt'\right)\left[\hat{a}, \hat{c}\right] \\
&\quad - \int d\omega\, \kappa(\omega) \left(e^{-i\omega(t-t_0)}\hat{b}_0(\omega) + \kappa(\omega)\int_{t_0}^{t} e^{-i\omega(t-t')}\hat{c}(t')\, dt'\right)\left[\hat{a}, \hat{c}^\dagger\right] \\
&= -\frac{i}{\hbar}\left[\hat{a}, \hat{H}_{\text{sys}}\right] \\
&\quad + \int d\omega\, \kappa(\omega) \left\{e^{i\omega(t-t_0)}\hat{b}_0^\dagger(\omega)\left[\hat{a}, \hat{c}\right] - \left[\hat{a}, \hat{c}^\dagger\right] e^{-i\omega(t-t_0)}\hat{b}_0(\omega)\right\} \\
&\quad + \int d\omega\, \kappa(\omega) \left\{\kappa^*(\omega)\int_{t_0}^{t} dt' \left(e^{i\omega(t-t')}\right)\hat{c}^\dagger(t')\left[\hat{a}, \hat{c}\right] - \left[\hat{a}, \hat{c}^\dagger\right]\kappa(\omega)\int_{t_0}^{t} dt' \left(e^{-i\omega(t-t')}\right)\hat{c}(t')\right\} \\
&= -\frac{i}{\hbar}\left[\hat{a}, \hat{H}_{\text{sys}}\right] \\
&\quad + \int d\omega\, \kappa(\omega) \left\{e^{i\omega(t-t_0)}\hat{b}^\dagger(\omega)\left[\hat{a}, \hat{c}\right] - \left[\hat{a}, \hat{c}^\dagger\right] e^{-i\omega(t-t_0)}\hat{b}_0(\omega)\right\} \\
&\quad + \int d\omega\, [\kappa(\omega)]^2 \int_{t_0}^{t} dt' \left\{e^{i\omega(t-t')}\hat{c}^\dagger(t')\left[\hat{a}, \hat{c}\right] - \left[\hat{a}, \hat{c}^\dagger\right] e^{-i\omega(t-t')}\hat{c}(t')\right\}.
\end{aligned}
$$

We introduce the first Markov approximation, which consists in the frequency independency of the coupling constant:

$$\kappa(\omega) = \sqrt{\gamma/2\pi}\,. \tag{3.7}$$

Here, two properties we will use:

$$\int_{-\infty}^{\infty} d\omega\, e^{-i\omega(t-t')} = 2\pi\delta(t-t'), \tag{3.8}$$

$$\int_{t_0}^{t} \hat{c}(t')\delta(t-t')\, dt' = \frac{1}{2}\hat{c}(t). \tag{3.9}$$

We also define an *in* field by

$$\hat{b}_{\text{in}}(t) = \frac{1}{\sqrt{2\pi}}\int d\omega\, e^{-i\omega(t-t_0)}\hat{b}_0(\omega), \tag{3.10}$$

which satisfies the commutation relation:

$$[\hat{b}_{\text{in}}(t), \hat{b}_{\text{in}}^\dagger(t')] = \delta(t-t'). \tag{3.11}$$

Using (3.8) - (3.10), we derive the quantum Langevin equation:

$$\begin{aligned}
\dot{\hat{a}} &= -\frac{i}{\hbar}\left[\hat{a}, \hat{H}_{\text{sys}}\right] \\
&\quad + \int_{-\infty}^{\infty} d\omega\, \kappa(\omega) \left\{ e^{i\omega(t-t_0)} \hat{b}^\dagger(\omega)[\hat{a}, \hat{c}] - [\hat{a}, \hat{c}^\dagger] e^{-i\omega(t-t_0)} \hat{b}_0(\omega) \right\} \\
&\quad + \int_{-\infty}^{\infty} d\omega\, [\kappa(\omega)]^2 \int_{t_0}^{t} dt' \left\{ e^{i\omega(t-t')} \hat{c}^\dagger(t')[\hat{a}, \hat{c}] - [\hat{a}, \hat{c}^\dagger] e^{-i\omega(t-t')} \hat{c}(t') \right\} \\
&= -\frac{i}{\hbar}\left[\hat{a}, \hat{H}_{\text{sys}}\right] \\
&\quad + \int_{-\infty}^{\infty} d\omega\, \frac{1}{\sqrt{2\pi}} \sqrt{\gamma}\, e^{i\omega(t-t_0)} \hat{b}^\dagger(\omega)[\hat{a}, \hat{c}] - \int_{-\infty}^{\infty} d\omega\, \frac{1}{\sqrt{2\pi}} \sqrt{\gamma}\, [\hat{a}, \hat{c}^\dagger] e^{-i\omega(t-t_0)} \hat{b}_0(\omega) \\
&\quad + \int_{-\infty}^{\infty} d\omega\, \frac{\gamma}{2\pi} \int_{t_0}^{t} dt' e^{i\omega(t-t')} \hat{c}^\dagger(t')[\hat{a}, \hat{c}] - \int_{-\infty}^{\infty} d\omega\, \frac{\gamma}{2\pi} \int_{t_0}^{t} dt' [\hat{a}, \hat{c}^\dagger] e^{-i\omega(t-t')} \hat{c}(t') \\
&= -\frac{i}{\hbar}\left[\hat{a}, \hat{H}_{\text{sys}}\right] \\
&\quad + \sqrt{\gamma}\, \hat{b}^\dagger_{\text{in}}(t)[\hat{a}, \hat{c}] - [\hat{a}, \hat{c}^\dagger] \sqrt{\gamma}\, \hat{b}_{\text{in}}(t) \\
&\quad + 2\pi\delta(t-t') \cdot \frac{\gamma}{2\pi} \int_{t_0}^{t} dt'\, \hat{c}^\dagger(t')[\hat{a}, \hat{c}] - 2\pi\delta(t-t') \cdot \frac{\gamma}{2\pi} \int_{t_0}^{t} dt'\, [\hat{a}, \hat{c}^\dagger]\, \hat{c}(t') \\
&= -\frac{i}{\hbar}\left[\hat{a}, \hat{H}_{\text{sys}}\right] + \sqrt{\gamma}\, \hat{b}^\dagger_{\text{in}}(t)[\hat{a}, \hat{c}] - [\hat{a}, \hat{c}^\dagger] \sqrt{\gamma}\, \hat{b}_{\text{in}}(t) + \frac{\gamma}{2} \hat{c}^\dagger [\hat{a}, \hat{c}] - [\hat{a}, \hat{c}^\dagger] \frac{\gamma}{2} \hat{c} \\
&= -\frac{i}{\hbar}\left[\hat{a}, \hat{H}_{\text{sys}}\right] - \left[\left[\hat{a}, \hat{c}^\dagger\right] \left(\frac{\gamma}{2} \hat{c} + \sqrt{\gamma}\, \hat{b}_{\text{in}}(t) \right) - \left(\frac{\gamma}{2} \hat{c}^\dagger + \sqrt{\gamma}\, \hat{b}^\dagger_{\text{in}}(t) \right) [\hat{a}, \hat{c}] \right].
\end{aligned}$$

Thus, the evolution of an arbitrary system operator $\hat{O}$ is given by the Markovian Quantum Langevin Equation (MQLE):

$$\dot{\hat{O}} = \frac{1}{i\hbar}\left[\hat{O}, \hat{H}_{\text{sys}}\right] - \left[\left[\hat{O}, \hat{a}^\dagger\right] \left(\frac{\gamma}{2} \hat{a} + \sqrt{\gamma}\, \hat{b}_{\text{in}}(t) \right) - \left(\frac{\gamma}{2} \hat{a}^\dagger + \sqrt{\gamma}\, \hat{b}^\dagger_{\text{in}}(t) \right) \left[\hat{O}, \hat{a}\right] \right]. \quad (3.12)$$

The terms proportional to γ are damping terms. Damping arises from the interaction of the system with the heat bath.

The terms depending on $\hat{b}_{\text{in}}(t)$ are to be taken as noise terms. However, they can only be interpreted as noise when the state of $\hat{b}_{\text{in}}(t)$ is incoherent, i.e. a thermal state. The case where $\hat{b}_{\text{in}}(t)$ is in a coherent state would represent a coherent driving field applied to the system (e.g. a pumping laser).

To be noticed, the existence of damping terms has nothing to do with the state of the bath - damping will occur even in a presence of a coherent driving field.

3.2 Standard Optomechanical Setup

In this section we recall the basic aspects of cavity-optomechanical systems. Much more about this topic can be found in standard papers [1] and textbooks [5].

We describe the standard optomechanical setup, which is the basis for the study of quantum optomechanics. Optomechanics refers to the study of the interaction between light and mechanical vibrations. We model the system and describe the interaction between the light field and the mechanical oscillator.

The standard optomechanical setup consists of a Fabry-Pérot cavity with one of its mirrors mounted on a mechanical oscillator [9]. The radiation mode is a standing mode of the cavity, of frequency ω_{cav}, which is driven by a laser at frequency ω_{las} through a semi-transparent mirror. The light field inside the cavity interacts with the mechanical oscillator.

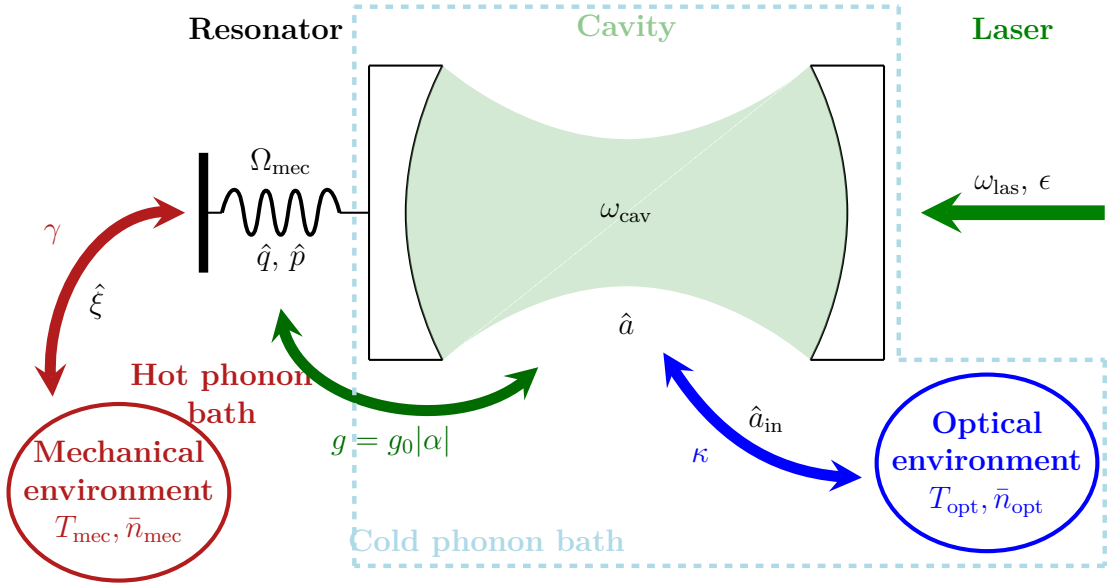

Figure 3.1: Standard optomechanical setup: a cavity with a moving-end mirror is driven by a laser. The mechanical resonator is in contact with a phonon reservoir at temperature T_{mec} and the cavity with a photon reservoir at temperature T_{opt}.

The thermodynamic system to be cooled consists of a mechanical resonator, which needs to have heat removed from it. This resonator is in contact with a hot phonon bath, causing the resonator to experience Brownian motion. Additionally, there is a photon bath characterized by the noise properties of the light field. This photon bath appears cold because its temperature is much lower than the energy scale of the photons. The photon bath interacts with the mechanical degrees of freedom through the driven optomechanical cavity (see Fig. 3.1).

Due to the large disparity in orders of magnitude between the mechanical and optical frequencies, the following inequality holds:

$$\hbar\Omega_{\text{mec}} \ll k_B T \ll \hbar\omega_{\text{cav}}. \tag{3.13}$$

The mean photon number of the optical environment is given by

$$\bar{n}_{\text{opt}}(\omega_{\text{cav}}) = \frac{1}{e^{\hbar\omega_{\text{cav}}/k_B T} - 1} \approx 0 \tag{3.14}$$

and the mean phonon number of the mechanical bath is given by

$$\bar{n}_{\mathrm{mec}}(\Omega_{\mathrm{mec}}) = \frac{1}{e^{\hbar\Omega_{\mathrm{mec}}/k_B T} - 1} \gg \bar{n}_{\mathrm{opt}}(\omega_{\mathrm{cav}}). \tag{3.15}$$

Due to 3.15, the effective temperature T_{mec} of the mechanical environment is much higher than the effective temperature T_{opt} of the optical environment. Therefore, unlike in conventional refrigerators, heat flows from the hot reservoir to the cold reservoir.

We model the cavity with a cavity mode of frequency ω_{cav} and annihilation operator $\hat{a}$ and the mechanical resonator with a mechanical mode of frequency Ω_{mec} and annihilation operator $\hat{b}$. The hamiltonian of the system is given by

$$\hat{H} = \hat{H}_{\mathrm{cavity}} + \hat{H}_{\mathrm{resonator}} + \hat{H}_{\mathrm{coupling}} + \hat{H}_{\mathrm{drive}},$$

where

- $\hat{H}_{\mathrm{cavity}} = \hbar\omega_{\mathrm{cav}}\hat{a}^\dagger\hat{a}$;
- $\hat{H}_{\mathrm{resonator}} = \hbar\Omega_{\mathrm{mec}}\hat{b}^\dagger\hat{b}$;
- $\hat{H}_{\mathrm{drive}} = \hbar(\epsilon\hat{a}^\dagger e^{-i\omega_p t} + \epsilon^*\hat{a}e^{i\omega_p t})$, where $|\epsilon|^2 = \frac{2\kappa P_{\mathrm{las}}}{\hbar\omega_{\mathrm{las}}}$.

The cavity modes are determined by the standing-wave-condition from electromagnetism [6]:

$$\omega_{\mathrm{cav}} = \frac{n\pi c}{L}, \tag{3.16}$$

c being the speed of light and L the length of the cavity.

However, the cavity mode couples to the mechanical resonator due to the radiation pressure of the light field and the moving-end mirror undergoes a displacement $\hat{q}$ and a momentum $\hat{p}$. Writing $L = L_0 + \hat{q}$ and considering only the first cavity mode in (3.16), we have

$$\begin{aligned}
\omega_{\mathrm{cav}} &= \frac{1 \cdot \pi c}{L_0 + \hat{q}} \\
&= \frac{\pi c}{L_0(1 + \frac{\hat{q}}{L_0})} \\
&= \frac{\pi c}{L_0} \cdot \frac{1}{1 + \frac{\hat{q}}{L_0}} \\
&\approx \frac{\pi c}{L_0}\left(1 - \frac{\hat{q}}{L_0}\right)
\end{aligned}$$

Thus, the cavity mode frequency depends on the position of the mirror:

$$\omega_{\mathrm{cav}}(\hat{q}) = \omega_{\mathrm{cav}} - \frac{\omega_{\mathrm{cav}}}{L_0}\hat{q}. \tag{3.17}$$

We therefore have a coupling between the number of photons $\hat{a}^\dagger\hat{a}$ and $\hat{q}$. This is called the radiation-pressure coupling. The periodic modulation of the cavity length gives rise to the optomechanical term. We define the single-photon-optomechanical-coupling strength as

$$g_0 = \frac{\delta\omega_{\mathrm{cav}}}{\delta x}|_{x=L_0}. \tag{3.18}$$

The single-photon-optomechanical-coupling strength is one of the central parameters in the field of quantum optomechanics [7]. From the point of view of the cavity field, for any cavity optomechanical geometry, the optomechanical coupling strength quantifies the linear dispersive shift in the optical resonance frequency induced by a mechanical displacement equal to the mechanical zero-point motion.

The system is described in the rotating frame of the laser frequency ω_{las},

$$\hat{H} = \hbar\Delta_0\hat{a}^\dagger\hat{a} + \hbar\Omega_{\mathrm{mec}}\hat{b}^\dagger\hat{b} - \hbar g_0\hat{a}^\dagger\hat{a}(\hat{b} + \hat{b}^\dagger) + \hbar(\epsilon\hat{a}^\dagger + \epsilon^*\hat{a}). \tag{3.19}$$

Thinking about it, a term such as $-fQ$ in a hamiltonian means a force f pushing the coordinate $\hat{q}$. This is exactly what we have here, except that now the force actually depends on the number of photons inside the cavity. The more photons we have, the more we push the mirror.

3.3 Sideband Cooling

We want to recall the concept of sideband cooling, which is a technique used to cool down the mechanical resonator to its ground state. This phenomenon is based on the light-matter interaction.

When photons are scattered by a material, most of them are elastically scattered (Rayleigh scattering), such that the scattered photons have the same energy as the incident photons. A smaller fraction of the scattered photons can be scattered inelastically (Raman scattering), with the scattered photons having an energy different from those of the incident photons. Because of conservation of energy, the material either gains or loses energy in the process.

Raman scattering is conceptualized as involving a virtual electronic energy level which corresponds to the energy of the exciting laser photons (see Fig. 3.2). Absorption of a photon excites the molecule to the imaginary state and re-emission leads to Raman or Rayleigh scattering. In both cases, the final state has the same electronic energy as the initial state but is higher in vibrational energy in the case of Stokes Raman scattering, lower in the case of anti-Stokes Raman scattering or the same in the case of Rayleigh scattering.

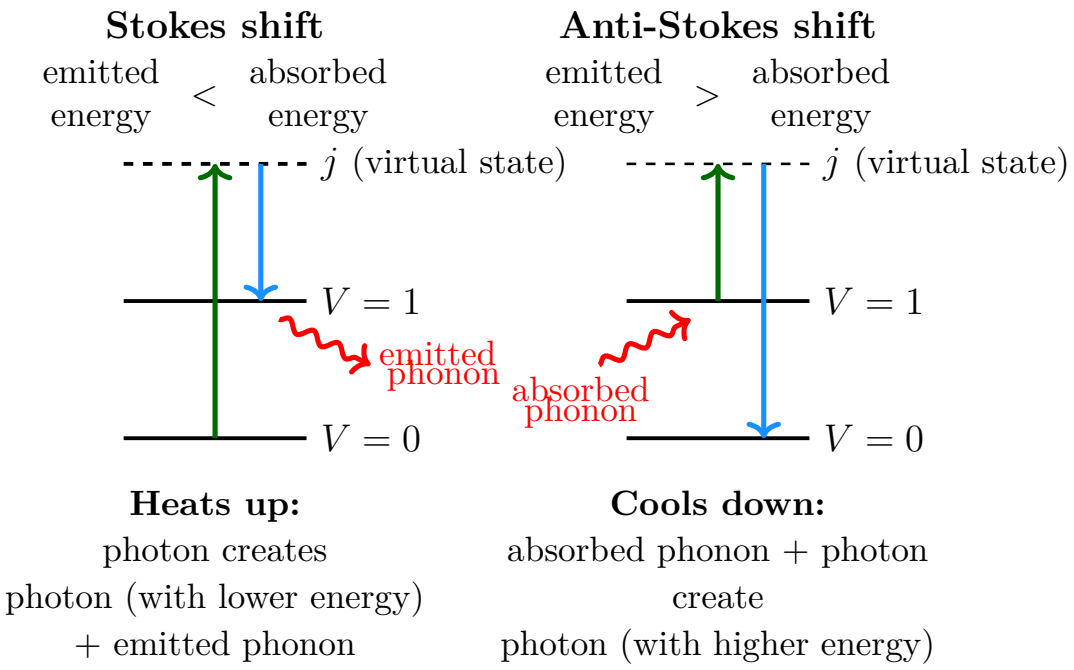

Figure 3.2: Raman-scattering picture: *On the left side*, a photon (green arrow) interacts with a molecule initially in the ground vibrational state ($V = 0$). The photon is absorbed and raises the molecule to a virtual energy state j. The molecule then relaxes to a higher vibrational state ($V = 1$), emitting a photon with less energy (blue arrow) than the absorbed one. This results in a scattered photon with a longer wavelength (lower energy) and is characterized by the emission of a phonon, effectively heating up the system. *On the right side*, the molecule starts in an excited vibrational state ($V = 1$). An incident photon (green arrow) excites the molecule to the virtual state j but the molecule then relaxes back to the ground state ($V = 0$), emitting a photon with higher energy (blue arrow) than the absorbed one. This scattered photon comes from the combination of the absorbed photon energy and the energy released as the molecule transitions to a lower vibrational state.

We can describe the cooling of a mechanical resonator in thermodynamical terms.
Due to the radiation pressure, the resonnator is coupled to the cavity mode and the cavity behaves as an additional reservoir for the resonator. As a consequence, the effective temperature of the mechanical mode will be intermediate between the temperature of the mechanical environment and the temperature of the optical environment, wich is almost zero (see Eq. 3.14). Therefore, mechanical ground-state cooling can be approached when the coupling rate g_0 between the cavity and the mechanical mode is larger than the damping rate γ of the mechanical mode.

Considering the resolved-sideband regime, that is $\kappa \ll \Omega_{\mathrm{mec}}$, we can sketch the principle of sideband cooling. In this regime, as illustrated by Fig. 3.3, three processes can occur:

- A photon from the laser can be absorbed by the cavity without changing the state of the resonator (in orange) ;
- A photon from the laser can create a photon in the cavity at lower frequency $\omega_{\text{las}} - \Omega_{\text{mec}}$ and a phonon (Stokes process, in magenta) ;
- A photon from the laser can, in combination with a phonon, create a photon at higher frequency $\omega_{\text{las}} + \Omega_{\text{mec}}$ (Anti-Stokes process, in blue).

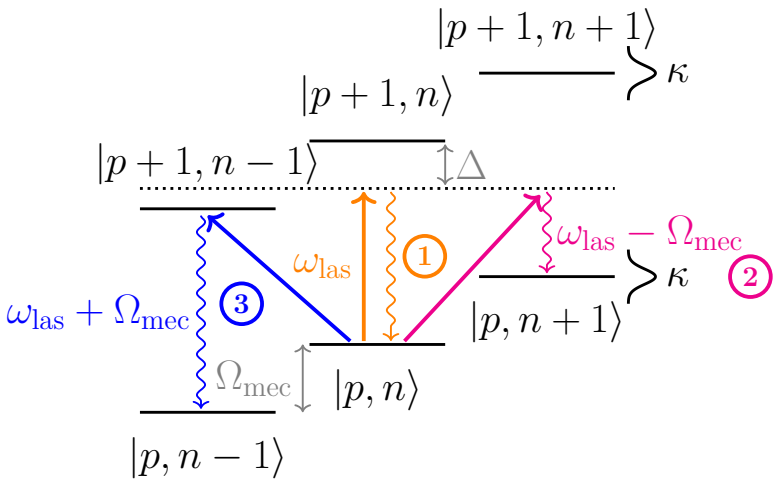

Figure 3.3: Principle of resolved-sideband cooling in the weak coupling limit in a Raman-scattering picture. The state $|p, n\rangle$ is described by p phonons and n photons.

Sideband-cooling is a technique based on the inelastic scattering of photons by the mechanical resonator. Thus, by choosing a cavity-laser detuning close to the mechanical frequency, the rates of the first two processes can be reduced, allowing effective cooling (see Fig. 3.4).

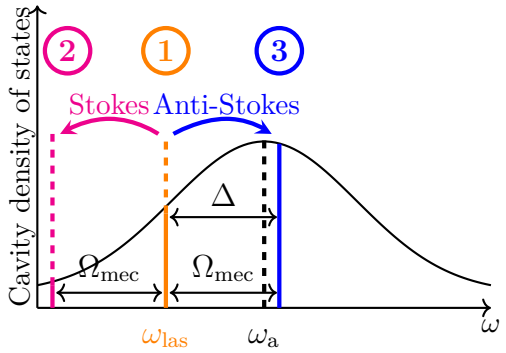

Figure 3.4: Cavity density of states. Δ is the effective detuning between the laser frequency (orange line) and the cavity resonance frequency (dashed black line), which is shifted with respect to Δ_0 by the optomechanical interaction (see 4.1.4).

4

Project

The project consists of two main parts: the theoretical study of the Fano-membrane-in-the-middle setup and the numerical simulations. The theoretical study aims to develop a model of the Fano-membrane-in-the-middle setup and to optimize its parameters to achieve ground-state cooling. The numerical simulations aim to validate the theoretical model. We aim to study the new Fano-membrane-in-the-middle setup with respect to already investigated setups to further understand the properties of the so-called Fano-membrane.

4.1 Membrane-in-the-middle + Fano-mode Setup

4.1.1 Motivation

4.1.1.1 Resolved and unresolved-sideband Regimes

In order to enhance the cooling of the mechanical resonnator, cooling rate should be higher than heating rate, that means Anti-Stokes process should be dominant over Stokes process. To do so, the cavity should be detuned from the laser frequency by the mechanical frequency and the cavity linewidth narrow enough to enhance Anti-Stokes process (see Fig. 4.1). The latter condition is the so-called resolved-sideband regime, defined by

$$\kappa \ll \Omega_{\mathrm{mec}}. \tag{4.1}$$

In the unresolved-sideband regime, Eq. (4.1) is not met and the cavity linewidth is larger than the mechanical frequency. This condition leads to an equal probability of the Stokes and Anti-Stokes processes, which is not favorable for cooling. Cooling is achieved by making the difference between the Anti-Stokes and Stokes processes as large as possible, that means placing the laser frequency at the most steeped left-part of the cavity density of states. We thus optimize sideband cooling regime.

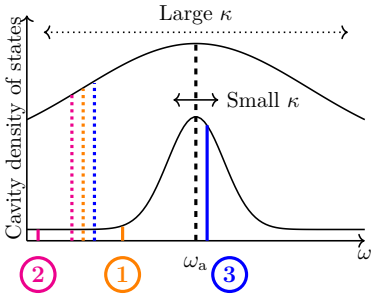

Figure 4.1: Cavity density of states. When the cavity linewidth is small enough with respect to the mechanical frequency, the system is in the resolved-sideband regime: Anti-Stokes process (blue line) is dominant over Stokes process (magenta line). On the contrary, when the cavity linewidth is large with respect to the mechanical frequency, the system is in the unresolved-sideband regime: Anti-Stokes and Stokes processes have equal probability (magenta and blue dashed lines).

4.1.1.2 Fano-membrane

A strategy to improve the optomechanical cooling is to make the density of states asymetric and narrower to further suppress the detrimental Stokes process (see Fig. 4.2). This can be achieved by adding a Fano-membrane [3] to the optomechanical system.

A Fano-membrane is a photonic crystal exhibiting a periodic dielectric structure that affects the propagation of electromagnetic waves. The interference between the discrete localized mode of the crystal and the broad continuum of states of the optical cavity creates an asymmetric line shape, known as Fano resonance. In particular, linewidth narrowing is one of the feature exhibited by photonic crystals [10], which is not accessible by conventional mirrors.

Introducing an auxiliary quantum mode and engineering its interaction with the optomechanical system is a possibility to cool down a system that is originally in the unresolved-sideband regime.

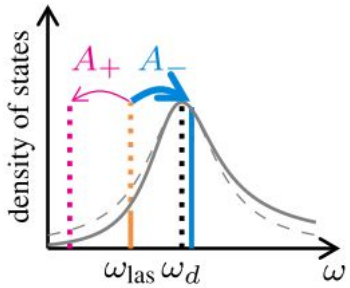

Figure 4.2: Cavity density of states (solid gray line) which is asymmetrical in a Fano-membrane setup. The dashed gray line represents the density of states of a standard cavity of equivalent linewidth. The Stokes and Anti-Stokes processes are represented by the magenta and cyan arrows, respectively (from [9]).

Thus, the most intriguing feature of the optomechanical system with a Fano-membrane is the presence of a optical-normal-mode resonance which has a very narrow linewidth, compared with the original linewidth of both the pure cavity and the Fano-membrane mode. This optical-normal-mode resonance, arising from pure interference effects, is a key feature of all Fano-membrane based optomechanical setups and will be further discussed in Sec. 4.2.

4.1.1.3 Different Fano-membrane-based Optomechanical Setups

The special property of optical-normal-mode resonance has been investigated in an optomechanical system where the left-hand side mirror of a cavity is replaced by a Fano-mirror [9, 8, 4]. This latter left-hand-side-Fano-mirror setup will serve as a reference for comparison with the setup we aim to study in this thesis, the Fano-membrane-in-the-middle setup. Sec. 4.2 will offer a detailed overview of the two different setups.

4.1.2 Setup

4.1.2.1 Fano-membrane in the middle of the Cavity

We describe the Fano-membrane-in-the-middle setup. This optomechanical system consists of an optical cavity with non-moving mirrors and a Fano-membrane placed in the middle. The Fano-membrane acts as the mechanical resonator.

We consider a single optical mode of frequency ω_{cav}, associated with the photon annihilation operator $\hat{a}$. A single harmonic mechanical mode of frequency Ω_{mec} is associated with the Fano-membrane with dimensionless position $\hat{p}$ and momentum $\hat{q}$ and an additional optical Fano-membrane mode of frequency ω_d, arising from the property of the Fano-membrane, is associated with the latter with annihilation operator $\hat{d}$.

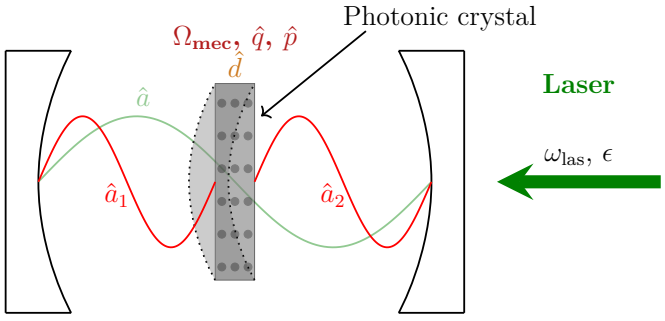

Figure 4.3: Cavity with Fano-membrane in the middle. In comparison with the standard optomechanical setup, the sides of the cavity are fixed and the Fano-membrane itself acts as the mechanical resonator. Thus, the Fano-membrane is associated with the mechanical and optical modes $\hat{q}$ and $\hat{d}$, respectively. The small reflectivity of the Fano-membrane allows the existence of a single cavity mode $\hat{a}$ (in green), whereas, in the opposite case, the cavity would support two different modes, $\hat{a}_1$ and $\hat{a}_2$ (in red).

4.1.2.2 Optomechanical Interactions

We model the interactions of the system with the different environments as follows:

- The cavity mode is coupled to the electromagnetic environments on both sides of the cavity, with loss rate κ_L for the left-hand side mirror and κ_R for the right-hand side one ;
- The mechanical mode of the Fano-membrane exhibits a loss rate γ ;
- The Fano-membrane mode is coupled to the Fano-membrane itself with loss rate κ_d.

The Fano-membrane being in the middle of the optical cavity, it is not coupled to the electromagnetic environment outside of the cavity. This is a key feature of the Fano-membrane-in-the-middle setup and it will be further compared in Sec. 4.2 with the already investigated left-hand-side-Fano-mirror setup, developped in [9, 8, 4].

The couplings between the different modes are defined as follows:

- The cavity mode coherently interacts with the Fano-membrane mode due to the overlap of their electric fields, with coupling strength λ ;
- The cavity mode interacts with the mechanical mode due to the radiation pressure, with single-photon-optomechanical coupling strength g_a^0 ;
- The Fano-membrane mode interacts with the mechanical mode due to the radiation pressure, with single-photon-optomechanical coupling strength g_d^0.

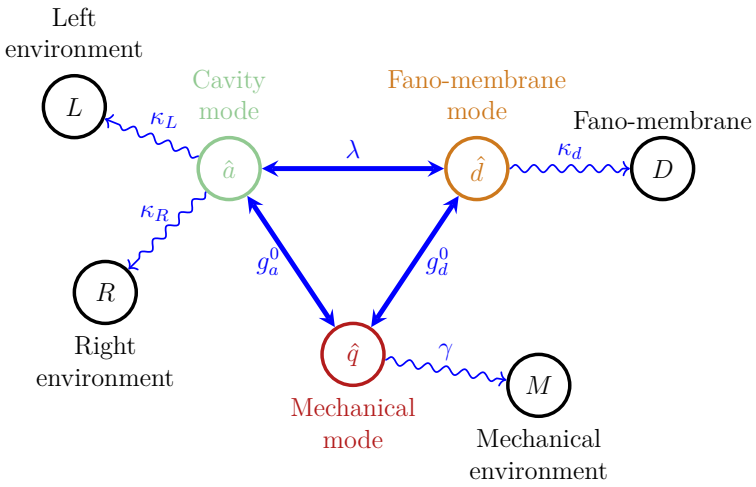

Figure 4.4: Sketch of the interactions among the modes. The mechanical and cavity modes are coupled through the radiation pressure, while the Fano-mirror and cavity modes are coupled through the overlap of their electromagnetic fields.

We assume that the optical cavity is driven by a laser with frequency ω_{las} and amplitude ϵ. The pumping amplitude

$$\epsilon = \sqrt{2\kappa_R P_{\text{las}}/(\hbar\omega_{\text{las}})} \tag{4.2}$$

(assumed to be real without loss of generality) is related to the power P_{las} of the pumping field and the loss rate κ_R (laser applied on the right-hand external side of the cavity).

4.1.2.3 Fluctuations Processes

The dynamics of the system are also determined by the fluctuation processes affecting the mechanical mode and the two optical modes. The mechanical mode is affected by a Brownian noise term $\hat{\xi}$ that obeys, in the white-noise approximation, the correlation function

$$\langle\hat{\xi}(t)\hat{\xi}(t')\rangle = (2\bar{n}_{\text{mec}} + 1)\delta(t - t'), \tag{4.3}$$

where $\bar{n}_{\text{mec}}$ is the mean phonon number, as in 3.15. The cavity mode is affected by the vacuum noise terms $\hat{a}_{\text{in,L}}$ and $\hat{a}_{\text{in,R}}$ associated with the left and right environments, respectively and whose correlation functions are given by

$$\langle\hat{a}_{\text{in,L,R}}(t)\hat{a}^{\dagger}_{\text{in,L,R}}(t')\rangle = (\bar{n}_{\text{opt}}(\omega_{\text{cav}}) + 1)\delta(t - t'), \tag{4.4}$$

and

$$\langle\hat{a}^{\dagger}_{\text{in,L,R}}(t)\hat{a}_{\text{in,L,R}}(t')\rangle = (\bar{n}_{\text{opt}}(\omega_{\text{cav}}))\delta(t - t'). \tag{4.5}$$

At optical frequencies, $\bar{n}_{\text{opt}}(\omega_{\text{cav}}) \approx 0$, so that only the correlation function of (4.4) is relevant. The Fano-membrane mode is affected by the vacuum noise term $\hat{d}_{\text{in}}$ whose correlation functions follow the same form as (4.4) and (4.5).

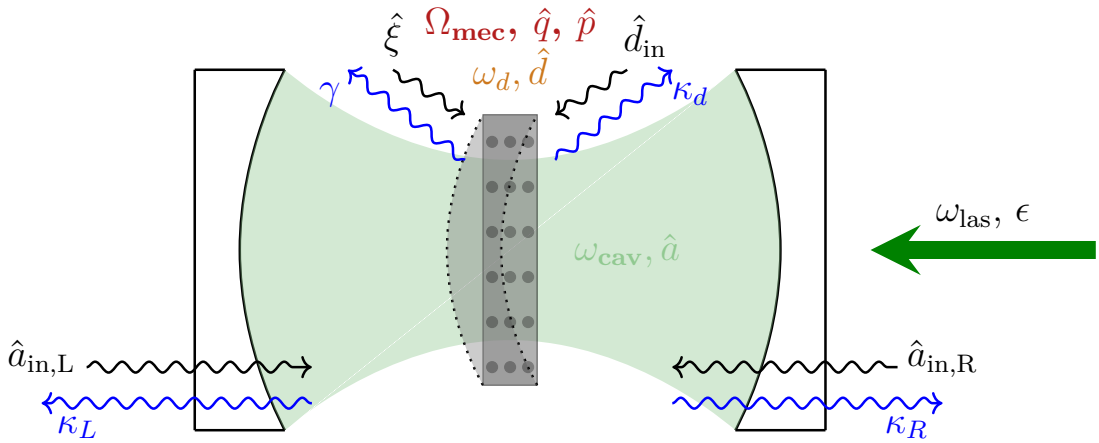

Figure 4.5: Inputs and outputs in the damped-optomechanical-Fano-membrane-in-the-middle system.

4.1.3 Derivation of the Langevin Equations

4.1.3.1 Construction of the Hamiltonian of the System

In order to fully describe the dynamics of the system with its hamiltonian, we need to build the interaction term between the cavity mode and the Fano-membrane mode. The general expression for an interaction term between two modes $\hat{O}_a$ and $\hat{O}_b$ is

$$g\hat{O}_a\hat{O}_b, \tag{4.6}$$

where g is the coupling strength. In our case, the interaction term reads

$$\begin{aligned} &\lambda\left(\hat{a}+\hat{a}^\dagger\right)\left(\hat{d}+\hat{d}^\dagger\right) \\ &= \lambda\left(\hat{a}\hat{d}+\hat{a}\hat{d}^\dagger+\hat{a}^\dagger\hat{d}+\hat{a}^\dagger\hat{d}^\dagger\right). \end{aligned} \tag{4.7}$$

The $\hat{a}\hat{d}$ and $\hat{a}^\dagger\hat{d}^\dagger$ terms correspond to the anhillation and the creation respectively of two photons both in the cavity and the Fano-membrane mode. Due to the small probability of having two photons in the cavity and the Fano-membrane mode, these terms are not considered in the interaction term. An alternative way to justify this assumption is by considering the optomechanical energy level diagram in Fig. 3.3. The scattering processes described by $\hat{a}\hat{d}$ and $\hat{a}^\dagger\hat{d}^\dagger$ are off-resonance and therefore suppressed if the system is in the resolved-sideband regime ($\kappa \ll \Omega_{\mathrm{mec}}$).

The interaction term writes finally as

$$\lambda\left(\hat{a}\hat{d}^\dagger+\hat{a}^\dagger\hat{d}\right). \tag{4.8}$$

We can write the hamiltonian of the Fano-membrane-in-the-middle setup, in the rotating frame at ω_{las},

$$\begin{aligned} \hat{H}_{\mathrm{Sys}} = &\hbar\Delta_a^0\hat{a}^\dagger\hat{a}+\hbar\Delta_d^0\hat{d}^\dagger\hat{d}+\hbar\Omega_{\mathrm{mec}}\hat{b}^\dagger\hat{b} \\ &-\hbar g_a^0\sqrt{2}\,\hat{a}^\dagger\hat{a}\hat{q}-\hbar g_d^0\sqrt{2}\,\hat{d}^\dagger\hat{d}\hat{q} \\ &+\hbar\lambda(\hat{a}^\dagger\hat{d}+\hat{d}^\dagger\hat{a})+\hbar(\epsilon\hat{a}^\dagger+\epsilon^*\hat{a}), \end{aligned} \tag{4.9}$$

where

- $\hbar\Delta_a^0\hat{a}^\dagger\hat{a}$, $\hbar\Delta_d^0\hat{d}^\dagger\hat{d}$ and $\hbar\Omega_{\mathrm{mec}}\hat{b}^\dagger\hat{b}$ are the energies of the cavity, the Fano-membrane mode and the mechanical mode, respectively ;
- $-\hbar g_a^0\sqrt{2}\,\hat{a}^\dagger\hat{a}\hat{q}$ and $-\hbar g_d^0\sqrt{2}\,\hat{d}^\dagger\hat{d}\hat{q}$ are the radiation pressure terms ;
- $\hbar\lambda(\hat{a}^\dagger\hat{d}+\hat{d}^\dagger\hat{a})$ is the interaction term between the cavity and the Fano-membrane mode ;
- $\hbar(\epsilon\hat{a}^\dagger+\epsilon^*\hat{a})$ is the pumping term.

4.1.3.2 Dynamics

We recall the idea of modelling open-system dynamics via quantum Langevin equations. The essential idea is to couple the system to a bath consisting of a large number (eventually infinite) of harmonic oscillators. In this way, the system dynamics may be substantially affected by the presence of the bath, while the effect of the system on each individual bath oscillator remains negligible. It is then possible to derive equations describing the system dynamics, without the requirement of also solving for the dynamics of the bath [7].

For a general mechanical observable $\hat{O}$, within the first Markov approximation, the quantum Langevin equation reads

$$\dot{\hat{O}} = \frac{1}{i\hbar}\left[\hat{O}, \hat{H}_{\text{sys}}\right] + i\sqrt{\gamma}\left[\hat{O}, \hat{q}\right]\hat{\xi}(t) + \frac{1}{2iQ}\left\{\left[\hat{O}, \hat{q}\right], \dot{\hat{q}}(t)\right\}_{+}, \quad Q = \frac{\Omega_{\text{mec}}}{\gamma}. \tag{4.10}$$

For the optical variables, we recall (3.12), generelazing the notion of dissipative term due to several environments:

$$\dot{\hat{O}} = \underbrace{\frac{1}{i\hbar}[\hat{O}, \hat{H}_{\text{sys}}]}_{\text{System}} \underbrace{- \sum_{\substack{\mu, \text{ all the} \\ \text{environments}}} \left([\hat{O}, \hat{c}_\mu^\dagger]\left(\kappa_\mu\, \hat{c}_\mu + \sqrt{2\,\kappa_\mu}\, \hat{b}_{\text{in},\mu}(t)\right) - \left(\kappa_\mu\, \hat{c}_\mu^\dagger + \sqrt{2\,\kappa_\mu}\, \hat{b}_{\text{in},\mu}^\dagger(t)\right)[\hat{O}, \hat{c}_\mu] \right)}_{\text{Dissipation}} \tag{4.11}$$

Optical environment, μ	Coupled optical mode, $\hat{c}_\mu$	External interaction term, κ_μ
L	$\hat{a}$	κ_L
R	$\hat{a}$	κ_R
D	$\hat{d}$	κ_d

Table 4.1: MQLE parameters for optical variables. For each optical mode, the MQLE takes into account the different optical environments and their corresponding dissipative external interaction terms.

The evolution of the Fano-membrane-in-the-middle system can be described with a set of MQLE:

$$\dot{\hat{a}} = -\left(i\Delta_a^0 + \kappa\right)\hat{a} + ig_a^0\sqrt{2}\,\hat{q}\hat{a} - i\lambda\hat{d} - i\epsilon - \sqrt{2\kappa_L}\,\hat{a}_{\text{in},L}(t) - \sqrt{2\kappa_R}\,\hat{a}_{\text{in},R}(t), \tag{4.12}$$

$$\dot{\hat{d}} = -\left(i\Delta_d^0 + \kappa_d\right)\hat{d} + ig_d^0\sqrt{2}\,\hat{q}\hat{d} - i\lambda\hat{a} - \sqrt{2\kappa_d}\,\hat{d}_{\text{in}}(t), \tag{4.13}$$

$$\dot{\hat{q}} = \Omega_{\text{mec}}\hat{p}, \tag{4.14}$$

$$\dot{\hat{p}} = -\Omega_{\text{mec}}\hat{q} - \gamma\,\hat{p} + g_a^0\sqrt{2}\,\hat{a}^\dagger\hat{a} + g_d^0\sqrt{2}\,\hat{d}^\dagger\hat{d} + \sqrt{\gamma}\,\hat{\xi}(t), \tag{4.15}$$

where we have defined the bare detunings:

$$\Delta_a^0 = \omega_{\text{cav}} - \omega_{\text{las}}, \tag{4.16}$$
$$\Delta_d^0 = \omega_d - \omega_{\text{las}}, \tag{4.17}$$

and

$$\kappa = \kappa_L + \kappa_R. \tag{4.18}$$

A detailled derivation of the Fano-membrane-in-the-middle-system MQLE can be found in Appendix B, Sec. B.1.

4.1.4 Linearization of the Langevin Equations

4.1.4.1 Mean-field Approximation

The hamiltonian describing the system is non-linear and so are the MQLE. Therefore, they can not be solved analytically. However, we can use a trick to obtain good approximations, wich is related to the driving laser intensity.

We assume that the cavity is strongly driven by the laser. In this case, the mean values of the operators will tend to align with the laser power, namely, the first moments $\langle\hat{a}\rangle$, $\langle\hat{d}\rangle$, $\langle\hat{p}\rangle$ and $\langle\hat{q}\rangle$ will tend to be much larger than the fluctuations (i.e. the second moments such as $\langle\hat{a}^\dagger\hat{a}\rangle$). This trick is called the mean-field approximation.

Summurazing, if the pumping is strong, the dynamics of the system can be linearized [1]. We thus split all the operators into a mean value and a fluctuation operator:

$$\hat{a} = \alpha + \delta\hat{a}, \tag{4.19}$$
$$\hat{d} = \delta + \delta\hat{d}, \tag{4.20}$$
$$\hat{p} = \overline{p} + \delta\hat{p}, \tag{4.21}$$
$$\hat{q} = \overline{q} + \delta\hat{q}, \tag{4.22}$$

and define the mean values

$$\langle\hat{a}\rangle = \alpha,$$
$$\langle\hat{d}\rangle = \delta,$$
$$\langle\hat{p}\rangle = \overline{p},$$
$$\langle\hat{q}\rangle = \overline{q},$$

with

$$\langle\delta\hat{a}\rangle = \langle\delta\hat{d}\rangle = \langle\delta\hat{p}\rangle = \langle\delta\hat{q}\rangle = 0. \tag{4.23}$$

4.1.4.2 Semi-classical Steady State

Let us consider the semi-classical approximation. Generaly speaking, considering two quantum operators $\hat{A}$ and $\hat{B}$, the expectation value of their product is

$$\langle \hat{A}\hat{B} \rangle = \langle \hat{A} \rangle \langle \hat{B} \rangle + \langle \delta\hat{A}\delta\hat{B} \rangle. \tag{4.24}$$

In the semi-classical approximation, we neglect the fluctuations, so that

$$\langle \hat{A}\hat{B} \rangle \approx \langle \hat{A} \rangle \langle \hat{B} \rangle. \tag{4.25}$$

Thus, assuming the semi-classical approximation means replacing the operators by their mean values. In this context, we derive the evolution equations for the first moments of each operator.

For the cavity operator, we obtain:

$$\begin{aligned}
\dot{\hat{a}} &= -\left(i\Delta_a^0 + \kappa\right)\hat{a} + ig_a^0\sqrt{2}\,\hat{q}\hat{a} - i\lambda\hat{d} - i\epsilon - \sqrt{2\kappa_L}\,\hat{a}_{\text{in},L}(t) - \sqrt{2\kappa_R}\,\hat{a}_{\text{in},R}(t), \\
\langle\dot{\hat{a}}\rangle &= -\left(i\Delta_a^0 + \kappa\right)\langle\hat{a}\rangle + ig_a^0\sqrt{2}\,\langle\hat{q}\hat{a}\rangle - i\lambda\langle\hat{d}\rangle - i\epsilon, \qquad (4.26) \\
\dot{\alpha} &= -\left(i\Delta_a^0 + \kappa\right)\alpha + ig_a^0\sqrt{2}\,\overline{q}\alpha - i\lambda\delta - i\epsilon. \qquad (4.27)
\end{aligned}$$

Then, for the Fano-optical operator:

$$\begin{aligned}
\dot{\hat{d}} &= -\left(i\Delta_d^0 + \kappa_d\right)\hat{d} + ig_d^0\sqrt{2}\,\hat{q}\hat{d} - i\lambda\hat{a} - \sqrt{2\kappa_d}\,\hat{d}_{\text{in}}(t), \\
\langle\dot{\hat{d}}\rangle &= -\left(i\Delta_d^0 + \kappa_d\right)\langle\hat{d}\rangle + ig_d^0\sqrt{2}\,\langle\hat{q}\hat{d}\rangle - i\lambda\langle\hat{a}\rangle, \qquad (4.28) \\
\dot{\delta} &= -\left(i\Delta_d^0 + \kappa_d\right)\delta + ig_d^0\sqrt{2}\,\overline{q}\delta - i\lambda\alpha. \qquad (4.29)
\end{aligned}$$

For the position operator:

$$\begin{aligned}
\dot{\hat{q}} &= \Omega_{\text{mec}}\hat{p}, \\
\langle\dot{\hat{q}}\rangle &= \Omega_{\text{mec}}\langle\hat{p}\rangle, \qquad (4.30) \\
\dot{\overline{q}} &= \Omega_{\text{mec}}\overline{p}. \qquad (4.31)
\end{aligned}$$

Using the property

$$\begin{aligned}
\langle\hat{a}^\dagger\hat{a}\rangle &= \langle\left(\alpha^\dagger + \delta\hat{a}^\dagger\right)(\alpha + \delta\hat{a})\rangle \\
&= \langle\alpha^\dagger\alpha + \alpha^\dagger\delta\hat{a} + \delta\hat{a}^\dagger\alpha + \delta\hat{a}^\dagger\delta\hat{a}\rangle \\
&= \langle\alpha^\dagger\alpha\rangle \\
&= |\alpha|^2 \qquad (4.32)
\end{aligned}$$

and similarly with $\langle\hat{d}^\dagger\hat{d}\rangle = |\delta|^2$,

we obtain, for the momentum operator:

$$\begin{aligned}
\dot{\hat{p}} &= -\Omega_{\text{mec}}\hat{q} - \gamma\hat{p} + g_a^0\sqrt{2}\,\hat{a}^\dagger\hat{a} + g_d^0\sqrt{2}\,\hat{d}^\dagger\hat{d} + \sqrt{\gamma}\hat{\xi}(t), \\
\langle\dot{\hat{p}}\rangle &= -\Omega_{\text{mec}}\langle\hat{q}\rangle - \gamma\langle\hat{p}\rangle + g_a^0\sqrt{2}\,\langle\hat{a}^\dagger\hat{a}\rangle + g_d^0\sqrt{2}\,\langle\hat{d}^\dagger\hat{d}\rangle, \qquad (4.33) \\
\dot{\overline{p}} &= -\Omega_{\text{mec}}\overline{q} - \gamma\overline{p} + g_a^0\sqrt{2}\,|\alpha|^2 + g_d^0\sqrt{2}\,|\delta|^2. \qquad (4.34)
\end{aligned}$$

Thus, the semi-classical steady state corresponding to the MQLE (4.12), (4.13), (4.14) and (4.15) is

$$\alpha = \frac{-i\,(\epsilon + \lambda\delta)}{\kappa + i\Delta_a}, \tag{4.35}$$

$$\delta = \frac{-i\lambda\alpha}{\kappa_d + i\Delta_d}, \tag{4.36}$$

$$\overline{q} = \frac{\sqrt{2}\,\left(g_a^0|\alpha|^2 + g_d^0|\delta|^2\right)}{\Omega_{\mathrm{mec}}}, \tag{4.37}$$

$$\overline{p} = 0, \tag{4.38}$$

where we have defined the effective detunings:

$$\Delta_a = \Delta_a^0 - g_a^0\sqrt{2}\,\overline{q}, \tag{4.39}$$

$$\Delta_d = \Delta_d^0 - g_d^0\sqrt{2}\,\overline{q}. \tag{4.40}$$

Although we have obtained a non-linear semi-classical steady state, we assume that we are in a parameter regime where the system is stable (see [7], Sec. 2.6 and 2.7).

4.1.4.3 Linearization around the semi-classical steady state

We linearize the MQLE around the semi-classical steady state, keeping terms up to the first order in the fluctuations:

$$\delta\dot{\hat{a}} = -\left(i\Delta_a + \kappa\right)\delta\hat{a} + ig_a\sqrt{2}\,\delta\hat{q} - i\lambda\delta\hat{d} - \sqrt{2\kappa_L}\,\hat{a}_{\mathrm{in},L}(t) - \sqrt{2\kappa_R}\,\hat{a}_{\mathrm{in},R}(t), \tag{4.41}$$

$$\delta\dot{\hat{d}} = -\left(i\Delta_d + \kappa_d\right)\delta\hat{d} + ig_d\sqrt{2}\,\delta\hat{q} - i\lambda\delta\hat{a} - \sqrt{2\kappa_d}\,\hat{d}_{\mathrm{in}}(t), \tag{4.42}$$

$$\delta\dot{\hat{q}} = \Omega_{\mathrm{mec}}\delta\hat{p}, \tag{4.43}$$

$$\delta\dot{\hat{p}} = -\Omega_{\mathrm{mec}}\delta\hat{q} - \gamma\delta\hat{p} + g_a^0\sqrt{2}\,\left(\alpha^\dagger\delta\hat{a} + \delta\hat{a}^\dagger\alpha\right) + g_d^0\sqrt{2}\,\left(\delta^\dagger\delta\hat{d} + \delta\hat{d}^\dagger\delta\right) + \sqrt{\gamma}\hat{\xi}(t), \tag{4.44}$$

where we have defined the effective optomechanical couplings

$$g_a = g_a^0\alpha, \tag{4.45}$$

$$g_d = g_d^0\delta, \tag{4.46}$$

describing the enhanced optomechanical interaction between the mechanical and cavity modes and the mechanical and optical Fano-membrane modes, respectively.

A detailled derivation of the linearization of the MQLE around the semi-classical steady state can be found in Appendix B, Sec. B.2.

4.1.4.4 Position and Momentum Optical Quadratures

We rewrite the linearized MQLE (4.41), (4.42), (4.43) and (4.44) in terms of the position and momentum quadratures. We define the position quadratures as

$$\delta\hat{X}_a = \frac{\delta\hat{a} + \delta\hat{a}^\dagger}{\sqrt{2}}, \tag{4.47}$$

$$\delta\hat{X}_d = \frac{\delta\hat{d} + \delta\hat{d}^\dagger}{\sqrt{2}}, \tag{4.48}$$

and the momentum quadratures as

$$\delta\hat{P}_a = \frac{\delta\hat{a} - \delta\hat{a}^\dagger}{i\sqrt{2}}, \tag{4.49}$$

$$\delta\hat{P}_d = \frac{\delta\hat{d} - \delta\hat{d}^\dagger}{i\sqrt{2}}. \tag{4.50}$$

From (4.41) we express

$$\delta\dot{\hat{a}}^\dagger = -\left(-i\Delta_a + \kappa\right)\delta\hat{a}^\dagger - ig_a^*\sqrt{2}\,\delta\hat{q}^\dagger + i\lambda\delta\hat{d}^\dagger - \sqrt{2\kappa_L}\,\hat{a}^\dagger_{\text{in},L}(t) - \sqrt{2\kappa_R}\,\hat{a}^\dagger_{\text{in},R}(t), \tag{4.51}$$

allowing us to derive the derivative of the optical-cavity-position quadrature:

$$\delta\dot{\hat{X}}_a = \frac{d}{dt}\delta\hat{X}_a = \frac{d}{dt}\left(\frac{\delta\hat{a} + \delta\hat{a}^\dagger}{\sqrt{2}}\right) = \frac{1}{\sqrt{2}}\left(\delta\dot{\hat{a}} + \delta\dot{\hat{a}}^\dagger\right).$$

Thus,

$$\begin{aligned}\delta\dot{\hat{X}}_a = \frac{1}{\sqrt{2}}\Bigg(&i\Delta_a\left(-\delta\hat{a} + \delta\hat{a}^\dagger\right) + \kappa\left(-\delta\hat{a} - \delta\hat{a}^\dagger\right) + ig_a\sqrt{2}\,\delta\hat{q} - ig_a^*\sqrt{2}\,\delta\hat{q}^\dagger \\ &+ i\lambda\left(-\delta\hat{d} + \delta\hat{d}^\dagger\right) - \sqrt{2\kappa_R}\left(\hat{a}_{\text{in},R}(t) + \hat{a}^\dagger_{\text{in},R}(t)\right) - \sqrt{2\kappa_L}\left(\hat{a}_{\text{in},L}(t) + \hat{a}^\dagger_{\text{in},L}(t)\right)\Bigg) \\ = \Delta_a\,\delta\hat{P}_a - \kappa\,\delta\hat{X}_a + i\left(g_a - g_a^*\right)\delta\hat{q} + \lambda\,\delta\hat{P}_d - \sqrt{2\kappa_R}\,\delta\hat{X}_{\text{in},R} - \sqrt{2\kappa_L}\,\delta\hat{X}_{\text{in},L}.\end{aligned} \tag{4.52}$$

However, for $Z \in \mathbb{C}$, $Z - Z^* = 2i\ \mathrm{Im}(Z)$. Then $i\left(g_a - g_a^*\right)\delta\hat{q} = -2\ \mathrm{Im}(g_a)\delta\hat{q}$.

Substituting, we then obtain

$$\delta\dot{\hat{X}}_a = \Delta_a\,\delta\hat{P}_a - \kappa\,\delta\hat{X}_a - 2\ \mathrm{Im}(g_a)\delta\hat{q} + \lambda\,\delta\hat{P}_d - \sqrt{2\kappa_R}\,\delta\hat{X}_{\text{in},R} - \sqrt{2\kappa_L}\,\delta\hat{X}_{\text{in},L} \tag{4.53}$$

In a similar way, we can derive the derivative of the optical-cavity-momentum quadrature:

$$\delta\dot{\hat{P}}_a = \frac{d}{dt}\delta\hat{P}_a = \frac{d}{dt}\left(\frac{\delta\hat{a} - \delta\hat{a}^\dagger}{i\sqrt{2}}\right) = \frac{1}{i\sqrt{2}}\left(\delta\dot{\hat{a}} - \delta\dot{\hat{a}}^\dagger\right). \tag{4.54}$$

Thus

$$\begin{aligned}\delta\dot{\hat{P}}_a &= \frac{1}{i\sqrt{2}}\Big(i\Delta_a\left(-\delta\hat{a}-\delta\hat{a}^\dagger\right)+\kappa\left(-\delta\hat{a}+\delta\hat{a}^\dagger\right)+ig_a\sqrt{2}\,\delta\hat{q}+ig_a^*\sqrt{2}\,\delta\hat{q}^\dagger \\ &\quad + i\lambda\left(-\delta\hat{d}-\delta\hat{d}^\dagger\right)-\sqrt{2\kappa_R}\left(\hat{a}_{\mathrm{in},R}(t)-\hat{a}^\dagger_{\mathrm{in},R}(t)\right)-\sqrt{2\kappa_L}\left(\hat{a}_{\mathrm{in},L}(t)-\hat{a}^\dagger_{\mathrm{in},L}(t)\right)\Big) \\ &= -\Delta_a\,\delta\hat{X}_a-\kappa\,\delta\hat{P}_a+(g_a+g_a^*)\,\delta\hat{q}-\lambda\,\delta\hat{X}_d-\sqrt{2\kappa_R}\,\delta\hat{P}_{\mathrm{in},R}-\sqrt{2\kappa_L}\,\delta\hat{P}_{\mathrm{in},L}.\end{aligned} \tag{4.55}$$

And for $Z\in\mathbb{C}$, $Z+Z^*=2\ \mathrm{Re}(Z)$. Then $(g_a+g_a^*)\,\delta\hat{q}=2\ \mathrm{Re}(g_a)\delta\hat{q}$.

Substituting, we then obtain

$$\delta\dot{\hat{P}}_a = -\Delta_a\,\delta\hat{X}_a-\kappa\,\delta\hat{P}_a+2\ \mathrm{Re}(g_a)\delta\hat{q}-\lambda\,\delta\hat{X}_d-\sqrt{2\kappa_R}\,\delta\hat{P}_{\mathrm{in},R}-\sqrt{2\kappa_L}\,\delta\hat{P}_{\mathrm{in},L}. \tag{4.56}$$

The same procedure is applied to the optical-Fano-membrane quadratures.

We obtain

$$\delta\dot{\hat{X}}_d = \Delta_d\,\delta\hat{P}_d-\kappa_d\,\delta\hat{X}_d-2\ \mathrm{Im}(g_d)\delta\hat{q}+\lambda\,\delta\hat{P}_a-\sqrt{2\kappa_d}\,\delta\hat{X}_{\mathrm{in},d}, \tag{4.57}$$

$$\delta\dot{\hat{P}}_d = -\Delta_d\,\delta\hat{X}_d-\kappa_d\,\delta\hat{P}_d+2\ \mathrm{Re}(g_d)\delta\hat{q}-\lambda\,\delta\hat{X}_a-\sqrt{2\kappa_d}\,\delta\hat{P}_{\mathrm{in},d}. \tag{4.58}$$

We derive a mathematical trick we will use right after:

$$\begin{aligned}2\left(\alpha^\dagger\delta\hat{a}+\delta\hat{a}^\dagger\alpha\right) &= 2\alpha^\dagger\delta\hat{a}+\alpha^\dagger\delta\hat{a}^\dagger-\alpha^\dagger\delta\hat{a}^\dagger+\alpha\delta\hat{a}-\alpha\delta\hat{a}+2\delta\hat{a}^\dagger\alpha \\ &= \alpha^\dagger\delta\hat{a}+\alpha^\dagger\delta\hat{a}^\dagger+\alpha\delta\hat{a}+\alpha\delta\hat{a}^\dagger \\ &\quad +\alpha^\dagger\delta\hat{a}-\alpha^\dagger\delta\hat{a}^\dagger-\alpha\delta\hat{a}+\alpha\delta\hat{a}^\dagger \\ &= \left(\alpha^\dagger+\alpha\right)\left(\delta\hat{a}+\delta\hat{a}^\dagger\right) \\ &\quad +\left(\alpha^\dagger-\alpha\right)\left(\delta\hat{a}-\delta\hat{a}^\dagger\right) \\ &= 2\sqrt{2}\ \mathrm{Re}(\alpha)\delta\hat{X}_a+2\sqrt{2}\ \mathrm{Im}(\alpha)\delta\hat{P}_a.\end{aligned}$$

For the around-semi-classical-steady-state-linearized MQLE of the momentum operator, we can write

$$\begin{aligned}\delta\dot{\hat{p}} &= -\Omega_{\mathrm{mec}}\delta\hat{q}-\gamma\delta\hat{p}+g_a^0\sqrt{2}\left(\alpha^\dagger\delta\hat{a}+\delta\hat{a}^\dagger\alpha\right)+g_d^0\sqrt{2}\left(\delta^\dagger\delta\hat{d}+\delta\hat{d}^\dagger\delta\right)+\sqrt{\gamma}\hat{\xi}(t) \\ &= -\Omega_{\mathrm{mec}}\delta\hat{q}-\gamma\delta\hat{p}+g_a^0\frac{2}{\sqrt{2}}\left(\alpha^\dagger\delta\hat{a}+\delta\hat{a}^\dagger\alpha\right)+g_d^0\frac{2}{\sqrt{2}}\left(\delta^\dagger\delta\hat{d}+\delta\hat{d}^\dagger\delta\right)+\sqrt{\gamma}\hat{\xi}(t).\end{aligned} \tag{4.59}$$

Sustituting

$$2\left(\alpha^\dagger\delta\hat{a}+\delta\hat{a}^\dagger\alpha\right) = 2\sqrt{2}\ \mathrm{Re}(\alpha)\delta\hat{X}_a+2\sqrt{2}\ \mathrm{Im}(\alpha)\delta\hat{P}_a \tag{4.60}$$

and

$$2\left(\delta^\dagger\delta\hat{d}+\delta\hat{d}^\dagger\delta\right)=2\sqrt{2}\ \mathrm{Re}(\delta)\delta\hat{X}_d+2\sqrt{2}\ \mathrm{Im}(\delta)\delta\hat{P}_d, \tag{4.61}$$

we get:

$$\begin{aligned}\delta\dot{\hat{p}} &= -\Omega_{\mathrm{mec}}\delta\hat{q}-\gamma\delta\hat{p}\\ &\quad+2g_a^0\ \mathrm{Re}(\alpha)\delta\hat{X}_a+2g_a^0\ \mathrm{Im}(\alpha)\delta\hat{P}_a+2g_d^0\ \mathrm{Re}(\delta)\delta\hat{X}_d+2g_d^0\ \mathrm{Im}(\delta)\delta\hat{P}_d+\sqrt{\gamma}\hat{\xi}(t)\\ &= -\Omega_{\mathrm{mec}}\delta\hat{q}-\gamma\delta\hat{p}\\ &\quad+2\ \mathrm{Re}(g_a)\delta\hat{X}_a+2\ \mathrm{Im}(g_a)\delta\hat{P}_a+2\ \mathrm{Re}(g_d)\delta\hat{X}_d+2\ \mathrm{Im}(g_d)\delta\hat{P}_d+\sqrt{\gamma}\hat{\xi}(t).\end{aligned} \tag{4.62}$$

For the around-semi-classical-steady-state-linearized MQLE of the position operator, we have

$$\delta\dot{\hat{q}}=\Omega_{\mathrm{mec}}\delta\hat{p}. \tag{4.63}$$

Thus, the system of around-semi-classical-steady-state-linearized MQLE written for the position and momentum quadratures of the Fano-mebrane-in-the-middle system reads:

$$\begin{aligned}\delta\dot{\hat{X}}_a &= \Delta_a\,\delta\hat{P}_a-\kappa\,\delta\hat{X}_a-2\ \mathrm{Im}(g_a)\delta\hat{q}+\lambda\,\delta\hat{P}_d-\sqrt{2\kappa_R}\,\delta\hat{X}_{\mathrm{in},R}-\sqrt{2\kappa_L}\,\delta\hat{X}_{\mathrm{in},L}\\ \delta\dot{\hat{P}}_a &= -\Delta_a\,\delta\hat{X}_a-\kappa\,\delta\hat{P}_a+2\ \mathrm{Re}(g_a)\delta\hat{q}-\lambda\,\delta\hat{X}_d-\sqrt{2\kappa_R}\,\delta\hat{P}_{\mathrm{in},R}-\sqrt{2\kappa_L}\,\delta\hat{P}_{\mathrm{in},L}\\ \delta\dot{\hat{X}}_d &= \Delta_d\,\delta\hat{P}_d-\kappa_d\,\delta\hat{X}_d-2\ \mathrm{Im}(g_d)\delta\hat{q}+\lambda\,\delta\hat{P}_a-\sqrt{2\kappa_d}\,\delta\hat{X}_{\mathrm{in},d}\\ \delta\dot{\hat{P}}_d &= -\Delta_d\,\delta\hat{X}_d-\kappa_d\,\delta\hat{P}_d+2\ \mathrm{Re}(g_d)\delta\hat{q}-\lambda\,\delta\hat{X}_a-\sqrt{2\kappa_d}\,\delta\hat{P}_{\mathrm{in},d}\\ \delta\dot{\hat{q}} &= \Omega_{\mathrm{mec}}\delta\hat{p}\\ \delta\dot{\hat{p}} &= -\Omega_{\mathrm{mec}}\delta\hat{q}-\gamma\delta\hat{p}+2\ \mathrm{Re}(g_a)\delta\hat{X}_a+2\ \mathrm{Im}(g_a)\delta\hat{P}_a+2\ \mathrm{Re}(g_d)\delta\hat{X}_d+2\ \mathrm{Im}(g_d)\delta\hat{P}_d+\sqrt{\gamma}\hat{\xi}(t)\end{aligned}$$

We can recast it in a into a compact matrix form:

$$\begin{bmatrix}\delta\dot{\hat{X}}_a\\ \delta\dot{\hat{P}}_a\\ \delta\dot{\hat{X}}_d\\ \delta\dot{\hat{P}}_d\\ \delta\dot{\hat{q}}\\ \delta\dot{\hat{p}}\end{bmatrix}=\begin{bmatrix}-\kappa & \Delta_a & 0 & \lambda & -2\ \mathrm{Im}(g_a) & 0\\ -\Delta_a & -\kappa & -\lambda & 0 & 2\ \mathrm{Re}(g_a) & 0\\ 0 & \lambda & -\kappa_d & \Delta_d & -2\ \mathrm{Im}(g_d) & 0\\ -\lambda & 0 & -\Delta_d & -\kappa_d & 2\ \mathrm{Re}(g_d) & 0\\ 0 & 0 & 0 & 0 & 0 & \Omega_{\mathrm{mec}}\\ 2\ \mathrm{Re}(g_a) & 2\ \mathrm{Im}(g_a) & 2\ \mathrm{Re}(g_d) & 2\ \mathrm{Im}(g_d) & -\Omega_{\mathrm{mec}} & -\gamma\end{bmatrix}\begin{bmatrix}\delta\hat{X}_a\\ \delta\hat{P}_a\\ \delta\hat{X}_d\\ \delta\hat{P}_d\\ \delta\hat{q}\\ \delta\hat{p}\end{bmatrix}+\begin{bmatrix}\text{Input}\\ \text{flux}\end{bmatrix} \tag{4.64}$$

This system of linear differential equations is the one we will solve to determine the final phonon number in the mechanical resonator. As we will see in the next section, it can be recast into a Lyapunov equation and solved numerically.

4.1.5 Lyapunov Equations

4.1.5.1 Final Phonon Number

We want to derive the final phonon number in the mechanical fluctuations. This number, defined by $\langle \delta\hat{b}^\dagger \delta\hat{b} \rangle$, is the one we are interested in to determine the final temperature of the mechanical resonator after the system has reached the steady state.

On one hand, we have

$$\begin{aligned}
\langle \delta\hat{q}^2 \rangle &= \langle \frac{\delta\hat{b}^\dagger + \delta\hat{b}}{\sqrt{2}} \cdot \frac{\delta\hat{b}^\dagger + \delta\hat{b}}{\sqrt{2}} \rangle \\
&= \frac{1}{2} \langle \delta\hat{b}^\dagger \delta\hat{b}^\dagger + \delta\hat{b}^\dagger \delta\hat{b} + \delta\hat{b}\delta\hat{b}^\dagger + \delta\hat{b}\delta\hat{b} \rangle \\
&= \frac{1}{2} \left(\langle \delta\hat{b}^\dagger \delta\hat{b}^\dagger \rangle + \langle \delta\hat{b}^\dagger \delta\hat{b} \rangle + \langle \delta\hat{b}\delta\hat{b}^\dagger \rangle + \langle \delta\hat{b}\delta\hat{b} \rangle \right).
\end{aligned} \tag{4.65}$$

On the other hand,

$$\begin{aligned}
\langle \delta\hat{p}^2 \rangle &= \langle \frac{\delta\hat{b}^\dagger - \delta\hat{b}}{i\sqrt{2}} \cdot \frac{\delta\hat{b}^\dagger - \delta\hat{b}}{i\sqrt{2}} \rangle \\
&= -\frac{1}{2} \langle \delta\hat{b}^\dagger \delta\hat{b}^\dagger - \delta\hat{b}^\dagger \delta\hat{b} - \delta\hat{b}\delta\hat{b}^\dagger + \delta\hat{b}\delta\hat{b} \rangle \\
&= -\frac{1}{2} \left(\langle \delta\hat{b}^\dagger \delta\hat{b}^\dagger \rangle - \langle \delta\hat{b}^\dagger \delta\hat{b} \rangle - \langle \delta\hat{b}\delta\hat{b}^\dagger \rangle + \langle \delta\hat{b}\delta\hat{b} \rangle \right)
\end{aligned} \tag{4.66}$$

Summing up both (4.65) and (4.66), we get

$$\begin{aligned}
\langle \delta\hat{q}^2 \rangle + \langle \delta\hat{p}^2 \rangle &= \frac{1}{2} \Big(\langle \delta\hat{b}^\dagger \delta\hat{b}^\dagger \rangle + \langle \delta\hat{b}^\dagger \delta\hat{b} \rangle + \langle \delta\hat{b}\delta\hat{b}^\dagger \rangle + \langle \delta\hat{b}\delta\hat{b} \rangle \\
&\qquad + \langle \delta\hat{b}^\dagger \delta\hat{b}^\dagger \rangle - \langle \delta\hat{b}^\dagger \delta\hat{b} \rangle - \langle \delta\hat{b}\delta\hat{b}^\dagger \rangle + \langle \delta\hat{b}\delta\hat{b} \rangle \Big) \\
&= \langle \delta\hat{b}^\dagger \delta\hat{b} \rangle + \langle \delta\hat{b}\delta\hat{b}^\dagger \rangle \\
&= \langle \delta\hat{b}^\dagger \delta\hat{b} + \delta\hat{b}\delta\hat{b}^\dagger - \delta\hat{b}^\dagger \delta\hat{b} + \delta\hat{b}^\dagger \delta\hat{b} \rangle \\
&= \langle 2\delta\hat{b}^\dagger \delta\hat{b} + [\delta\hat{b}, \delta\hat{b}^\dagger] \rangle \\
&= \langle 2\delta\hat{b}^\dagger \delta\hat{b} + 1 \rangle.
\end{aligned} \tag{4.67}$$

Then, the final phonon number is given by:

$$\langle \delta\hat{b}^\dagger \delta\hat{b} \rangle = \frac{\langle \delta\hat{q}^2 \rangle + \langle \delta\hat{p}^2 \rangle - 1}{2}. \tag{4.68}$$

Thus, the final phonon number is given by the second-order moments of the mechanical quadratures, $\langle \delta\hat{q}^2 \rangle$ and $\langle \delta\hat{p}^2 \rangle$.

4.1.5.2 Evolution of the Second-order Moments

The MQLE-matrix system (4.64) that we have derived in Sec. 4.1.4.4 can be written in a compact differential-equation form

$$\dot{\hat{Y}} = M\hat{Y} + \hat{f} \tag{4.69}$$

where

$$\hat{Y} = \begin{bmatrix} \delta\hat{X}_a & \delta\hat{P}_a & \delta\hat{X}_d & \delta\hat{P}_d & \delta\hat{q} & \delta\hat{p} \end{bmatrix}^T, \tag{4.70}$$

is a vector of fluctuation operators,

$$M = \begin{bmatrix} -\kappa & \Delta_a & 0 & \lambda & -2\ \mathrm{Im}(g_a) & 0 \\ -\Delta_a & -\kappa & -\lambda & 0 & 2\ \mathrm{Re}(g_a) & 0 \\ 0 & \lambda & -\kappa_d & \Delta_d & -2\ \mathrm{Im}(g_d) & 0 \\ -\lambda & 0 & -\Delta_d & -\kappa_d & 2\ \mathrm{Re}(g_d) & 0 \\ 0 & 0 & 0 & 0 & 0 & \Omega_{\mathrm{mec}} \\ 2\ \mathrm{Re}(g_a) & 2\ \mathrm{Im}(g_a) & 2\ \mathrm{Re}(g_d) & 2\ \mathrm{Im}(g_d) & -\Omega_{\mathrm{mec}} & -\gamma \end{bmatrix} \tag{4.71}$$

and

$$\hat{f} = \begin{bmatrix} \text{Input} \\ \text{flux} \end{bmatrix}. \tag{4.72}$$

However, we demonstrate in Appendix C, Sec. C.1, that the covariance matrix element

$$V_{ij} = \frac{1}{2}\left\langle \hat{Y}_i\hat{Y}_j + \hat{Y}_j\hat{Y}_i \right\rangle - \left\langle \hat{Y}_i \right\rangle \left\langle \hat{Y}_j \right\rangle,$$

whose vector of operators $\hat{Y}$ is a vector of fluctuation operators and follows the differential equation

$$\dot{\hat{Y}} = A\hat{Y} + \hat{f}, \quad \text{where } \hat{f} \text{ is a fluctuation operator,} \tag{4.73}$$

is a solution of the Lyapunov equation

$$\frac{dV}{dt} = AV + VA^T + B. \tag{4.74}$$

Thus, the second-order moments of the optomechanical-system quadratures (coordinates of our vector of operators (4.70)) evolve in a form of a Lyapunov equation (4.74). The matrix A is the matrix M obtained from the MQLE-matrix system (4.64) and the matrix B is the diagonal matrix whose elements are obtained from the correlation functions of Eq. (4.3) and Eq. (4.4) of the input-noise operators (see Appendix C, Sec. C.1).

For the Fano-membrane-in-the-middle system, the matrix B is reads

$$B = \begin{bmatrix} \kappa & 0 & 0 & 0 & 0 & 0 \\ 0 & \kappa & 0 & 0 & 0 & 0 \\ 0 & 0 & \kappa_d & 0 & 0 & 0 \\ 0 & 0 & 0 & \kappa_d & 0 & 0 \\ 0 & 0 & 0 & 0 & 0 & 0 \\ 0 & 0 & 0 & 0 & 0 & \gamma(2\bar{n}_{\mathrm{mec}} + 1) \end{bmatrix}. \tag{4.75}$$

A detailed derivation of the elements of the matrix B can be found in Appendix C, Sec. C.2.

We are interested in the steady state of the system, where the time derivative of the covariance matrix is zero. Namely,

$$MV + VM^T = -B. \tag{4.76}$$

Solving numerically the steady-state-Lyapunov equation (4.76) gives access to the phonon number in the mechanical fluctuations:

$$\langle \delta\hat{b}^\dagger \delta\hat{b} \rangle = \frac{1}{2}(\langle \delta\hat{q}^2 \rangle + \langle \delta\hat{p}^2 \rangle - 1) = \frac{1}{2}\left(V_{55} + V_{66} - 1\right). \tag{4.77}$$

4.2 Fano-membrane-based Optomechanical Systems

Let's take a moment to recap and reflect on what we have developed and described so far.

- We have introduced the concept of optomechanical system and described the standard optomechanical setup ;
- We have found that, in the limit of the unresolved-sideband regime, we needed to find a way to enhance the cooling process ;
- We then introduced the concept of Fano-membrane-based optomechanical system, which enhances the optomechanical cooling of the mechanical resonator due to the special properties of the photonic crystal ;
- We have described the Fano-membrane-in-the-middle system and derived the equation for the final phonon number in the mechanical resonator ;
- We have mentioned the existence of an alternative Fano-membrane-based optomechanical setup: the left-hand-side-Fano-mirror setup ;
- We have now reached the stage where we will explore the optical-normal-mode theory and its properties within the equations of both the left-hand-side-Fano-mirror setup and the Fano-membrane-in-the-middle setup and how we can optimize the cooling of the mechanical resonator.

4.2.1 The Optical-Normal-Mode Theory

Here is a picture of what we call the normal-mode theory. Let us consider two general quantum modes. When those two modes strongly couple, they hybridize and form new modes we call "normal modes". Normal-mode theory is a way to simplify the description of the system by introducing a new set of operators that are linear combinations of the original operators. This is what we aim to do in this section.

We will describe the strong interaction between two bosonic modes, the cavity mode and the Fano-membrane mode, and we will find the normal modes of the system.

Neglecting the mechanical mode is based on the assumption that in most optomechanical setups, the mechanical damping rate is order of magnitudes smaller compared to the other relevant frequencies.

An alternative way to justify that we can neglect the mechanical mode is to consider that we are in the weak-optomechanical-coupling regime (see Fig. 4.6). In this regime, the mechanical mode is weakly coupled to the cavity mode. In a standard optomechanical setup, we deal with only two modes: a single optical mode (the cavity mode) and a single mechanical one. However, in the Fano-membrane-based optomechanical systems we describe, we have two optical modes (the cavity and the Fano-membrane modes) and a single mechanical mode. Thus, in order to be able to compare to the standard optomechanical setup, we need to merge the two optical modes into a single one. This is what we do when dealing with the optical-normal-mode theory.

Therefore, assuming the weak optomechanical coupling regime enables us to merge the two optical modes into a normal one and we can mimic the standard optomechanica setup.

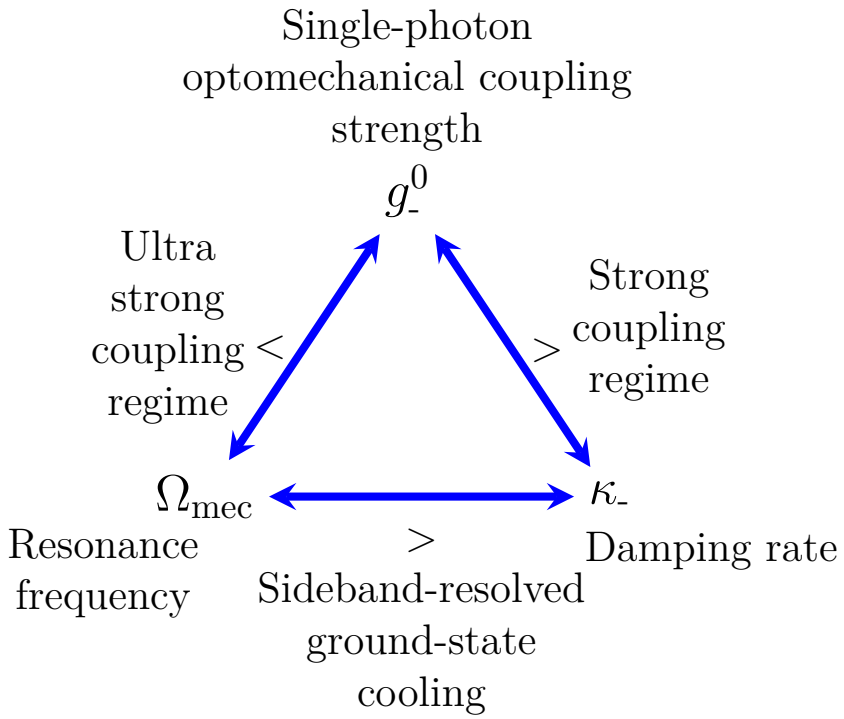

Figure 4.6: The different optomechanical regimes. In this work, we are mainly interested in the Sideband-resolved-ground-state-cooling regime.

4.2.1.1 Optical-Normal-Mode Theory for the Fano-membrane-in-the-middle Setup

Here we describe the optical-normal-mode theory for the setup we aim to study in this work: the Fano-membrane-in-the-middle setup.

Due to the overlap of the cavity and Fano-membrane modes, those two modes hybridize and can be described by the hamiltonian

$$\hat{H}_{\text{opt}} = \hbar\omega_a \hat{a}^\dagger \hat{a} + \hbar\omega_d \hat{d}^\dagger \hat{d} + \hbar\lambda(\hat{a}^\dagger \hat{d} + \hat{d}^\dagger \hat{a}). \tag{4.78}$$

The Langevin equations are given by

$$\dot{a} = -i(\Delta_a^0 - i\kappa)a - i\lambda d, \tag{4.79}$$
$$\dot{d} = -i(\Delta_d^0 - i\kappa_d)d - i\lambda a, \tag{4.80}$$

where

$$\kappa = \kappa_R + \kappa_L, \tag{4.81}$$
$$\Delta_a^0 = \omega_{\text{cav}} - \omega_{las}, \tag{4.82}$$
$$\Delta_d^0 = \omega_d - \omega_{las}. \tag{4.83}$$

This system of equations can be written in matrix form as

$$\begin{bmatrix} \dot{\hat{a}} \\ \dot{\hat{d}} \end{bmatrix} = -i \begin{bmatrix} \Delta_a^0 - i\kappa & \lambda \\ \lambda & \Delta_d^0 - i\kappa_d \end{bmatrix} \begin{bmatrix} \hat{a} \\ \hat{d} \end{bmatrix} + \text{input flux}, \tag{4.84}$$

where the input flux is a vector of noise terms.

The optical-normal-mode theory is a way to diagonalize the hamiltonian of the system and to find the normal modes of the system. The normal modes are the eigenmodes of the optical system and they are the modes that are excited when the system is in a steady state.

Whithout the rotating wave approximation, the eigenvalues of the matrix system (4.84) are given by

$$\Omega_\pm = \frac{1}{2}\left(\omega_{\text{cav}} + \omega_d - i(\kappa + \kappa_d)\right) \pm \sqrt{(\frac{1}{2}(\omega_{\text{cav}} - \omega_d) - i\frac{1}{2}(\kappa - \kappa_d))^2 + \lambda^2}. \tag{4.85}$$

Those eigenvalues correspond to the effective resonant frequencies and effective linewidths of the system:

$$\Delta_\pm = \text{Re}[\Omega_\pm], \tag{4.86}$$
$$\kappa_\pm = -\text{Im}[\Omega_\pm], \tag{4.87}$$

4.2.1.2 Optical-Normal-Mode Theory for the left-hand-side-Fano-mirror Setup

Here we describe the left-hand-side-Fano-mirror setup. This setup has been investigated in the literature [9, 8, 4].

This study, whose setup is depicted in Fig. 4.7, has provided an extensive analysis of a Fano-mirror coupled to an optical cavity. Both dispersive as well as dissipative optomechanical couplings are considered. This is the main difference with the Fano-membrane-in-the-middle setup, where only the dissipative optomechanical coupling is considered and where the Fano-membrane is placed in the middle of the cavity (and therefore does not interact with the external environments).

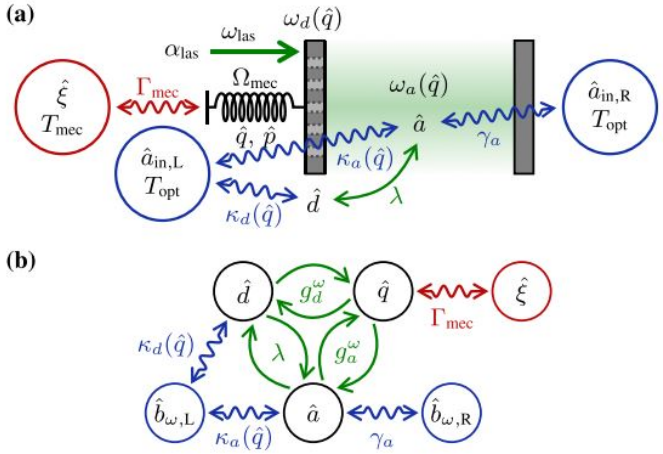

Figure 4.7: (a) Sketch of the optomechanical setup, consisting of a double-sided optical cavity with one movable Fano-mirror. (b) Coupled-mode-setup picture. In this setup, the left-hand-side Fano-mirror is coupled both to the cavity and the left-environment modes. (from [8])

In the rotating frame of the laser frequency, the Langevin equations for this setup are given by

$$\begin{bmatrix} \dot{\hat{a}} \\ \dot{\hat{d}} \end{bmatrix} = -i \begin{bmatrix} \Delta_a - i(\kappa_a + \gamma_a) & G \\ G & \Delta_d - i\kappa_d \end{bmatrix} \begin{bmatrix} \hat{a} \\ \hat{d} \end{bmatrix} + \text{input fluctuations}, \tag{4.88}$$

where we have introduced the total optical coupling strenght G:

$$G = \lambda - i\sqrt{\kappa_a \kappa_d}. \tag{4.89}$$

The dissipative part of G is $\sqrt{\kappa_a \kappa_d}$.

Without the rotating wave approximation, the eigenvalues of the matrix system (4.88) in the above equation are given by

$$\Omega_\pm = \frac{1}{2}\left(\omega_{cav} + \omega_d - i(\kappa_a + \kappa_d)\right) \pm \sqrt{\left(\frac{1}{2}(\omega_{cav} - \omega_d) - i\frac{1}{2}\left(\kappa_a - \kappa_d\right)\right)^2 - \kappa_a \kappa_d + \lambda^2}. \tag{4.90}$$

4.2.2 Optimization

We recall that the goal of this work is to optimize the cooling of the mechanical resonator. Thus, we need to find the smallest κ in order to narrow as much as possible the effective linewidth of the normal modes.

The effective linewidth of the normal modes is given by the imaginary part of the eigenvalues, Eq. (4.87).

Thus, the discussion comes down to deal with the imaginary parts of the eigenvalues of the two setups. And for the convenience of the discussion, we take $\omega_{\text{cav}} = \omega_d$.

In the Fano-membrane-in-the-middle setup, where we do not take the dispersive couplings into account, the eigenvalues are described by

$$\Omega_{\pm} = ... - i\,\frac{\kappa + \kappa_d}{2} \pm \sqrt{(... - i\,\frac{\kappa - \kappa_d}{2})^2 + \lambda^2}. \tag{4.91}$$

In the left-hand-side-Fano-mirror setup, where the dispersive couplings are taken into account, the eigenvalues are described by

$$\Omega_{\pm} = ... - i\,\frac{\kappa_a + \kappa_d}{2} \pm \sqrt{(... - i\,\frac{\kappa_a - \kappa_d}{2})^2 - \kappa_a\kappa_d + \lambda^2}. \tag{4.92}$$

In both case, the coherent coupling λ between the two optical modes is a detrimental positiv sign term that tends to reduce the linewidth spliting of the normal modes. We thus need to overcome this term.

In the case where there is no dispersive coupling and in the limit where $\lambda = 0$, Eq. (4.91) reads

$$-i\,\frac{\kappa + \kappa_d}{2} \pm i\,\frac{\kappa - \kappa_d}{2}$$

and the only way to have an effective linewidth as narrow as possible is to have $\kappa_d = 0$, what leads to an effective linewidth almost equal to 0.

In the case where there is dispersive coupling and in the limit where $\lambda = 0$, Eq. (4.92) reads

$$-i\,\frac{\kappa + \kappa_d}{2} \pm \sqrt{-\left(\frac{\kappa - \kappa_d}{2}\right)^2 - \kappa_a\kappa_d}$$

and the main idea to obtain an effective linewidth as narrow as possible is to have κ_d as large as possible, so that the dispersive term $\kappa_a\kappa_d$ is big enough and makes the effective linewidth to drop down.

Let us summarize the main idea of the optimization possibilities for the two setups:

- In the Fano-membrane-in-the-middle setup, the fact that the membrane is in the middle of the cavity and therefore does not interact with the external environments leads to a smaller κ_d. In the limit case where $\kappa_d = 0$, the effective linewidth tends to 0. A small κ_d should be used to overcome the detrimental additional positiv-sign term λ^2 ;

- In the left-hand-side-Fano-mirror setup, the fact that the Fano-mirror interacts with the left environment leads to an additional negative-sign term $\kappa_a\kappa_d$ in the effective linewidth. This negative-sign term should be large to overcome the detrimental additional positiv-sign term λ^2 term.

5

Results

5.1 Ground-state Cooling Simulation

In this section, we present the results of the ground-state cooling simulations we performed during this work.

- The first goal of those simulations is to check the validity of the developed theory and to compare the results with the literature.
- The second goal is to compare the results of the Fano-membrane-in-the-middle setup with the standard optomechanical setup. By choosing the parameters of the simulation, we can either choose the standard-optomechanical setup or the Fano-membrane-in-the-middle setup.
- The third goal is to study the effect of the Fano-membrane-in-the-middle setup on the ground-state cooling of the mechanical resonator. We aim to determine the optimal parameters of the Fano-membrane-in-the-middle setup, as explained in the previous section, Sec. 4.2.2.

The ground-state cooling criterion reads

$$\log_{10}(\bar{n}_{\mathrm{mec}}) < 0. \tag{5.1}$$

As shown in Fig. 5.1, the ground-state cooling is achieved for the standard optomechanical setup. The ground state is reached for the value of $\omega_{\mathrm{las}} = \Delta_{\text{-}} - \Omega_{\mathrm{mec}}$, meaning that the effective detuning is equal to the mechanical frequency: the cavity density of states is resonant with the cooling Anti-Stokes process.

Fig. 5.2 shows the simulation performed with the Fano-membrane-in-the-middle setup. The Y-axis represents the final mechanical phonon number n_{fin} normalized by the mechanical phonon number n_{mec}. Here, $n_{\mathrm{mec}} = 4502$. Ground-state cooling is not achieved.

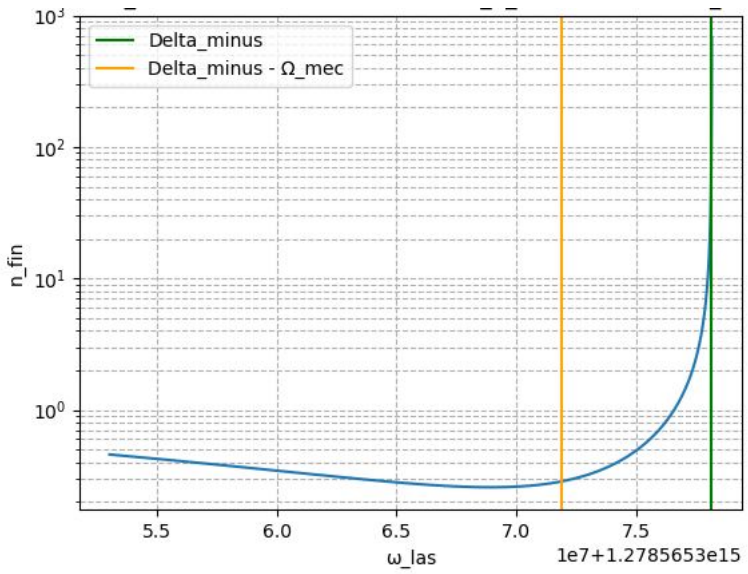

Figure 5.1: Ground-state cooling is achieved for the standard optomechanical setup. The mechanical resonator is cooled to the mechanical ground-state. The simulation is performed with the following parameters: $\omega_{\text{mec}} = 2\pi \times 10^6$ Hz, $\omega_{\text{cav}} = 2\pi \times 10^{14}$ Hz, $\kappa = 2\pi \times 400$ kHz, $g = 2\pi \times 845$ Hz, $\gamma = 2\pi \times 10^{-}1$ Hz, $T = 300$ K.

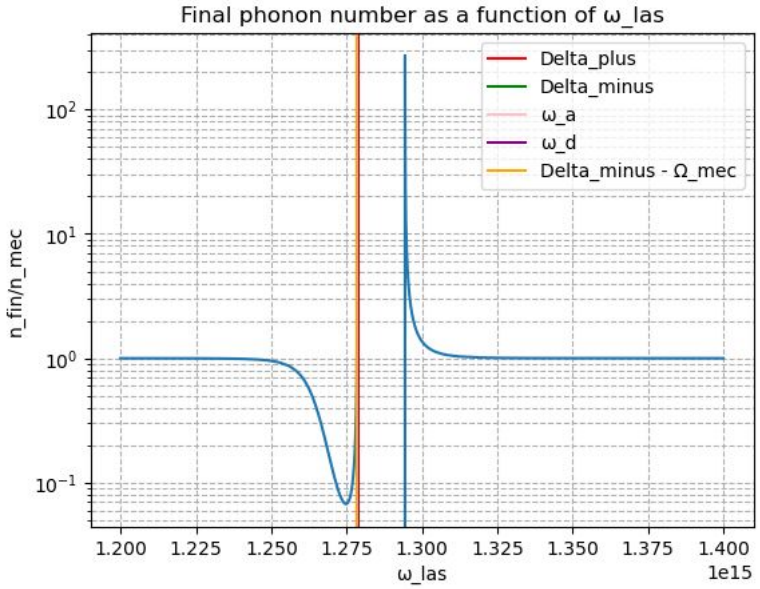

Figure 5.2: Simulation performed with the Fano-membrane-in-the-middle setup. We aim to reach the ground-state of the mechanical resonator for the normal modes of the system.

5.2 Optimization of the Fano-membrane-in-the-middle System Parameters

We aim to determine the optimal parameters of the Fano-membrane-in-the-middle setup to achieve ground-state cooling. To do so, we perform an optimization

of the parameters (see Fig. 5.3).

The optimization is performed by varying the parameters of the Fano-membrane-in-the-middle setup. We aim to minimize the effective linewidth $\kappa_{\text{eff}} = f(\omega_d, \kappa_d, \lambda)$ of the cavity for a given cavity frequancy ω_a. We perform a so called gradient-descent protocol to numerically minimize the effective linewidth.

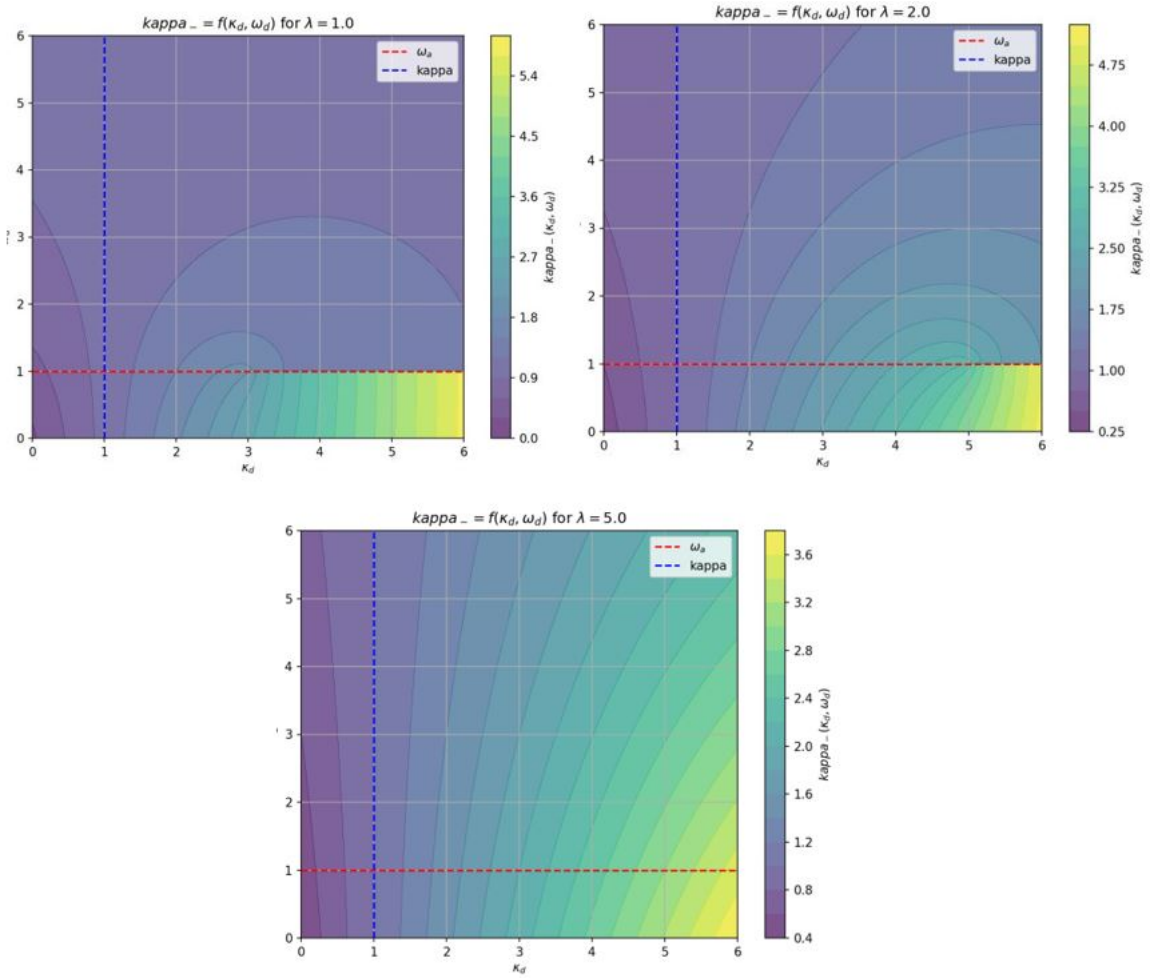

Figure 5.3: Optimization of the Fano-membrane-in-the-middle system parameters with the gradient descent protocol.

The optimization has not given satisfactory results yet. The optimization is still ongoing and is the reason of the extension of the internship for the month of October 2024.

6
Conclusion

At the end of this study, the importance of optomechanical systems in the field of quantum technologies becomes more evident. The theoretical framework developed here serves as a powerful tool for studying the cooling of mechanical resonators and optimizing the cooling process. Achieving this requires a deep understanding of the physics of the system and the ability to manipulate inherent parameters to develop and refine the desired system.

The concept of optomechanical systems was introduced alongside a description of the standard optomechanical setup. In exploring the unresolved-sideband regime, it became clear that an enhancement to the cooling process was necessary. This led to the introduction of the Fano-membrane-based optomechanical system, which improves the cooling of the mechanical resonator due to the unique properties of the photonic crystal. The Fano-membrane-in-the-middle system was described in detail, and the equation for the final phonon number in the mechanical resonator was derived. Additionally, the alternative left-hand-side-Fano-mirror setup was mentioned.

Subsequent exploration of the optical-normal-mode theory and its application to both the left-hand-side-Fano-mirror setup and the Fano-membrane-in-the-middle setup revealed insights into optimizing the cooling of the mechanical resonator. It was found that the key to improving the cooling process lies in overcoming the detrimental positive-sign term λ^2 in the effective linewidth of the normal modes.

This study represents a first step toward optimizing the cooling of mechanical resonators in optomechanical systems. It provides a theoretical framework for studying and improving the cooling process, paving the way for future work. The next step would involve continuing developing the numerical model to simulate and further refine the system. This work contributes to the broader field of quantum technologies and the advancement of quantum devices.

Optomechanical ground state cooling with Fano-membrane in the middle

Aymeric Frerejean

Department of Microtechnology and Nanoscience (MC2), Chalmers University of Technology, SE-412 96, Göteborg, Sweden

Abstract: Laser cooling techniques offer general methods for preparing microscopic resonators in their motional ground state. We report on theoretical investigations of an optomechanical system which comprises a frequency-dependent photonic-crystal membrane (Fano mirror) placed in the middle of an optical cavity. The quantum Langevin equations are derived for a single cavity mode, a guided optical (Fano) mode of the membrane, and a mechanical mode accounting for the out-of-plane displacement of the membrane, due to its very small reflectivity. We exhibit the linear behaviours of the optomechanical interaction by placing the membrane in between a node and an anti-node of the cavity standing wave. The Fano-mirror setup shows enhanced sideband cooling through the reduction of the spectral linewidth of the cavity compared to conventional systems lacking the Fano mode. This enhancement allows for ground-state cooling of the mechanical mode, even in the (deeply) unresolved-sideband regime. Furthermore, we investigate the effective quality factor of the cavity and normal modes formed by the coupled cavity and Fano modes. The normal modes show two complex eigenfrequencies, whose real $\omega_\pm = \Re(\omega_\pm)$ and imaginary $\kappa_\pm = -\Im(\omega_\pm)$ parts correspond to their effective resonance frequencies and loss rates, respectively. This formalism provides an intuitive framework for determining the optimal manufacturing parameters needed to achieve ground-state cooling.

1 Motivations

Quantum Ground State Preparation
- Bring a mechanical oscillator down to its quantum ground state

➡ Quantum effects become significant!

Quantum Information Processing
- Quantum Transducers: convert quantum states between light and microwaves

Precision Measurements and Sensors
- Force Sensing: weak magnetic fields or gravitational waves
- Displacement Sensing at the atomic scale
- Mass Sensing: detecting single molecules

2 Standard setup for optomechanical cooling

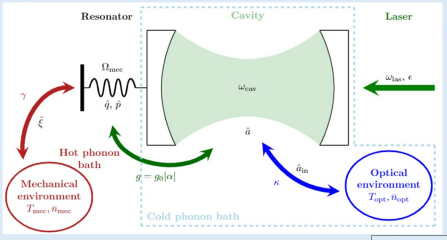

Tricky point: How can the significant disparity in orders of magnitude between optical and mechanical frequencies be effectively managed?

Cavity with a moving-end mirror driven by a laser, coupled to a photon and a phonon bath ➡ Energy loss of the resonator through the cavity using large optical decay rate

3 Principle of resolved-sideband cooling

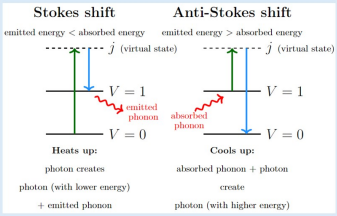

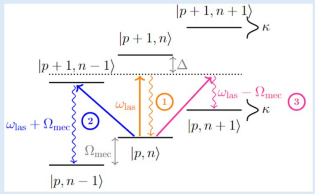

Resolved-sideband cooling condition: $\kappa \ll \Omega_{\mathrm{mec}}$

4 Objective

How to cool down even if large κ ?

Make short cavity
But short cavity has a higher κ ➡
- System parameter control for enhanced anti-Stokes process
- Use a Fano (photonic crystal) membrane

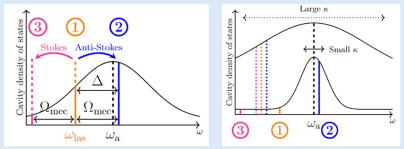

5 Membrane in the middle + Fano mirror setup

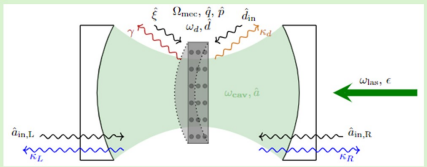

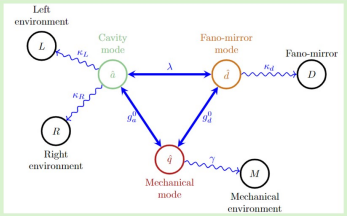

Fano mirror:
- movable photonic crystal membrane
- guided optical mode

➡ Cool and control optomechanical systems that are originally in the unresolved-sideband regime

6 Assumptions of the model

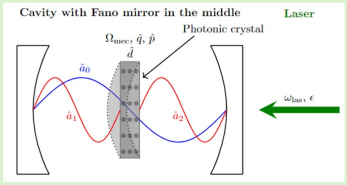

$$g_0 = \left.\frac{\delta\omega_a}{\delta x}\right|_{x=x_0}$$

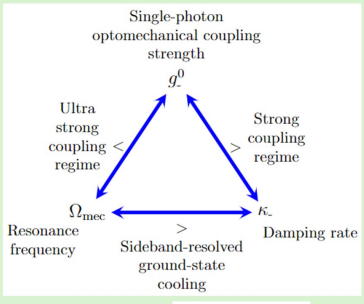

Linearization condition: $g_{a/d}^0/\Omega_{\mathrm{mec}} \approx 10^{-3}$

7 Derivation

$$\hat{H}_{\mathrm{Sys}} = \overbrace{\hbar\omega_a \hat{a}^\dagger \hat{a}}^{\text{Cavity}} + \overbrace{\hbar\omega_d \hat{d}^\dagger \hat{d}}^{\text{Fano-mirror}} + \overbrace{\hbar\Omega_{\mathrm{mec}} \hat{b}^\dagger \hat{b}}^{\text{Mechanics}} \underbrace{- \hbar g_a^0 \sqrt{2}\hat{a}^\dagger \hat{a}\hat{q} - \hbar g_d^0 \sqrt{2}\hat{d}^\dagger \hat{d}\hat{q}}_{\text{Coupling}} + \underbrace{\hbar\lambda(\hat{a}^\dagger \hat{d} + \hat{d}^\dagger \hat{a})}_{\text{Non linear term}} + \overbrace{\hbar(\epsilon \hat{a}^\dagger + \epsilon^* \hat{a})}^{\text{Drive}},$$

$$\begin{pmatrix} \dot{\hat{a}} \\ \dot{\hat{d}} \end{pmatrix} = -i \begin{pmatrix} \Delta_a^0 - i\kappa & \lambda \\ \lambda & \Delta_d^0 - i\kappa_d \end{pmatrix} \begin{pmatrix} \hat{a} \\ \hat{d} \end{pmatrix} + \text{input flux}$$

$$\Omega_\pm = \frac{1}{2}\left(\omega_a + \omega_d - i(\kappa + \kappa_d)\right) \pm \sqrt{\left(\frac{1}{2}(\omega_a - \omega_d) - i\frac{1}{2}(\kappa - \kappa_d)\right)^2 + \lambda^2}$$

$$\dot{\hat{O}} = \underbrace{\frac{i}{\hbar}[\hat{O}, \hat{H}_{\mathrm{sys}}]}_{\text{System}} - \underbrace{\sum_{\mu,\ \text{all the environments}} \left([\hat{O}, \hat{c}_\mu^\dagger]\left(\kappa_\mu \hat{c}_\mu + \sqrt{2\kappa_\mu}\hat{b}_{\mathrm{in},\mu}(t)\right) - \left(\kappa_\mu \hat{c}_\mu^\dagger + \sqrt{2\kappa_\mu}\hat{b}_{\mathrm{in},\mu}^\dagger(t)\right)[\hat{O}, \hat{c}_\mu]\right)}_{\text{Dissipation}}$$

➡ Effective resonant frequencies and damping rates of the system:

$$\Delta_+ = \mathrm{Re}[\Omega_+], \quad \Delta_- = \mathrm{Re}[\Omega_-], \quad \kappa_+ = -\mathrm{Im}[\Omega_+], \quad \kappa_- = -\mathrm{Im}[\Omega_-].$$

➡ $\dfrac{\kappa}{\Omega_{\mathrm{mec}}} \ll 1$

8 Results

$$n_{\mathrm{fin}} = \frac{1}{2}\left(\langle \delta q^2 \rangle + \langle \delta p^2 \rangle - 1\right)$$

➡ Criterion of mechanical ground-state cooling: $\log_{10}(n_{\mathrm{fin}}) < 0$

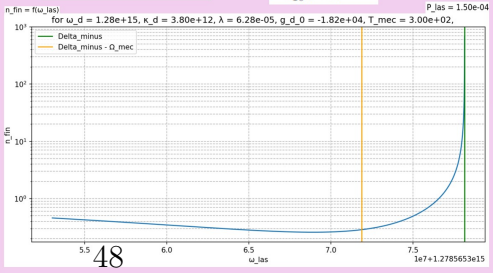

Minimization of kappa using a gradient descent protocol:

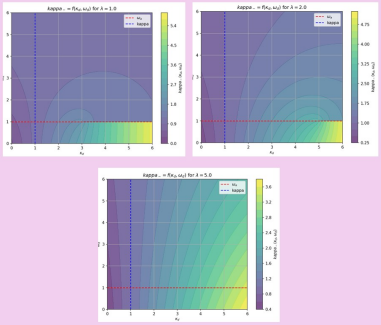

9 Outlook

- Evaluate the final phonon number in an optomechanical system with a Fano mirror
- Explore the possible values for the coupling parameter λ
- Determine the optimal parameters to achieve ground state cooling

➡
- Achieve ground-state cooling in the (deeply) unresolved-sideband regime
- Reverse process: heating

Bibliography

[1] Markus Aspelmeyer, Tobias J. Kippenberg, and Florian Marquardt. Cavity optomechanics. *Rev. Mod. Phys.*, 86:1391–1452, Dec 2014.

[2] C. W. Gardiner and M. J. Collett. Input and output in damped quantum systems: Quantum stochastic differential equations and the master equation. *Phys. Rev. A*, 31:3761–3774, Jun 1985.

[3] Ond řej Černotík, Aurélien Dantan, and Claudiu Genes. Cavity quantum electrodynamics with frequency-dependent reflectors. *Phys. Rev. Lett.*, 122:243601, Jun 2019.

[4] Sushanth Kini Manjeshwar, Anastasiia Ciers, Juliette Monsel, Hannes Pfeifer, Cindy Peralle, Shu Min Wang, Philippe Tassin, and Witlef Wieczorek. Integrated microcavity optomechanics with a suspended photonic crystal mirror above a distributed bragg reflector. *Optics Express*, 31(19):30212, August 2023.

[5] Gabriel T. Landi. *Quantum Information and Quantum Noise*. University of Sao Paulo, Sao Paulo, 2018.

[6] C. K. Law. Interaction between a moving mirror and radiation pressure: A hamiltonian formulation. *Phys. Rev. A*, 51:2537–2541, Mar 1995.

[7] Warwick P. Bowen Gerard J. Milburn. *Quantum Optomechanics*. CRC Press, STaylor and Francis Group 6000 Broken Sound Parkway NW Suite 300 Boca Raton FL 33487-2742, 2016.

[8] Juliette Monsel, Anastasiia Ciers, Sushanth Kini Manjeshwar, Witlef Wieczorek, and Janine Splettstoesser. Dissipative and dispersive cavity optomechanics with a frequency-dependent mirror. *Phys. Rev. A*, 109:043532, Apr 2024.

[9] Juliette Monsel, Nastaran Dashti, Sushanth Kini Manjeshwar, Jakob Eriksson, Henric Ernbrink, Ebba Olsson, Emelie Torneus, Witlef Wieczorek, and Janine Splettstoesser. Optomechanical cooling with coherent and squeezed light: The thermodynamic cost of opening the heat valve. *Phys. Rev. A*, 103:063519, Jun 2021.

[10] Andreas Naesby and Aurélien Dantan. Microcavities with suspended subwavelength structured mirrors. *Opt. Express*, 26(23):29886–29894, Nov 2018.

A

Appendix A

A.1 Useful quantum mechanics Relations

The following relations are useful results in quantum mechanics.

$$\begin{aligned}
\hat{p}^2 + \hat{q}^2 &= \left(\frac{i}{\sqrt{2}}\left(\hat{b}^\dagger - \hat{b}\right)\right)^2 + \left(\frac{1}{\sqrt{2}}\left(\hat{b}^\dagger + \hat{b}\right)\right)^2 \\
&= -\frac{1}{2}\left(\hat{b}^\dagger\hat{b}^\dagger + \hat{b}\hat{b} - \hat{b}^\dagger\hat{b} - \hat{b}\hat{b}^\dagger\right) \\
&\quad + \frac{1}{2}\left(\hat{b}^\dagger\hat{b}^\dagger + \hat{b}\hat{b} + \hat{b}^\dagger\hat{b} + \hat{b}\hat{b}^\dagger\right) \\
&= \hat{b}^\dagger\hat{b} + \hat{b}\hat{b}^\dagger \\
&= \hat{b}^\dagger\hat{b} + \hat{b}\hat{b}^\dagger - \hat{b}^\dagger\hat{b} + \hat{b}^\dagger\hat{b} \\
&= 2\hat{b}^\dagger\hat{b} + [\hat{b}, \hat{b}^\dagger] \\
&= 2\hat{b}^\dagger\hat{b} + 1
\end{aligned} \tag{A.1}$$

$$\begin{aligned}
[\hat{q}, \hat{p}] &= \left[\frac{1}{\sqrt{2}}(\hat{b}^\dagger + \hat{b}), \frac{i}{\sqrt{2}}(\hat{b}^\dagger - \hat{b})\right] \\
&= \frac{i}{2}\left[\hat{b}^\dagger + \hat{b}, \hat{b}^\dagger - \hat{b}\right] \\
&= \frac{i}{2}\left([\hat{b}^\dagger, \hat{b}^\dagger] + [\hat{b}^\dagger, -\hat{b}] + [\hat{b}, \hat{b}^\dagger] + [\hat{b}, -\hat{b}]\right) \\
&= \frac{i}{2}\left(0 + [\hat{b}, \hat{b}^\dagger] - [\hat{b}^\dagger, \hat{b}] - 0\right) \\
&= \frac{i}{2} \cdot 2 \\
&= i
\end{aligned} \tag{A.2}$$

$$\begin{aligned}\left[\hat{p},\hat{q}^2\right] &= \hat{p}\hat{q}^2 - \hat{q}^2\hat{p} \\ &= \hat{p}\hat{q}^2 - \hat{q}\hat{p}\hat{q} + \hat{q}\hat{p}\hat{q} - \hat{q}^2\hat{p} \\ &= (\hat{p}\hat{q} - \hat{q}\hat{p})\,\hat{q} + \hat{q}\,(\hat{p}\hat{q} - \hat{q}\hat{p}) \\ &= [\hat{p},\hat{q}]\,\hat{q} + \hat{q}\,[\hat{p},\hat{q}] \\ &= (-i)\hat{q} + \hat{q}(-i) \\ &= -2i\hat{q} \end{aligned} \tag{A.3}$$

$$\begin{aligned}\left[\hat{q},\hat{p}^2\right] &= \hat{q}\hat{p}^2 - \hat{p}^2\hat{q} \\ &= \hat{q}\hat{p}^2 - \hat{p}\hat{q}\hat{p} + \hat{p}\hat{q}\hat{p} - \hat{p}^2\hat{q} \\ &= (\hat{q}\hat{p} - \hat{p}\hat{q})\,\hat{p} + \hat{p}\,(\hat{q}\hat{p} - \hat{p}\hat{q}) \\ &= [\hat{q},\hat{p}]\,\hat{p} + \hat{p}\,[\hat{q},\hat{p}] \\ &= i\hat{p} + \hat{p}i \\ &= 2i\hat{p} \end{aligned} \tag{A.4}$$

$$\left[\hat{a}^\dagger\hat{a},\hat{a}\right] = (-1)\hat{a} \tag{A.5}$$

$$\begin{aligned}\left[\hat{a}^\dagger\hat{a},\left[\hat{a}^\dagger\hat{a},\hat{a}\right]\right] &= \left[\hat{a}^\dagger\hat{a},(-1)\hat{a}\right] \\ &= (-1)\left[\hat{a}^\dagger\hat{a},\hat{a}\right] \\ &= (-1)(-1)\hat{a} \end{aligned} \tag{A.6}$$

B

Appendix B

B.1 Derivation of the MQLE for the Fano-membrane-in-the-middle Setup

In this section, we detail the derivation of the the Markovian Quantum Langevin Equation for the Fano-membrane-in-the-middle setup.

The hamiltonian of the Fano-membrane-in-the-middle setup is, in the rotating frame at $\omega_{\rm las}$,

$$\begin{aligned}\hat{H}_{\rm Sys} = {} & \hbar\Delta_a^0\hat{a}^\dagger\hat{a} + \hbar\Delta_d^0\hat{d}^\dagger\hat{d} + \hbar\Omega_{\rm mec}\hat{b}^\dagger\hat{b} - \hbar g_a^0\sqrt{2}\,\hat{a}^\dagger\hat{a}\hat{q} - \hbar g_d^0\sqrt{2}\,\hat{d}^\dagger\hat{d}\hat{q} \\ & + \hbar\lambda(\hat{a}^\dagger\hat{d} + \hat{d}^\dagger\hat{a}) + \hbar(\epsilon\hat{a}^\dagger + \epsilon^*\hat{a}),\end{aligned} \tag{B.1}$$

For the position operator, we have

$$\begin{aligned}\dot{\hat{q}} &= \frac{1}{i\hbar}\left[\hat{q}, \hat{H}_{\rm sys}\right] + i\sqrt{\gamma}\,[\hat{q},\hat{q}]\,\hat{\xi}(t) + \frac{1}{2iQ}\left\{[\hat{q},\hat{q}], \dot{\hat{q}}(t)\right\}_+ \\ &= \frac{1}{i\hbar}\left[\hat{q}, \hat{H}_{\rm sys}\right] \\ &= \frac{1}{i\hbar}\Big[\hat{q}, \hbar\Delta_a^0\hat{a}^\dagger\hat{a} + \hbar\Delta_d^0\hat{d}^\dagger\hat{d} + \hbar\Omega_{\rm mec}\hat{b}^\dagger\hat{b} - \hbar g_a^0\sqrt{2}\,\hat{a}^\dagger\hat{a}\hat{q} \\ &\qquad -\hbar g_d^0\sqrt{2}\,\hat{d}^\dagger\hat{d}\hat{q} + \hbar\lambda(\hat{a}^\dagger\hat{d} + \hat{d}^\dagger\hat{a}) + \hbar(\epsilon\hat{a}^\dagger + \epsilon^*\hat{a})\Big] \\ &= \frac{1}{i\hbar}\left[\hat{q}, \hbar\Omega_{\rm mec}\hat{b}^\dagger\hat{b}\right] \\ &= \frac{1}{i\hbar}\left[\hat{q}, \hbar\Omega_{\rm mec}\frac{\hat{p}^2+\hat{q}^2}{2}\right] \\ &= \frac{\Omega_{\rm mec}}{2i}\left[\hat{q}, \hat{p}^2\right] \\ &= \frac{\Omega_{\rm mec}}{2i}\Big(\hat{p}[\hat{q},\hat{p}] + [\hat{q},\hat{p}]\hat{p}\Big) \\ &= \frac{\Omega_{\rm mec}}{2i}\left(\hat{p}\cdot i + i\cdot\hat{p}\right) \\ &= \frac{\Omega_{\rm mec}}{2i}\left(i\hat{p} + i\hat{p}\right) \\ &= \Omega_{\rm mec}\hat{p}.\end{aligned} \tag{B.2}$$

For the momentum operator, we have

$$
\begin{aligned}
\dot{\hat{p}} &= \frac{1}{i\hbar}\left[\hat{p}, \hat{H}_{\mathrm{sys}}\right] + i\sqrt{\gamma}\,[\hat{p}, \hat{q}]\,\hat{\xi}(t) + \frac{1}{2iQ}\left\{[\hat{p}, \hat{q}], \dot{\hat{q}}(t)\right\}_+ \\
&= \frac{1}{i\hbar}\Big[\hat{p}, \hbar\Delta_a^0 \hat{a}^\dagger\hat{a} + \hbar\Delta_d^0 \hat{d}^\dagger\hat{d} + \hbar\Omega_{\mathrm{mec}}\hat{b}^\dagger\hat{b} - \hbar g_a^0\sqrt{2}\,\hat{a}^\dagger\hat{a}\hat{q} \\
&\qquad -\hbar g_d^0\sqrt{2}\,\hat{d}^\dagger\hat{d}\hat{q} + \hbar\lambda(\hat{a}^\dagger\hat{d} + \hat{d}^\dagger\hat{a}) + \hbar(\epsilon\hat{a}^\dagger + \epsilon^*\hat{a})\Big] \\
&\quad + \sqrt{\gamma}\,\hat{\xi}(t) + \frac{1}{2iQ}\left\{-i, \dot{\hat{q}}(t)\right\}_+ \\
&= \frac{1}{i\hbar}\left(\left[\hat{p}, \frac{\hbar\Omega_{\mathrm{mec}}}{2}(\hat{p}^2 + \hat{q}^2)\right] + i\hbar g_a^0\sqrt{2}\,\hat{a}^\dagger\hat{a} + i\hbar g_d^0\sqrt{2}\,\hat{d}^\dagger\hat{d}\right) \\
&\quad + \sqrt{\gamma}\,\hat{\xi}(t) - \frac{1}{2Q}\cdot 2\dot{\hat{q}}(t) \\
&= \frac{1}{i\hbar}\left(\frac{\hbar\Omega_{\mathrm{mec}}}{2}\left[\hat{p}, \hat{q}^2\right] + i\hbar g_a^0\sqrt{2}\,\hat{a}^\dagger\hat{a} + i\hbar g_d^0\sqrt{2}\,\hat{d}^\dagger\hat{d}\right) \\
&\quad + \sqrt{\gamma}\,\hat{\xi}(t) - \left(\frac{\Omega_{\mathrm{mec}}}{\gamma}\right)^{-1}\dot{\hat{q}}(t) \\
&= \frac{\Omega_{\mathrm{mec}}}{2i}\left[\hat{p}, \hat{q}^2\right] + g_a^0\sqrt{2}\,\hat{a}^\dagger\hat{a} + g_d^0\sqrt{2}\,\hat{d}^\dagger\hat{d} + \sqrt{\gamma}\,\hat{\xi}(t) - \gamma\,\hat{p} \\
&= \frac{\Omega_{\mathrm{mec}}}{2i}\,(-2i\hat{q}) + g_a^0\sqrt{2}\,\hat{a}^\dagger\hat{a} + g_d^0\sqrt{2}\,\hat{d}^\dagger\hat{d} + \sqrt{\gamma}\,\hat{\xi}(t) - \gamma\,\hat{p} \\
&= -\Omega_{\mathrm{mec}}\hat{q} - \gamma\,\hat{p} + g_a^0\sqrt{2}\,\hat{a}^\dagger\hat{a} + g_d^0\sqrt{2}\,\hat{d}^\dagger\hat{d} + \sqrt{\gamma}\,\hat{\xi}(t). \qquad \text{(B.3)}
\end{aligned}
$$

For the cavity operator, we have

$$
\begin{aligned}
\dot{\hat{a}} &= \frac{1}{i\hbar}\left[\hat{a}, \hat{H}_{\text{sys}}\right] - \left(\left[\hat{a}, \hat{d}^\dagger\right]\left(\kappa_d \hat{d} + \sqrt{2\kappa_d}\,\hat{d}_{\text{in}}(t)\right) - \left(\kappa_d \hat{d}^\dagger + \sqrt{2\kappa_d}\,\hat{d}^\dagger_{\text{in}}(t)\right)\left[\hat{a}, \hat{d}\right]\right) \\
&\quad - \left(\left[\hat{a}, \hat{a}^\dagger\right]\left(\kappa_L \hat{a} + \sqrt{2\kappa_L}\,\hat{a}_{\text{in},L}(t)\right) - \left(\kappa_L \hat{a}^\dagger + \sqrt{2\kappa_L}\,\hat{a}^\dagger_{\text{in},L}(t)\right)[\hat{a}, \hat{a}]\right) \\
&\quad - \left(\left[\hat{a}, \hat{a}^\dagger\right]\left(\kappa_R \hat{a} + \sqrt{2\kappa_R}\,\hat{a}_{\text{in},R}(t)\right) - \left(\kappa_R \hat{a}^\dagger + \sqrt{2\kappa_R}\,\hat{a}^\dagger_{\text{in},R}(t)\right)[\hat{a}, \hat{a}]\right) \\
&= \frac{1}{i\hbar}\Big[\hat{a}, \hbar\Delta_a^0 \hat{a}^\dagger\hat{a} + \hbar\Delta_d^0 \hat{d}^\dagger\hat{d} + \hbar\Omega_{\text{mec}}\hat{b}^\dagger\hat{b} - \hbar g_a^0\sqrt{2}\,\hat{a}^\dagger\hat{a}\hat{q} - \hbar g_d^0\sqrt{2}\,\hat{d}^\dagger\hat{d}\hat{q} \\
&\quad + \hbar\lambda(\hat{a}^\dagger\hat{d} + \hat{d}^\dagger\hat{a}) + \hbar(\epsilon\hat{a}^\dagger + \epsilon^*\hat{a})\Big] \\
&\quad - \left[\hat{a}, \hat{a}^\dagger\right]\left(\kappa_L \hat{a} + \sqrt{2\kappa_L}\,\hat{a}_{\text{in},L}(t)\right) \\
&\quad - \left[\hat{a}, \hat{a}^\dagger\right]\left(\kappa_R \hat{a} + \sqrt{2\kappa_R}\,\hat{a}_{\text{in},R}(t)\right) \\
&= \frac{1}{i\hbar}\left(\left[\hat{a}, \hbar\Delta_a^0 \hat{a}^\dagger\hat{a}\right] - \left[\hat{a}, \hbar g_a^0\sqrt{2}\,\hat{a}^\dagger\hat{a}\hat{q}\right] + \left[\hat{a}, \hbar\lambda(\hat{a}^\dagger\hat{d} + \hat{d}^\dagger\hat{a})\right] + \left[\hat{a}, \hbar(\epsilon\hat{a}^\dagger + \epsilon^*\hat{a})\right]\right) \\
&\quad - (\kappa_L + \kappa_R)\,\hat{a} - \sqrt{2\kappa_L}\,\hat{a}_{\text{in},L}(t) - \sqrt{2\kappa_R}\,\hat{a}_{\text{in},R}(t) \\
&= \frac{1}{i\hbar}\Big(\hbar\Delta_a^0\left(\hat{a}\hat{a}^\dagger\hat{a} - \hat{a}^\dagger\hat{a}\hat{a}\right) - \hbar g_a^0\sqrt{2}\,\hat{q}\left(\hat{a}\hat{a}^\dagger\hat{a} - \hat{a}^\dagger\hat{a}\hat{a}\right) \\
&\quad + \hbar\lambda\left(\hat{a}\hat{a}^\dagger\hat{d} - \hat{a}^\dagger\hat{d}\hat{a} + \hat{a}\hat{d}^\dagger\hat{a} - \hat{d}^\dagger\hat{a}\hat{a}\right) + \hbar\left(\hat{a}\epsilon\hat{a}^\dagger - \epsilon\hat{a}^\dagger\hat{a} + \hat{a}\epsilon^*\hat{a} - \epsilon^*\hat{a}\hat{a}\right)\Big) \\
&\quad - (\kappa_L + \kappa_R)\,\hat{a} - \sqrt{2\kappa_L}\,\hat{a}_{\text{in},L}(t) - \sqrt{2\kappa_R}\,\hat{a}_{\text{in},R}(t) \\
&= \frac{1}{i\hbar}\left(\hbar\Delta_a^0\left[\hat{a}, \hat{a}^\dagger\right]\hat{a} - \hbar g_a^0\sqrt{2}\,\hat{q}\left[\hat{a}, \hat{a}^\dagger\right]\hat{a} + \hbar\lambda\hat{d}\left[\hat{a}, \hat{a}^\dagger\right] + \hbar\epsilon\left[\hat{a}, \hat{a}^\dagger\right]\right) \\
&\quad - (\kappa_L + \kappa_R)\,\hat{a} - \sqrt{2\kappa_L}\,\hat{a}_{\text{in},L}(t) - \sqrt{2\kappa_R}\,\hat{a}_{\text{in},R}(t) \\
&= -\left(i\Delta_a^0 + \kappa\right)\hat{a} + ig_a^0\sqrt{2}\,\hat{q}\hat{a} - i\lambda\hat{d} - i\epsilon \\
&\quad - \sqrt{2\kappa_L}\,\hat{a}_{\text{in},L}(t) - \sqrt{2\kappa_R}\,\hat{a}_{\text{in},R}(t), \quad \kappa = \kappa_L + \kappa_R.
\end{aligned}
\tag{B.4}
$$

For the Fano-optical operator, we have

$$\begin{aligned}
\dot{\hat{d}} &= \frac{1}{i\hbar}\left[\hat{d}, \hat{H}_{\rm sys}\right] - \left(\left[\hat{d}, \hat{d}^\dagger\right]\left(\kappa_d \hat{d} + \sqrt{2\kappa_d}\,\hat{d}_{\rm in}(t)\right) - \left(\kappa_d \hat{d}^\dagger + \sqrt{2\kappa_d}\,\hat{d}^\dagger_{\rm in}(t)\right)\left[\hat{d}, \hat{d}\right]\right) \\
&= \frac{1}{i\hbar}\Big[\hat{d}, \hbar\Delta_a^0 \hat{a}^\dagger\hat{a} + \hbar\Delta_d^0 \hat{d}^\dagger\hat{d} + \hbar\Omega_{\rm mec}\hat{b}^\dagger\hat{b} - \hbar g_a^0\sqrt{2}\,\hat{a}^\dagger\hat{a}\hat{q} - \hbar g_d^0\sqrt{2}\,\hat{d}^\dagger\hat{d}\hat{q} \\
&\quad + \hbar\lambda(\hat{a}^\dagger\hat{d} + \hat{d}^\dagger\hat{a}) + \hbar(\epsilon\hat{a}^\dagger + \epsilon^*\hat{a})\Big] \\
&\quad - \kappa\hat{d} - \sqrt{2\kappa_d}\,\hat{d}_{\rm in}(t) \\
&= -\frac{i}{\hbar}\Big(\hbar\Delta_d^0\left(\hat{d}\hat{d}^\dagger\hat{d} - \hat{d}^\dagger\hat{d}\hat{d}\right) - \hbar g_d^0\sqrt{2}\,\hat{q}\left(\hat{d}\hat{d}^\dagger\hat{d} - \hat{d}^\dagger\hat{d}\hat{d}\right) + \hbar\lambda\left(\hat{d}\hat{a}^\dagger\hat{d} - \hat{a}^\dagger\hat{d}\hat{d} + \hat{d}\hat{d}^\dagger\hat{a} - \hat{d}^\dagger\hat{a}\hat{d}\right)\Big) \\
&\quad - \kappa\hat{d} - \sqrt{2\kappa_d}\,\hat{d}_{\rm in}(t) \\
&= -\frac{i}{\hbar}\Big(\hbar\Delta_d^0\left[\hat{d}, \hat{d}^\dagger\right]\hat{d} - \hbar g_d^0\sqrt{2}\,\hat{q}\left[\hat{d}, \hat{d}^\dagger\right]\hat{d} + \hbar\lambda\hat{a}\left[\hat{d}, \hat{d}^\dagger\right]\Big) \\
&\quad - \kappa\hat{d} - \sqrt{2\kappa_d}\,\hat{d}_{\rm in}(t) \\
&= -\left(i\Delta_d^0 + \kappa_d\right)\hat{d} + ig_d^0\sqrt{2}\,\hat{q}\hat{d} - i\lambda\hat{a} - \sqrt{2\kappa_d}\,\hat{d}_{\rm in}(t). \qquad \text{(B.5)}
\end{aligned}$$

B.2 Linearization of the MQLE around the semi-classical steady state for the Fano-membrane-in-the-middle Setup

For the cavity operator, from (B.4)

$$\dot{\hat{a}} = -\left(i\Delta_a^0 + \kappa\right)\hat{a} + ig_a^0\sqrt{2}\,\hat{q}\hat{a} - i\lambda\hat{d} - i\epsilon - \sqrt{2\kappa_L}\,\hat{a}_{\mathrm{in},L}(t) - \sqrt{2\kappa_R}\,\hat{a}_{\mathrm{in},R}(t),$$

we derive

$$\begin{aligned}\frac{d}{dt}(\alpha+\delta\hat{a}) = &-\left(i\Delta_a^0+\kappa\right)(\alpha+\delta\hat{a}) + ig_a^0\sqrt{2}\,(\overline{q}+\delta\hat{q})(\alpha+\delta\hat{a})\\ &- i\lambda(\delta+\delta\hat{d}) - i\epsilon - \sqrt{2\kappa_L}\,\hat{a}_{\mathrm{in},L}(t) - \sqrt{2\kappa_R}\,\hat{a}_{\mathrm{in},R}(t).\end{aligned} \tag{B.6}$$

So

$$\begin{aligned}\delta\dot{\hat{a}} &= -\left(i\Delta_a^0+\kappa\right)(\alpha+\delta\hat{a}) + ig_a^0\sqrt{2}\,(\overline{q}\alpha+\overline{q}\delta\hat{a}+\delta\hat{q}\alpha+\delta\hat{q}\delta\hat{a})\\ &\quad - i\lambda(\delta+\delta\hat{d}) - i\epsilon - \sqrt{2\kappa_L}\,\hat{a}_{\mathrm{in},L}(t) - \sqrt{2\kappa_R}\,\hat{a}_{\mathrm{in},R}(t)\\ &= -\left(i\Delta_a^0+\kappa\right)\alpha - \left(i\Delta_a^0+\kappa\right)\delta\hat{a}\\ &\quad + ig_a^0\sqrt{2}\,\overline{q}\alpha + ig_a^0\sqrt{2}\,\overline{q}\delta\hat{a} + ig_a^0\sqrt{2}\,\delta\hat{q}\alpha + ig_a^0\sqrt{2}\,\delta\hat{q}\delta\hat{a}\\ &\quad - i\lambda\delta - i\lambda\delta\hat{d} - i\epsilon - \sqrt{2\kappa_L}\,\hat{a}_{\mathrm{in},L}(t) - \sqrt{2\kappa_R}\,\hat{a}_{\mathrm{in},R}(t)\\ &= -\left(\kappa + i(\Delta_a^0 - g_a^0\sqrt{2}\,\overline{q})\right)\alpha - \left(\kappa + i(\Delta_a^0 - g_a^0\sqrt{2}\,\overline{q})\right)\delta\hat{a}\\ &\quad + ig_a^0\sqrt{2}\delta\hat{q}\alpha\\ &\quad - i\lambda\delta - i\lambda\delta\hat{d} - i\epsilon - \sqrt{2\kappa_L}\,\hat{a}_{\mathrm{in},L}(t) - \sqrt{2\kappa_R}\,\hat{a}_{\mathrm{in},R}(t).\end{aligned} \tag{B.7}$$

Sustituting $\alpha = \frac{-i(\epsilon+\lambda\delta)}{\kappa+i\Delta_a}$, we get:

$$\delta\dot{\hat{a}} = -\left(i\Delta_a + \kappa\right)\delta\hat{a} + ig_a\sqrt{2}\,\delta\hat{q} - i\lambda\delta\hat{d} - \sqrt{2\kappa_L}\,\hat{a}_{\mathrm{in},L}(t) - \sqrt{2\kappa_R}\,\hat{a}_{\mathrm{in},R}(t). \tag{B.8}$$

For the Fano-optical operator, from (B.5),

$$\dot{\hat{d}} = -\left(i\Delta_d^0 + \kappa_d\right)\hat{d} + ig_d^0\sqrt{2}\,\hat{q}\hat{d} - i\lambda\hat{a} - \sqrt{2\kappa_d}\,\hat{d}_{\mathrm{in}}(t),$$

we derive

$$\begin{aligned}\frac{d}{dt}(\delta+\delta\hat{d}) = &-\left(i\Delta_d^0+\kappa_d\right)(\delta+\delta\hat{d}) + ig_d^0\sqrt{2}\,(\overline{q}+\delta\hat{q})(\delta+\delta\hat{d})\\ &- i\lambda(\alpha+\delta\hat{a}) - \sqrt{2\kappa_d}\,\hat{d}_{\mathrm{in}}(t).\end{aligned} \tag{B.9}$$

So

$$\begin{aligned}\delta\dot{\hat{d}} &= -\left(i\Delta_d^0+\kappa_d\right)(\delta+\delta\hat{d}) + ig_d^0\sqrt{2}\,\left(\overline{q}\delta+\overline{q}\delta\hat{d}+\delta\hat{q}\delta+\delta\hat{q}\delta\hat{d}\right)\\ &\quad - i\lambda(\alpha+\delta\hat{a}) - \sqrt{2\kappa_d}\,\hat{d}_{\text{in}}(t)\\ &= -\left(i\Delta_d^0+\kappa_d\right)\delta - \left(i\Delta_d^0+\kappa_d\right)\delta\hat{d}\\ &\quad + ig_d^0\sqrt{2}\,\overline{q}\delta + ig_d^0\sqrt{2}\,\overline{q}\delta\hat{d} + ig_d^0\sqrt{2}\,\delta\hat{q}\delta + ig_d^0\sqrt{2}\,\delta\hat{q}\delta\hat{d}\\ &\quad - i\lambda\alpha - i\lambda\delta\hat{a} - \sqrt{2\kappa_d}\,\hat{d}_{\text{in}}(t)\\ &= -\left(\kappa_d+i(\Delta_d^0-g_d^0\sqrt{2}\,\overline{q})\right)\delta - \left(\kappa_d+i(\Delta_d^0-g_d^0\sqrt{2}\,\overline{q})\right)\delta\hat{d}\\ &\quad + ig_d^0\sqrt{2}\,\delta\hat{q}\delta\\ &\quad - i\lambda\alpha - i\lambda\delta\hat{a} - \sqrt{2\kappa_d}\,\hat{d}_{\text{in}}(t). \end{aligned} \tag{B.10}$$

Sustituting $\delta = \frac{-i\lambda\alpha}{\kappa_d+i\Delta_d}$, we get:

$$\delta\dot{\hat{d}} = -\left(i\Delta_d+\kappa_d\right)\delta\hat{d} + ig_d\sqrt{2}\,\delta\hat{q} - i\lambda\delta\hat{a} - \sqrt{2\kappa_d}\,\hat{d}_{\text{in}}(t). \tag{B.11}$$

For the position operator, from (B.2),

$$\dot{\hat{q}} = \Omega_{\text{mec}}\hat{p},$$

we derive

$$\frac{d}{dt}(\overline{q}+\delta\hat{q}) = \Omega_{\text{mec}}(\overline{p}+\delta\hat{p}), \tag{B.12}$$

and we get

$$\delta\dot{\hat{q}} = \Omega_{\text{mec}}\delta\hat{p}. \tag{B.13}$$

And for the momentum operator, from (B.3),

$$\dot{\hat{p}} = -\Omega_{\text{mec}}\hat{q} - \gamma\hat{p} + g_a^0\sqrt{2}\,\hat{a}^\dagger\hat{a} + g_d^0\sqrt{2}\,\hat{d}^\dagger\hat{d} + \sqrt{\gamma}\hat{\xi}(t),$$

we derive

$$\begin{aligned}\frac{d}{dt}(\overline{p}+\delta\hat{p}) &= -\Omega_{\text{mec}}(\overline{q}+\delta\hat{q}) - \gamma(\overline{p}+\delta\hat{p})\\ &\quad + g_a^0\sqrt{2}\,\left(\alpha+\delta\hat{a}\right)^\dagger(\alpha+\delta\hat{a})\\ &\quad + g_d^0\sqrt{2}\,\left(\delta+\delta\hat{d}\right)^\dagger\left(\delta+\delta\hat{d}\right)\\ &\quad + \sqrt{\gamma}\hat{\xi}(t). \end{aligned} \tag{B.14}$$

So

$$\begin{aligned}\delta\dot{\hat{p}} &= -\Omega_{\text{mec}}\overline{q} - \Omega_{\text{mec}}\delta\hat{q} - \gamma\delta\hat{p}\\ &\quad + g_a^0\sqrt{2}\,\left(\alpha^\dagger\alpha+\alpha^\dagger\delta\hat{a}+\delta\hat{a}^\dagger\alpha+\delta\hat{a}^\dagger\delta\hat{a}\right)\\ &\quad + g_d^0\sqrt{2}\,\left(\delta^\dagger\delta+\delta^\dagger\delta\hat{d}+\delta\hat{d}^\dagger\delta+\delta\hat{d}^\dagger\delta\hat{d}\right)\\ &\quad + \sqrt{\gamma}\hat{\xi}(t). \end{aligned} \tag{B.15}$$

Sustituting $\overline{q} = \frac{\sqrt{2}\left(g_a^0|\alpha|^2+g_d^0|\delta|^2\right)}{\Omega_{\text{mec}}}$, we get:

$$\delta\dot{\hat{p}} = -\Omega_{\text{mec}}\delta\hat{q} - \gamma\delta\hat{p} + g_a^0\sqrt{2}\,\left(\alpha^\dagger\delta\hat{a}+\delta\hat{a}^\dagger\alpha\right) + g_d^0\sqrt{2}\,\left(\delta^\dagger\delta\hat{d}+\delta\hat{d}^\dagger\delta\right) + \sqrt{\gamma}\hat{\xi}(t). \tag{B.16}$$

B.3 Derivation of the Fano-optical Quadratures for the Fano-membrane-in-the-middle Setup

From (B.11), we express

$$\delta\dot{\hat{d}}^\dagger = -\left(-i\Delta_d + \kappa_d\right)\delta\hat{d}^\dagger - ig_d^*\sqrt{2}\,\delta\hat{q}^\dagger + i\lambda\delta\hat{a}^\dagger - \sqrt{2\kappa_d}\,\hat{d}_{\mathrm{in}}^\dagger(t), \tag{B.17}$$

allowing us to derive the derivative of the Fano-optical position quadrature:

$$\delta\dot{\hat{X}}_d = \frac{d}{dt}\delta\hat{X}_d = \frac{d}{dt}\left(\frac{\delta\hat{d} + \delta\hat{d}^\dagger}{\sqrt{2}}\right) = \frac{1}{\sqrt{2}}\left(\delta\dot{\hat{d}} + \delta\dot{\hat{d}}^\dagger\right). \tag{B.18}$$

Thus

$$\begin{aligned}
\delta\dot{\hat{X}}_d = \frac{1}{\sqrt{2}}\Bigg(&i\Delta_d\left(-\delta\hat{d} - \delta\hat{d}^\dagger\right) + \kappa_d\left(-\delta\hat{d} - \delta\hat{d}^\dagger\right) + ig_d\sqrt{2}\,\delta\hat{q} - ig_d^*\sqrt{2}\,\delta\hat{q}^\dagger \\
&+ i\lambda\left(-\delta\hat{a} + \delta\hat{a}^\dagger\right) - \sqrt{2\kappa_d}\left(\hat{d}_{\mathrm{in}}(t) + \hat{d}_{\mathrm{in}}^\dagger(t)\right)\Bigg) \\
= {}&\Delta_d\,\delta\hat{P}_d - \kappa_d\,\delta\hat{X}_d + i\left(g_d - g_d^*\right)\delta\hat{q} + \lambda\,\delta\hat{P}_a - \sqrt{2\kappa_d}\,\delta\hat{X}_{\mathrm{in},d} \\
= {}&\Delta_d\,\delta\hat{P}_d - \kappa_d\,\delta\hat{X}_d - 2\ \mathrm{Im}(g_d)\delta\hat{q} + \lambda\,\delta\hat{P}_a - \sqrt{2\kappa_d}\,\delta\hat{X}_{\mathrm{in},d}.
\end{aligned} \tag{B.19}$$

In a similar way, we can express the derivative of the Fano-optical momentum quadrature:

$$\begin{aligned}
\delta\dot{\hat{P}}_d = \frac{1}{i\sqrt{2}}\Bigg(&i\Delta_d\left(-\delta\hat{d} - \delta\hat{d}^\dagger\right) + \kappa_d\left(-\delta\hat{d} + \delta\hat{d}^\dagger\right) + ig_d\sqrt{2}\,\delta\hat{q} + ig_d^*\sqrt{2}\,\delta\hat{q}^\dagger \\
&+ i\lambda\left(-\delta\hat{a} - \delta\hat{a}^\dagger\right) - \sqrt{2\kappa_d}\left(\hat{d}_{\mathrm{in}}(t) - \hat{d}_{\mathrm{in}}^\dagger(t)\right)\Bigg) \\
= {}&-\Delta_d\,\delta\hat{X}_d - \kappa_d\,\delta\hat{P}_d + \left(g_d + g_d^*\right)\delta\hat{q} - \lambda\,\delta\hat{X}_a - \sqrt{2\kappa_d}\,\delta\hat{P}_{\mathrm{in},d} \\
= {}&-\Delta_d\,\delta\hat{X}_d - \kappa_d\,\delta\hat{P}_d + 2\ \mathrm{Re}(g_d)\delta\hat{q} - \lambda\,\delta\hat{X}_a - \sqrt{2\kappa_d}\,\delta\hat{P}_{\mathrm{in},d}.
\end{aligned} \tag{B.20}$$

C

Appendix C

C.1 Solution of the Lyapunov Equation

Given the vector of operators

$$\hat{Y} = \begin{bmatrix} \hat{q}_1 & \hat{p}_1 & ... & \hat{q}_N & \hat{p}_N \end{bmatrix}^T, \tag{C.1}$$

we define the covariance matrix V as

$$\hat{V}_{ij} = \frac{1}{2}\left\langle \hat{Y}_i\hat{Y}_j + \hat{Y}_j\hat{Y}_i \right\rangle - \left\langle \hat{Y}_i \right\rangle \left\langle \hat{Y}_j \right\rangle. \tag{C.2}$$

We demonstrate that the covariance matrix element V_{ij}, whose vector of operators $\hat{Y}$ is a vector of fluctuation operators and follows the differential equation

$$\dot{\hat{Y}} = A\hat{Y} + \hat{f}, \quad \text{where } \hat{f} \text{ is a fluctuation operator,} \tag{C.3}$$

is a solution of the Lyapunov equation

$$\frac{dV}{dt} = AV + VA^T + B. \tag{C.4}$$

We start by considering a vector of fluctuation operators

$$\hat{Y} = \begin{bmatrix} \delta\hat{q}_1 & \delta\hat{p}_1 & ... & \delta\hat{q}_N & \delta\hat{p}_N \end{bmatrix}^T. \tag{C.5}$$

Then,

$$\forall i, \quad \left\langle \hat{Y}_i \right\rangle = 0 \tag{C.6}$$

because we are dealing with fluctuation operators. We can then rewrite the covariance matrix element V_{ij} as

$$\hat{V}_{ij} = \frac{1}{2}\left\langle \hat{Y}_i\hat{Y}_j + \hat{Y}_j\hat{Y}_i \right\rangle. \tag{C.7}$$

We differentiate (C.7):

$$\begin{aligned} \frac{d\hat{V}_{ij}}{dt} &= \frac{1}{2}\frac{d}{dt}\langle \hat{Y}_i\hat{Y}_j + \hat{Y}_j\hat{Y}_i \rangle \\ &= \frac{1}{2}\left(\langle \dot{\hat{Y}}_i\hat{Y}_j \rangle + \langle \hat{Y}_i\dot{\hat{Y}}_j \rangle + \langle \dot{\hat{Y}}_j\hat{Y}_i \rangle + \langle \hat{Y}_j\dot{\hat{Y}}_i \rangle \right). \end{aligned}$$

We assume that the equation of motion for $\hat{Y}_i$ is given by

$$\dot{\hat{Y}}_i = \sum_k A_{ik}\hat{Y}_k + \hat{f}_i(t), \tag{C.8}$$

where

$$\hat{f}_i(t) = \sqrt{\gamma_i}\,\hat{a}_{\text{in}}(t) \tag{C.9}$$

is a general fluctuation operator satisfying the correlation function

$$\langle \hat{f}_i(t)\hat{f}_k(t')\rangle = \gamma\,\delta_{ik}\,\delta(t-t'). \tag{C.10}$$

Substituting, we get

$$\begin{aligned}
\dot{\hat{V}}_{ij} &= \frac{1}{2}\sum_k \Big(\langle A_{ik}\hat{Y}_k\hat{Y}_j\rangle + \langle \hat{f}_i(t)\hat{Y}_j\rangle + \langle \hat{Y}_i A_{jk}\hat{Y}_k\rangle + \langle \hat{Y}_i\hat{f}_j\rangle \\
&\quad + \langle A_{jk}\hat{Y}_k\hat{Y}_i\rangle + \langle \hat{f}_j\hat{Y}_i\rangle + \langle \hat{Y}_j A_{ik}\hat{Y}_k\rangle + \langle \hat{Y}_j\hat{f}_i(t)\rangle\Big) \\
&= \sum_k \Big(\langle A_{ik}\left(\hat{Y}_k\hat{Y}_j + \hat{Y}_j\hat{Y}_k\right)\rangle + \langle A_{jk}\left(\hat{Y}_k\hat{Y}_i + \hat{Y}_i\hat{Y}_k\right)\rangle \\
&\quad + \frac{1}{2}\langle\left\{\hat{f}_i(t),\hat{Y}_j\right\}_+ + \left\{\hat{f}_j,\hat{Y}_i\right\}_+\rangle\Big) \\
&= \sum_k \left(A_{ik}\hat{V}_{kj} + A_{jk}\hat{V}_{ik} + \frac{1}{2}\langle\left\{\hat{f}_i(t),\hat{Y}_j\right\}_+ + \left\{\hat{f}_j,\hat{Y}_i\right\}_+\rangle\right) \\
&= AV + VA^T + \frac{1}{2}\langle\left\{\hat{f}_i(t),\hat{Y}_j\right\}_+ + \left\{\hat{f}_j,\hat{Y}_i\right\}_+\rangle.
\end{aligned}$$

We verify that

$$\hat{y}(t) = e^{At}\int_0^t ds\, e^{-As}\hat{f}(s) + \hat{y}(0) \tag{C.11}$$

is a solution to (C.8):

$$\begin{aligned}
\dot{\hat{y}}(t) &= Ae^{At}\left(\int_0^t ds\, e^{-As}\hat{f}(s) + \hat{y}(0)\right) + e^{At}e^{-At}\hat{f}(t) \\
&= A\hat{y}(t) + \hat{f}(t).
\end{aligned}$$

We then derive

$$\begin{aligned}
\frac{1}{2}\langle\hat{f}_i(t)\hat{Y}_j\rangle &= \frac{1}{2}\langle\hat{f}_i(t)\left(\sum_k\int_0^t ds\,[e^{A(t-s}]_{jk}\hat{f}_k(s)+\hat{y}_j(0)\right)\rangle \\
&= \frac{1}{2}\langle\hat{f}_i(t)\sum_k\int_0^t ds\,[e^{A(t-s)}]_{jk}\hat{f}_k(s)\rangle + \frac{1}{2}\langle\hat{f}_i(t)\hat{y}_j(0)\rangle \\
&= \frac{1}{2}\sum_k\int_0^t ds\,[e^{A(t-s)}]_{jk}\langle\hat{f}_i(t)\hat{f}_k(s)\rangle + \frac{1}{2}\langle\hat{f}_i(t)\rangle\hat{y}_j(0) \\
&= \frac{1}{2}\sum_k\int_0^t ds\,[e^{A(t-s)}]_{jk}\gamma_k\,\delta_{ik}\,\delta(t-s)+0 \\
&= \frac{\gamma}{2}\sum_k\int_0^t [e^{A(t-s)}]_{jk}\delta_{ik}\,ds \\
&= \frac{\gamma}{2}\sum_k\delta_{ik}\frac{1}{2}\mathbb{1}_{jk} \\
&= \frac{\gamma}{4}\delta_{ik}\delta_{jk}\mathbb{1} \\
&= \frac{\gamma}{4}\delta_{ij}\mathbb{1}.
\end{aligned}$$

We then have

$$\begin{aligned}
\frac{1}{2}\langle\left\{\hat{f}_i(t),\hat{Y}_j\right\}_+ + \left\{\hat{f}_j(t),\hat{Y}_i\right\}_+\rangle &= \frac{1}{2}\langle\left\{\hat{f}_i(t),\hat{Y}_j\right\}_+\rangle + \frac{1}{2}\langle\left\{\hat{f}_j(t),\hat{Y}_i\right\}_+\rangle \\
&= \frac{1}{2}\langle\hat{f}_i(t)\hat{Y}_j+\hat{Y}_j\hat{f}_i(t)\rangle + \frac{1}{2}\langle\hat{f}_j(t)\hat{Y}_i+\hat{Y}_i\hat{f}_j(t)\rangle \\
&= \frac{1}{2}\left(\langle\hat{f}_i(t)\hat{Y}_j\rangle + \langle\hat{Y}_j\hat{f}_i(t)\rangle + \langle\hat{f}_j(t)\hat{Y}_i\rangle + \langle\hat{Y}_i\hat{f}_j(t)\rangle\right) \\
&= \gamma\,\delta_{ij}\,\mathbb{1}. \qquad \text{(C.12)}
\end{aligned}$$

Thus,

$$\frac{d\hat{V}_{ij}}{dt} = AV + VA^T + B, \qquad \text{(C.13)}$$

where B is a diagonal matrix whose elements are the square of the fluctuation-operator prefactor.

C.2 Derivation of the B-matrix Elements

We derive the elements of the B-matrix for the optomechanical system.

The matrix B is defined as

$$B = \begin{bmatrix} u & 0 & 0 & 0 & 0 & 0 \\ 0 & v & 0 & 0 & 0 & 0 \\ 0 & 0 & w & 0 & 0 & 0 \\ 0 & 0 & 0 & x & 0 & 0 \\ 0 & 0 & 0 & 0 & y & 0 \\ 0 & 0 & 0 & 0 & 0 & z \end{bmatrix}, \tag{C.14}$$

where

$$u = \langle \sqrt{2\kappa_L}\, \delta\hat{X}_{\mathrm{in},L}(t) \cdot \sqrt{2\kappa_L}\, \delta\hat{X}_{\mathrm{in},L}(t') \rangle + \langle \sqrt{2\kappa_R}\, \delta\hat{X}_{\mathrm{in},R}(t) \cdot \sqrt{2\kappa_R}\, \delta\hat{X}_{\mathrm{in},R}(t') \rangle, \tag{C.15}$$

$$v = \langle \sqrt{2\kappa_L}\, \delta\hat{P}_{\mathrm{in},L}(t) \cdot \sqrt{2\kappa_L}\, \delta\hat{P}_{\mathrm{in},L}(t') \rangle + \langle \sqrt{2\kappa_R}\, \delta\hat{P}_{\mathrm{in},R}(t) \cdot \sqrt{2\kappa_R}\, \delta\hat{P}_{\mathrm{in},R}(t') \rangle, \tag{C.16}$$

$$w = \langle \sqrt{2\kappa_d}\, \delta\hat{X}_{\mathrm{in},d}(t) \cdot \sqrt{2\kappa_d}\, \delta\hat{X}_{\mathrm{in},d}(t') \rangle, \tag{C.17}$$

$$x = \langle \sqrt{2\kappa_d}\, \delta\hat{P}_{\mathrm{in},d}(t) \cdot \sqrt{2\kappa_d}\, \delta\hat{P}_{\mathrm{in},d}(t') \rangle, \tag{C.18}$$

$$y = 0, \tag{C.19}$$

$$z = \langle \sqrt{\gamma}\, \hat{\xi}(t) \cdot \sqrt{\gamma}\, \hat{\xi}(t') \rangle. \tag{C.20}$$

We perform the calculations for each element in the following.

$$\begin{aligned}
u &= \langle \sqrt{2\kappa_L}\, \frac{\delta\hat{a}_{\mathrm{in},L}(t) + \delta\hat{a}^\dagger_{\mathrm{in},L}(t)}{\sqrt{2}} \cdot \sqrt{2\kappa_L}\, \frac{\delta\hat{a}_{\mathrm{in},L}(t') + \delta\hat{a}^\dagger_{\mathrm{in},L}(t')}{\sqrt{2}} \rangle \\
&\quad + \langle \sqrt{2\kappa_R}\, \frac{\delta\hat{a}_{\mathrm{in},R}(t) + \delta\hat{a}^\dagger_{\mathrm{in},R}(t)}{\sqrt{2}} \cdot \sqrt{2\kappa_R}\, \delta \frac{\delta\hat{a}_{\mathrm{in},R}(t') + \hat{a}^\dagger_{\mathrm{in},R}(t')}{\sqrt{2}} \rangle \\
&= \frac{1}{2} \Big(\langle \sqrt{2\kappa_L}\, \delta\hat{a}_{\mathrm{in},L}(t) \cdot \sqrt{2\kappa_L}\, \delta\hat{a}_{\mathrm{in},L}(t') \rangle + \langle \sqrt{2\kappa_L}\, \delta\hat{a}_{\mathrm{in},L}(t) \cdot \sqrt{2\kappa_L}\, \delta\hat{a}^\dagger_{\mathrm{in},L}(t') \rangle \\
&\quad + \langle \sqrt{2\kappa_L}\, \delta\hat{a}^\dagger_{\mathrm{in},L}(t) \cdot \sqrt{2\kappa_L}\, \delta\hat{a}_{\mathrm{in},L}(t') \rangle + \langle \sqrt{2\kappa_L}\, \delta\hat{a}^\dagger_{\mathrm{in},L}(t) \cdot \sqrt{2\kappa_L}\, \delta\hat{a}^\dagger_{\mathrm{in},L}(t') \rangle \Big) \\
&\quad + \frac{1}{2} \Big(\langle \sqrt{2\kappa_R}\, \delta\hat{a}_{\mathrm{in},R}(t) \cdot \sqrt{2\kappa_R}\, \delta\hat{a}_{\mathrm{in},R}(t') \rangle + \langle \sqrt{2\kappa_R}\, \delta\hat{a}_{\mathrm{in},R}(t) \cdot \sqrt{2\kappa_R}\, \delta\hat{a}^\dagger_{\mathrm{in},R}(t') \rangle \\
&\quad + \langle \sqrt{2\kappa_R}\, \delta\hat{a}^\dagger_{\mathrm{in},R}(t) \cdot \sqrt{2\kappa_R}\, \delta\hat{a}_{\mathrm{in},R}(t') \rangle + \langle \sqrt{2\kappa_R}\, \delta\hat{a}^\dagger_{\mathrm{in},R}(t) \cdot \sqrt{2\kappa_R}\, \delta\hat{a}^\dagger_{\mathrm{in},R}(t') \rangle \Big) \\
&= \frac{1}{2} \left(2\kappa_L \delta(t-t') + 2\kappa_L \delta(t-t')\right) + \frac{1}{2} \left(2\kappa_R \delta(t-t') + 2\kappa_R \delta(t-t')\right) \\
&= \kappa_L \delta(t-t') + \kappa_R \delta(t-t') \\
&= (\kappa_L + \kappa_R) \delta(t-t') \\
&= \kappa \delta(t-t')
\end{aligned} \tag{C.21}$$

$$
\begin{aligned}
v &= \langle \sqrt{2\kappa_L}\,\frac{\delta\hat{a}_{\mathrm{in},L}(t)-\delta\hat{a}^{\dagger}_{\mathrm{in},L}(t)}{i\sqrt{2}}\cdot\sqrt{2\kappa_L}\,\frac{\delta\hat{a}_{\mathrm{in},L}(t')-\delta\hat{a}^{\dagger}_{\mathrm{in},L}(t')}{i\sqrt{2}}\rangle \\
&\quad + \langle \sqrt{2\kappa_R}\,\frac{\delta\hat{a}_{\mathrm{in},R}(t)-\delta\hat{a}^{\dagger}_{\mathrm{in},R}(t)}{i\sqrt{2}}\cdot\sqrt{2\kappa_R}\,\frac{\delta\hat{a}_{\mathrm{in},R}(t')-\delta\hat{a}^{\dagger}_{\mathrm{in},R}(t')}{i\sqrt{2}}\rangle \\
&= -\frac{1}{2}\Big(\langle\sqrt{2\kappa_L}\,\delta\hat{a}_{\mathrm{in},L}(t)\cdot\sqrt{2\kappa_L}\,\delta\hat{a}_{\mathrm{in},L}(t')\rangle - \langle\sqrt{2\kappa_L}\,\delta\hat{a}_{\mathrm{in},L}(t)\cdot\sqrt{2\kappa_L}\,\delta\hat{a}^{\dagger}_{\mathrm{in},L}(t')\rangle \\
&\quad - \langle\sqrt{2\kappa_L}\,\delta\hat{a}^{\dagger}_{\mathrm{in},L}(t)\cdot\sqrt{2\kappa_L}\,\delta\hat{a}_{\mathrm{in},L}(t')\rangle + \langle\sqrt{2\kappa_L}\,\delta\hat{a}^{\dagger}_{\mathrm{in},L}(t)\cdot\sqrt{2\kappa_L}\,\delta\hat{a}^{\dagger}_{\mathrm{in},L}(t')\rangle\Big) \\
&\quad - \frac{1}{2}\Big(\langle\sqrt{2\kappa_R}\,\delta\hat{a}_{\mathrm{in},R}(t)\cdot\sqrt{2\kappa_R}\,\delta\hat{a}_{\mathrm{in},R}(t')\rangle - \langle\sqrt{2\kappa_R}\,\delta\hat{a}_{\mathrm{in},R}(t)\cdot\sqrt{2\kappa_R}\,\delta\hat{a}^{\dagger}_{\mathrm{in},R}(t')\rangle \\
&\quad - \langle\sqrt{2\kappa_R}\,\delta\hat{a}^{\dagger}_{\mathrm{in},R}(t)\cdot\sqrt{2\kappa_R}\,\delta\hat{a}_{\mathrm{in},R}(t')\rangle + \langle\sqrt{2\kappa_R}\,\delta\hat{a}^{\dagger}_{\mathrm{in},R}(t)\cdot\sqrt{2\kappa_R}\,\delta\hat{a}^{\dagger}_{\mathrm{in},R}(t')\rangle\Big) \\
&= -\frac{1}{2}\left(-2\kappa_L\delta(t-t') - 2\kappa_L\delta(t-t')\right) - \frac{1}{2}\left(-2\kappa_R\delta(t-t') - 2\kappa_R\delta(t-t')\right) \\
&= \kappa_L\delta(t-t') + \kappa_R\delta(t-t') \\
&= (\kappa_L+\kappa_R)\delta(t-t') \\
&= \kappa\delta(t-t')
\end{aligned}
\tag{C.22}
$$

$$
\begin{aligned}
w &= \langle \sqrt{2\kappa_d}\,\frac{\delta\hat{d}_{\mathrm{in}}(t)+\delta\hat{d}^{\dagger}_{\mathrm{in}}(t)}{\sqrt{2}}\cdot\sqrt{2\kappa_d}\,\frac{\delta\hat{d}_{\mathrm{in}}(t')+\delta\hat{d}^{\dagger}_{\mathrm{in}}(t')}{\sqrt{2}}\rangle \\
&= \frac{1}{2}\Big(\langle\sqrt{2\kappa_d}\,\delta\hat{d}_{\mathrm{in}}(t)\cdot\sqrt{2\kappa_d}\,\delta\hat{d}_{\mathrm{in}}(t')\rangle + \langle\sqrt{2\kappa_d}\,\delta\hat{d}_{\mathrm{in}}(t)\cdot\sqrt{2\kappa_d}\,\delta\hat{d}^{\dagger}_{\mathrm{in}}(t')\rangle \\
&\quad + \langle\sqrt{2\kappa_d}\,\delta\hat{d}^{\dagger}_{\mathrm{in}}(t)\cdot\sqrt{2\kappa_d}\,\delta\hat{d}_{\mathrm{in}}(t')\rangle + \langle\sqrt{2\kappa_d}\,\delta\hat{d}^{\dagger}_{\mathrm{in}}(t)\cdot\sqrt{2\kappa_d}\,\delta\hat{d}^{\dagger}_{\mathrm{in}}(t')\rangle\Big) \\
&= \frac{1}{2}\left(2\kappa_d\delta(t-t') + 2\kappa_d\delta(t-t')\right) \\
&= \kappa_d\delta(t-t')
\end{aligned}
\tag{C.23}
$$

$$
\begin{aligned}
x &= \langle \sqrt{2\kappa_d}\,\frac{\delta\hat{d}_{\mathrm{in}}(t)-\delta\hat{d}^{\dagger}_{\mathrm{in}}(t)}{i\sqrt{2}}\cdot\sqrt{2\kappa_d}\,\frac{\delta\hat{d}_{\mathrm{in}}(t')-\delta\hat{d}^{\dagger}_{\mathrm{in}}(t')}{i\sqrt{2}}\rangle \\
&= -\frac{1}{2}\Big(\langle\sqrt{2\kappa_d}\,\delta\hat{d}_{\mathrm{in}}(t)\cdot\sqrt{2\kappa_d}\,\delta\hat{d}_{\mathrm{in}}(t')\rangle - \langle\sqrt{2\kappa_d}\,\delta\hat{d}_{\mathrm{in}}(t)\cdot\sqrt{2\kappa_d}\,\delta\hat{d}^{\dagger}_{\mathrm{in}}(t')\rangle \\
&\quad - \langle\sqrt{2\kappa_d}\,\delta\hat{d}^{\dagger}_{\mathrm{in}}(t)\cdot\sqrt{2\kappa_d}\,\delta\hat{d}_{\mathrm{in}}(t')\rangle + \langle\sqrt{2\kappa_d}\,\delta\hat{d}^{\dagger}_{\mathrm{in}}(t)\cdot\sqrt{2\kappa_d}\,\delta\hat{d}^{\dagger}_{\mathrm{in}}(t')\rangle\Big) \\
&= -\frac{1}{2}\left(-2\kappa_d\delta(t-t') - 2\kappa_d\delta(t-t')\right) \\
&= \kappa_d\delta(t-t')
\end{aligned}
\tag{C.24}
$$

$$
y = 0 \tag{C.25}
$$

$$\begin{aligned} z &= \langle \sqrt{\gamma}\,\hat{\xi}(t) \cdot \sqrt{\gamma}\,\hat{\xi}(t') \rangle \\ &= \gamma \langle \hat{\xi}(t) \cdot \hat{\xi}(t') \rangle \\ &= \gamma(2\bar{n}_{\mathrm{mec}} + 1)\delta(t - t') \end{aligned} \tag{C.26}$$

Thus, the matrix B reads

$$B = \begin{bmatrix} \kappa & 0 & 0 & 0 & 0 & 0 \\ 0 & \kappa & 0 & 0 & 0 & 0 \\ 0 & 0 & \kappa_d & 0 & 0 & 0 \\ 0 & 0 & 0 & \kappa_d & 0 & 0 \\ 0 & 0 & 0 & 0 & 0 & 0 \\ 0 & 0 & 0 & 0 & 0 & \gamma(2\bar{n}_{\mathrm{mec}} + 1) \end{bmatrix}. \tag{C.27}$$

Abstract

Laser cooling techniques offer general methods for preparing microscopic resonators in their motional ground state. We report on theoretical investigations of an optomechanical system which comprises a frequency-dependent photonic-crystal membrane (Fano mirror) placed in the middle of an optical cavity. The quantum Langevin equations are derived for a single cavity mode, a guided optical (Fano) mode of the membrane, and a mechanical mode accounting for the out-of-plane displacement of the membrane, due to its very small reflectivity. We exhibit the linear behaviours of the optomechanical interaction by placing the membrane in between a node and an anti-node of the cavity standing wave. The Fano-mirror setup shows enhanced sideband cooling through the reduction of the spectral linewidth of the cavity compared to conventional systems lacking the Fano mode. This enhancement allows for ground-state cooling of the mechanical mode, even in the (deeply) unresolved-sideband regime.

Furthermore, we investigate the effective quality factor of the cavity and normal modes formed by the coupled cavity and Fano modes. The normal modes show two complex eigenfrequencies, whose real $\Delta_{\pm} = \mathrm{Re}(\Omega_{\pm})$ and imaginary $\kappa_{\pm} = -\,\mathrm{Im}(\Omega_{\pm})$, parts correspond to their effective resonance frequencies and loss rates, respectively. This formalism provides an intuitive framework for determining the optimal manufacturing parameters needed to achieve ground-state cooling.

Keywords: Laser Cooling, Optomechanical System, Photonic-Crystal Membrane, Quantum Langevin Equations, Sideband Cooling, Unresolved-Sideband Regime, Resonance Frequencies, Loss Rate, Ground-State Cooling.

Riassunto

Le tecniche di raffreddamento laser offrono metodi generali per preparare risonatori microscopici nel loro stato fondamentale di moto. In questo report si riportano indagini teoriche su un sistema optomeccanico, che comprende una membrana di cristallo fotonico dipendente dalla frequenza (specchio di Fano) posta al centro di una cavità ottica. Le equazioni di Langevin quantistiche sono derivate per una singola modalità della cavità, una modalità ottica guidata (di Fano) della membrana, e una modalità meccanica che tiene conto dello spostamento fuori dal piano della membrana, a causa della sua riflettività molto bassa. Mostriamo i comportamenti lineari dell'interazione optomeccanica posizionando la membrana tra un nodo e un antinodo dell'onda stazionaria della cavità. L'allestimento con lo specchio di Fano mostra un raffreddamento a banda laterale migliorato grazie alla riduzione della larghezza spettrale della cavità rispetto ai sistemi convenzionali privi della modalità di Fano. Questo miglioramento consente il raffreddamento allo stato fondamentale della modalità meccanica, anche nel regime di banda laterale fortemente irrisolta.

Inoltre, indaghiamo il fattore di qualità effettivo della cavità e le modalità normali formate dall'accoppiamento tra la cavità e le modalità di Fano. Le modalità normali mostrano due autofrequenze complesse, le cui parti reali $\Delta_\pm = \mathrm{Re}(\Omega_\pm)$ e immaginarie $\kappa_\pm = -\,\mathrm{Im}(\Omega_\pm)$ corrispondono rispettivamente alle loro frequenze di risonanza effettive e ai tassi di perdita. Questo formalismo fornisce un quadro intuitivo per determinare i parametri di fabbricazione ottimali necessari per ottenere il raffreddamento allo stato fondamentale.

Parole chiave: Raffreddamento Laser, Sistema Optomeccanico, Membrana di Cristallo Fotonico, Equazioni di Langevin Quantistiche, Raffreddamento a Banda Laterale, Regime di Banda Laterale Irrisolta, Frequenze di Risonanza, Tasso di Perdita, Raffreddamento allo Stato Fondamentale.

Résumé

Le refroidissement par laser est une méthode permettant de réduire les fluctuations quantiques des résonateurs microscopiques jusqu'à ce que ces derniers soient dans leur état quantique fondamental. Nous présentons une étude théorique d'un système optomécanique comprenant une cavité optique dans laquelle est suspendu un cristal photonique, appelé également miroir de Fano. Nous établissons les équations quantiques de Langevin pour chacun des trois modes du système : le mode de la cavité optique, le mode optique lié au cristal photonique et le mode mécanique dû au déplacement de la membrane. La faible réflectivité de la membrane permet à cette dernière d'entrer en résonance. Nous démontrons que l'interaction optomécanique revêt un caractère linéaire lorsque la membrane est placée entre un nœud et un ventre de l'onde stationnaire qui s'établit dans la cavité. Par rapport aux systèmes optomécaniques standard qui ne possèdent pas de cristal photonique, le système que nous étudions améliore le processus de refroidissement de l'oscillateur mécanique en réduisant la largeur spectrale de la cavité. Cette configuration permet d'atteindre l'état fondamental du résonateur mécanique, bien que la largeur spectrale de la cavité ne présente initialement pas les caractéristiques physiques optimales nécessaires à l'apparition du processus de refroidissement.

En outre, nous étudions l'effectif facteur de qualité de la cavité et les modes normaux issus du couplage entre la cavité et le mode du cristal photonique. Ces modes normaux présentent deux fréquences propres complexes, dont les parties réelles $\Delta_{\pm} = \mathrm{Re}(\Omega_{\pm})$ correspondent aux fréquences de résonance et les parties imaginaires $\kappa_{\pm} = -\,\mathrm{Im}(\Omega_{\pm})$ aux facteurs de dissipation. Cette étude théorique offre une approche intuitive du système optomécanique étudié et permet de mieux cerner les paramètres physiques fondamentaux nécessaires à la fabrication de ce dispositif optique.

Mots-clés : Refroidissement par laser, Système optomécanique, Cristal photonique, Équations quantiques de Langevin, Refroidissement par effet fréquentiel, Large spectre fréquentiel, Fréquences de résonance, Dissipation, Etat quantique fondamental.

DEPARTMENT OF MICROTECHNOLOGY AND NANOSCIENCE - MC2
CHALMERS UNIVERSITY OF TECHNOLOGY
Gothenburg, Sweden
www.chalmers.se